On Aspects of Anyons and Quantum Graphs

Babak Majidzadeh Garjani

Abstract

This thesis consists of two distinct parts. The first part, based on the first two accompanied papers, is in the field of topological phases of matter and the second part, based on the third accompanied paper, looks at a problem in the field of quantum graphs, a rapidly growing field of mathematical physics.

First, we investigate the entanglement property of the Laughlin state by looking at the rank of the reduced density operator when particles are divided into two groups. We show that the problem of determining this rank translates itself into a question about symmetric polynomials, namely, one has to determine the lower bound for the *degree* in each variable of the symmetric polynomials that vanish under a transformation that clusters the particles into groups of equal size and then brings the particles in each group together. Although we were not able to prove this, but we were able to determine the lower bound for the *total* degree of symmetric polynomials that vanish under the transformation described. Moreover, we were able to characterize all symmetric polynomials that vanish under this transformation.

In the second paper, we introduce a one-dimensional model of interacting $su(2)_k$ anyons. The specific feature of this model is that, through pairing terms present in the Hamiltonian, the number of anyons of the chain can fluctuate. We also take into account the possibility that anyons hop to empty neighboring sites. We investigate the model in five different points of the parameter space. At one of these points, the Hamiltonian of the model becomes a sum of projectors and we determine the explicit form of all the zero-energy ground states for odd values of k. At the other four points, the system is integrable and we determine the behavior of the model at these integrable points. In particular, we show that the system is critical and determine the CFT describing the system at these points.

It is known that there are non-Hermitian Hamiltonians whose spectra are entirely real. This property can be understood in terms of a certain symmetry of these Hamiltonians, known as *PT*-symmetry. It is also known that the spectrum of a non-Hermitian *PT*-symmetric Hamiltonian has reflection symmetry with respect to the real axis. We then ask the reverse question whether or not the reflection symmetry of a non-Hermitian Hamiltonian necessarily implies that the Hamiltonian is *PT*-symmetric. In the context of quantum graphs, we introduce a model for which the answer to this question is positive.

Department of Physics

Stockholm University, 106 91 Stockholm

On Aspects of Anyons and Quantum Graphs

Babak Majidzadeh Garjani

On Aspects of Anyons and Quantum Graphs

Babak Majidzadeh Garjani

This thesis is dedicated to my wife, Shadi

Abstract

This thesis consists of two distinct parts. The first part, based on the first two accompanied papers, is in the field of topological phases of matter and the second part, based on the third accompanied paper, looks at a problem in the field of quantum graphs, a rapidly growing field of mathematical physics.

First, we investigate the entanglement property of the Laughlin state by looking at the rank of the reduced density operator when particles are divided into two groups. We show that the problem of determining this rank translates itself into a question about symmetric polynomials, namely, one has to determine the lower bound for the *degree* in each variable of the symmetric polynomials that vanish under a transformation that clusters the particles into groups of equal size and then brings the particles in each group together. Although we were not able to prove this, but we were able to determine the lower bound for the *total* degree of symmetric polynomials that vanish under the transformation described above. Moreover, we were able to characterize all symmetric polynomials that vanish under this transformation.

In the second paper, we introduce a one-dimensional model of interacting $\mathfrak{su}(2)_k$ anyons. The specific feature of this model is that, through pairing terms present in the Hamiltonian, the number of anyons of the chain can fluctuate. We also take into account the possibility that anyons hop to empty neighboring sites. We investigate the model at five different points of the parameter space. At one of these points, the Hamiltonian of the model becomes a sum of projectors and we determine, for odd values of k, the explicit form of all the zero-energy ground states. At the other four points, the system is integrable and we determine the behavior of the model at these integrable points. In particular, we show that the system is critical and determine the conformal field theories describing the system at these points.

It is known that there are non-Hermitian Hamiltonians whose spectra are entirely real. This property can be understood in terms of a certain symmetry of these Hamiltonians, known as $\mathcal{PT}$-symmetry. It is also known that the spectrum of a non-Hermitian $\mathcal{PT}$-symmetric Hamiltonian has reflection symmetry with respect to the real axis. We then ask the reverse question that whether or not the reflection symmetry of a non-Hermitian Hamiltonian necessarily implies that the Hamiltonian is $\mathcal{PT}$-symmetric. In the context of quantum graphs, we introduce a model for which the answer to this question is positive.

Svensk Sammanfattning

Denna avhandling består av två olika delar. Den första delen, som är baserad på de första två bifogade pappren, handlar om topologiska materiefaser. Den andra delen, som är baserad på det tredje bifogade pappret, handlar om ett problem angående kvantgrafer, som är ett snabbt växande område inom matematisk fysik.

I det första pappret tittar vi på sammanflätningsegenskaper för Laughlintillståndet, genom att undersöka den reducerade täthetsmatrisen när man delar upp partiklarna i tillståndet i två olika grupper. Mer specifikt tittar vi på matrisrangen av täthetsmatrisen. Vi visar att för att beräkna rangen, är detta likvärdigt med ett visst problem som handlar om symmetriska polynom. Mer precist måste man hitta den lägsta möjliga graden av en variabel för ett polynom, som blir noll när man grupperar variablerna i lika stora grupper, och man sätter alla variabler i en grupp lika med varandra. Även om vi inte lyckades med att lösa det här problemet, lyckades vi med att visa vad den minimala totala graden av en sådant polynom är. Dessutom lyckades vi med att karakterisera polynom av den här typen.

I det andra pappret introducerar vi en en-dimensionell modell av växelverkande anyoner av typ $\mathfrak{su}(2)_k$. Specifikt för den här modellen är att antalet anyoner kan fluktuera, via en parbildningsterm. Anyonera kan också flytta sig till en angränsande position, om den är tom. Vi undersöker den här modellen i fem olika punkter i parameterrummet. Vid en av dessa punkter kan man skriva Hamiltonianen som en summa av projektorer, och vi hittade alla grundtillstånd med noll energi för udda k. Vid de andra fyra punkter är modellen exakt lösbar, och vi undersökte beteendet av modellen vid de här punkterna. Vi visade att modellen är kritisk, och vi bestämde den konforma fältteori-beskrivningen.

Det är känt att det finns icke-Hermitska Hamiltonianer, som har reella spektra. Den här egenskapen kan förklaras med hjälp av en viss symmetri, känd som $\mathcal{PT}$-symmetri. Det är också känt att spektrumet hos en $\mathcal{PT}$-symmetrisk Hamiltonian är symmetriskt med avseende på den reella axeln. Vi frågar oss nu om det motsatta också är sant: om man har en icke-Hermitsk Hamiltonian, som har ett spektrum som är symmetriskt med avseende på den reella axeln, har den här Hamiltonianen då automatisk $\mathcal{PT}$-symmetri? Vi introducerar en modell i området kvantgrafer, för vilken vi visar att svaret på den här frågan är positivt.

Contribution to Papers

Paper 1 I proved the main theorem in the paper and contributed equally in writing the paper.

Paper 2 I participated in both the design and analysis of the Hamiltonian. I did the numerical investigations for the Hamiltonian of the model. I contributed equally in writing the paper.

Paper 3 I did almost all the calculations and wrote the majority of the paper. My contribution to the whole article is at least 50 percent.

Note Chapters 1 and 2, except Section 1.6, are based on [MG15].

Acknowledgements

I also appreciate Najib Alhashemi Alharari, a good friend who has always encouraged me to believe in myself. Thank you so much Najib.

I respectfully appreciate Donald Knuth for his (LA)TEX system and being so generous to distribute it for free. I have been always fascinated by the level of beauty that this system can bring to one's writings. Thank you so much Donald.

Last but not least, I am thankful to Sweden, this beautiful country with nice and friendly people. I wish the bests for you. Heja Sverige!.

Contribution to Papers

Paper 1 I proved the main theorem in the paper and contributed equally in writing the paper.

Paper 2 I participated in both the design and analysis of the Hamiltonian. I did the numerical investigations for the Hamiltonian of the model. I contributed equally in writing the paper.

Paper 3 I did almost all the calculations and wrote the majority of the paper.

Note   Chapters 1 and 2, except Section 1.6, are based on [MG15].

Contents

Introduction and Outline

0.1 Introduction

The first part of this thesis is based on the first two accompanied papers. Generally speaking, the objects of interest in each one of these papers are particles called *anyon*s. In the first paper our focus is on *Abelian* anyons and in the second paper our focus is on a model of *non-Abelian* anyons. In the next few lines we describe these terms first.

As the reader might know from her quantum mechanics courses, the *elementary* particles of the universe in which we, apparently, live—the universe with one temporal dimension and *three* spatial ones—fall into two categories. An elementary particle is either a *boson* or a *fermion*. The argument to explain this goes along the following lines.

Consider a system consisting of two *identical* elementary particles, described by the wave-function $\psi(\boldsymbol{r}_1, \boldsymbol{r}_2)$. Rotate the particles by 180° about the midpoint of the line-segment joining them. This gives rise to an exchange of the two particles. Since the particles are assumed to be identical, exchanging them must not affect the expectation value of any dynamical variable associated with the system. This then implies that

$$|\psi(\boldsymbol{r}_1, \boldsymbol{r}_2)|^2 = |\psi(\boldsymbol{r}_2, \boldsymbol{r}_1)|^2, \tag{1}$$

or, equivalently,

$$\psi(\boldsymbol{r}_1, \boldsymbol{r}_2) = e^{i\pi\theta}\, \psi(\boldsymbol{r}_2, \boldsymbol{r}_1), \tag{2}$$

for some real θ in the interval $[0, 2)$. Continuing the rotation of the particles for another 180° around the same point and in the same direction, the system returns to its initial state and, therefore,

$$\psi(\boldsymbol{r}_1, \boldsymbol{r}_2) = e^{2i\pi\theta}\, \psi(\boldsymbol{r}_1, \boldsymbol{r}_2). \tag{3}$$

Thus, there are two possibilities for θ, namely, $\theta \equiv 0, 1 \pmod{2}$. The possibility $\theta = 0$ corresponds to *bosons* and $\theta = 1$ corresponds to *fermions*. Since zero and one are both integers, bosons and fermions are said to obey *integer* statistics.

However, if we lived in a universe with one temporal dimension and only *two* spatial ones, the above innocent argument—as was first mentioned by Jon Magne Leinaas and Jan Myrheim [LM77] and later by Frank Wilczek
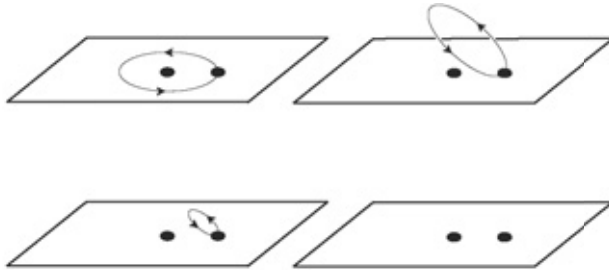
Figure 0.1: Deformation of the trajectory in 3D. (Figure by Eddy Ardonne)

[Wil82a]—has a delicate loophole stemming from *topological* properties of the world-lines traced by particles in space-time. The point, as is explained below, is that, in two spatial dimensions, a 360° rotation of two identical particles about their midpoint does not necessarily bring the system back into its initial state.

First consider the case of three spatial dimensions and a system consisting of two identical particles, either both bosons or both fermions. Consider two scenarios, scenario number one in which one particle goes around the other and comes back to its original position in *space*, and scenario number two in which none of the two particles moves at all. Although visualizing the world-line of the particles in four-dimensional space-time is complicated, nevertheless, the series of pictures in Fig. 0.1 illustrate that, in the first scenario, it is always possible to *continuously* deform and shrink to zero the trajectory of the moving particle, getting the trajectory, that is, no trajectory at all corresponding to the second scenario. This then implies that the two pictures, one for each scenario and each consisting of two world-lines, are topologically "equivalent".

Consider now the same two scenarios as before, but assume that the particles in the system under investigation, each has only two spatial degrees of freedom. This time, one can easily visualize the world-lines corresponding to each scenario as curves in three-dimensional space-time, as is indicated in Fig. 0.2. It is clear that in this case the corresponding world-lines are no longer topologically equivalent. In fact, the world-lines are now tied making a knot and to untie them, keeping the endpoints fixed, one has to rip one of the world-lines and glue it back again. Thus, in two dimensions, the counterpart of Eq. (3), is

$$\psi'(\boldsymbol{r}_1, \boldsymbol{r}_2) = \mathrm{e}^{2i\pi\theta}\, \psi(\boldsymbol{r}_1, \boldsymbol{r}_2), \tag{4}$$

where, in general, ψ' is different from ψ. Thus, $\theta \equiv \alpha \pmod{2}$ with α in $[0, 1]$. As discussed above, $\alpha = 0$ corresponds to bosons and $\alpha = 1$ corresponds to fermions. The particles for which α is a *fraction* in $(0, 1)$ are coined anyons by Wilczek [Wil82b] and it is said that they obey fractional statistics. Each value of α is associated with a different *type* of anyon and α is called the *statistics*
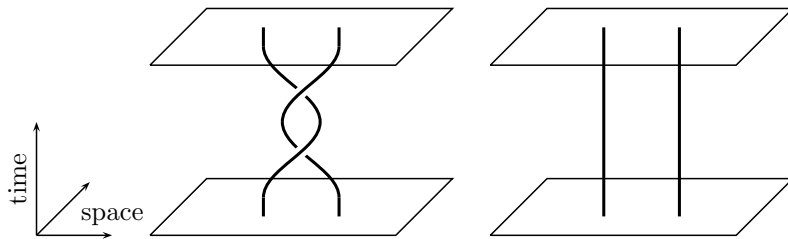
Figure 0.2: Braiding of two anyons in 2D. (Figure by Eddy Ardonne)

of that particular type of anyon. The process in which one anyon goes around another anyon is called *braiding*. To be more precise, the anyons described above, for which braiding two of them gives rise to a non-trivial phase factor for the corresponding wave-function, are called Abelian anyons, since the phases in this case, which are just complex numbers, commute.

There is another type of anyons, called non-Abelian anyons, for which different braidings do not in general commute. To explain this, consider a $(2+1)$-dimensional system consisting of a number of identical particles at fixed positions. Moreover, assume that this state is not unique but, say, d-fold degenerate and also assume that the system is gapped. This state then can be considered as a d-dimensional column vector. Now consider an adiabatic process in which some of these particles are braided around each other such that the final positions of particles are the same as the initial positions of particles. Although the adiabatic theorem implies that the final energy of the system is the same as the initial energy of the system, but it cannot guarantee that the system ends up in exactly the same state that it started from. The most thing that the adiabatic theorem asserts is that the system ends up in a state that is a linear combination of the d degenerate states. In which state the system will end up, depends on the topology of the knot of the braiding processes. Therefore, braiding process can be considered as a matrix acting on the initial d-dimensional state vector. Since, in general, two matrices do not commute, these kind of anyons are called non-Abelian.

In the first paper, we look at the entanglement properties of the Laughlin state, which hosts the Abelian anyons. In the second paper, we consider a one-dimensional model of a chain of non-Abelian anyons and investigate some of its properties. In particular, we investigate the model at four integrable points and determine the exact zero-energy ground states at another point.

In the second part of this thesis, which is based on the third accompanied paper, we look at an axiom of quantum mechanics which asserts that the physical observables are represented by Hermitian operators. This axiom is in fact a mathematical sufficient condition that guarantees the reality of the spectrum of the physical observable that the Hermitian operator represents, which is of

course expected to be the case for a physical theory. However, the Hermiticity
of the operators in quantum mechanics is not a necessary condition for the
spectrum of the operator to be a subset of real numbers.

In this part, we first express the fact that there are *non-Hermitian* linear
operators whose spectra are entirely *real*. One simple example in this regard is
the non-Hermitian "Hamiltonian" H defined by:

$$H = P^2 + \mathrm{i}\, X^3, \tag{5}$$

where P is the momentum operator and X is the position operator. The fact
that the spectrum of H is entirely real and positive was first conjectured by
Bessis and Zinn-Justin in 1998. Soon afterwards, Bender and Boettcher con-
firmed this *numerically* to a very high accuracy [BB98]. Finally, in 2001, a proof
for this conjecture was given by Dorey et al [DDT01]. Bender and Boettcher
associated the reality of the spectrum of H, despite of its non-Hermiticiy, to a
symmetry possessed by H, namely, $\mathcal{PT}$ symmetry, where $\mathcal{P}$ and $\mathcal{T}$ are the (lin-
ear) parity and the (anti-linear) time-reversal operators, respectively. A Hamil-
tonian H is called $\mathcal{PT}$-symmetric if it commutes with $\mathcal{PT}$, that is, $[H, \mathcal{PT}] = 0$.
We see that the spectrum of a $\mathcal{PT}$-symmetric Hamiltonian, either Hermitian
or non-Hermitian, has reflection symmetry with respect to the real axis of the
complex energy plane, namely, the eigenvalues are either real or come in con-
jugate pairs. The last statement gives rise to a natural question, namely, if the
spectrum of a non-Hermitian Hamiltonian H has reflection symmetry with re-
spect to the real axis, does this imply that H is $\mathcal{PT}$-symmetric? Investigating
if this opposite statement holds is harder. In the third accompanied paper, we
investigate this question in the context of *quantum graphs*. A quantum graph
is a graph-like object equipped with a differential operator together with a set
of boundary conditions, called vertex conditions. In this paper, we consider
a simple model, namely, a equilateral quantum star-graph equipped with the
Laplacian as the operator acting on it, subject to such vertex conditions that
make the Laplace operator non-Hermitian. We show in this paper that the
answer to the question above is positive for this model.

0.2   Outline of the Thesis

This thesis contains two distinct parts A and B. Part A, which includes four
chapters, starts by a chapter on the integer and fractional quantum Hall ef-
fects. It introduces the trial wave-function proposed by Laughlin to explain
the fraction quantum Hall effect, and also introduces Abelian and non-Abelian
quantum Hall states, corresponding to Abelian and non-Abelian anyons, respec-
tively. This chapter provides the physical background necessary for Chapter 2.

Chapter 2, which is based on the first accompanied paper [GEA15], is de-
voted to the entanglement property of a fractional quantum Hall system mod-
eled by the Laughlin state and subject to a decomposition scheme, known as

the particle-cut. The notion of interest in this chapter is the rank of the reduced density operator corresponding to the smaller subsystem when the larger subsystem is traced out. In Chapter 2, we relate this rank to the number of summands present in the sum (2.49), which presents a weak-Schmidt decomposition *form* for the Laughlin state Ψ_m, and reduce the problem of determining this rank to proving that this sum is *indeed* a weak-Schmidt decomposition of the corresponding Laughlin state. Then we reduce this latter problem to determining a lower bound for the degree, in each variable, of symmetric polynomials that vanish under a linear transformation, which we call the clustering transformation.

Chapter 3 is devoted to the general theory of anyons and treats the subject on an abstract level. It discusses the notions of fusion rules, F-symbols and R-symbols, and general aspects of the Hilbert spaces corresponding to anyon models. It also contains concrete examples regarding these concepts. Essentially, this chapter provides the necessary tools needed for the next chapter.

Chapter 4 describes the main content of the second accompanied paper [GA17]. It introduces a one-dimensional chain of non-Abelian $\mathfrak{su}(2)_k$ anyons. The model considered in this chapter includes terms in its Hamiltonian that allow for spin-1/2 anyons to interact, a spin-1/2 anyon can hop to the adjacent empty site, and a pair of spin-1/2 anyons can be created out of the vacuum or a pair of spin-1/2 anyons can annihilated into the vacuum. The latter possibility is actually a characteristic feature of our model. In this chapter, we analyze the model at five different points of the parameter space. At one of these points, the Hamiltonian of the model becomes a sum of projection operators, where we are able to determine the explicit form of all zero-energy ground states of the model. We continue our analysis of the model in the subsequent sections and determine four other points of the parameter space at which the system is integrable. This we do by mapping our model onto a restricted solid-on-solid model investigated in [WNS92]. We also discuss the criticality of the system at these integrable points.

Part B of the thesis includes a single chapter and that is Chapter 5. This chapter, which is based on the third accompanied paper [KMG17], starts with an introduction to the notion of $\mathcal{PT}$-symmetric quantum mechanics. There we see that there are non-Hermitian $\mathcal{PT}$-symmetric Hamiltonians whose spectra are entirely real. There we also see that it is a feature of $\mathcal{PT}$-symmetric Hamiltonians that their spectrum have reflection symmetry with respect to the real axis in the energy complex plane. In the context of quantum graphs, which is introduced in the same chapter, we construct a simple model of a non-Hermitian operator whose spectrum has this reflection symmetry and we show that the Hamiltonian is indeed $\mathcal{PT}$-symmetric, where $\mathcal{T}$ is the anti-linear complex-conjugation operator and $\mathcal{P}$ is an edge-permuting symmetry of the graph.

Part A

The Quantum Hall Effect and Anyon Chains

Chapter 1

The Quantum Hall Effect, Abelian and Non-Abelian Anyons

The outline of this chapter is as follows. Section 1.1, after recalling Landau's theory of symmetry breaking to explain the phase transition, introduces the integer and fractional quantum Hall effects. In this section, the fractional quantum Hall state is introduced as a new phase of matter, namely, the topological phase. Section 1.2 starts with the classical Hall effect and points the relation between the classical and quantum Hall effects. Section 1.3 is devoted to the quantum mechanical investigation of an electron in two spatial dimensions subject to a uniform perpendicular magnetic field, that is, the well-known problem of Landau levels. Section 1.4 introduces the Laughlin wave-function and explains how Laughlin came to this approximate wave-function to describe the FQHE. In Section 1.5, the Laughlin quasi-holes with fractional charge and statistics. The last section introduces non-Abelian quasi-holes. This chapter, except Section 1.6, is based on [MG15].

1.1   Topological Phase and Topological Order

From personal experience, we know that matter is found in three different states or phases, namely, solid, liquid, and gas. For example, a bunch of water molecules can be found in all these three states as ice, liquid water, and steam. Cooling an amount of liquid water down to its freezing temperature transforms it into solid ice. The liquid phase transforms to the solid phase and it is said that a *phase transition* has occurred. Although a full description of these states needs quantum physics as well, but these three states traditionally belong to a category called *classical states* of matter. Another important phase of matter is the *ferromagnetic* phase, which is already known from the time of Ancient Greek in the form of permanent magnets. At high temperatures, the magnetic moments of a magnetic material are *disordered* and the average magnetic moment is zero. Cooling the material down to the temperature known as the *Curie* temperature, the magnetic moments align and the average magnetic moment does no longer vanish and the material is said to be in the ferromagnetic phase. Other examples of phases of matter are the *superfluid*, the *superconducting*, and the *liquid crystal* phases.

What distinguishes these phases from each other is their internal structure, which is referred to as the *internal order*. Consider a monatomic gas as an

example. The interaction between atoms is almost zero and, therefore, each atom is moving without being affected by the motion of other atoms. Thus, one can say that the gaseous state is a very disordered one and that the gas is symmetric under a translation with respect to any vector of an arbitrary magnitude and direction. At low temperatures, the kinetic energy of atoms is lower and the interaction of atoms becomes more important. Hence, the motion of any individual atom influences others and a regular pattern known as a *crystal* or *lattice* is formed. This lattice is symmetric with respect to only those translations whose corresponding vector is an integer multiple of the lattice vector. This then means that the *continuous* translational symmetry is *broken* to a *discrete* translational symmetry. In the ferromagnetism phenomenon mentioned earlier, at high temperatures, the system has a continuous rotational symmetry known as $SO(3)$ symmetry. Below the Curie temperature, however, the magnetic moments of the system align and this gives rise to a non-zero magnetic moment and the ferromagnetic state emerges. In this case the $SO(3)$ rotational symmetry is broken to the $SO(2)$ symmetry.

Taking into account the relation between the internal order and the symmetries underlying various phases of matter, Russian physicist Lev Landau developed a theory, Landau's theory of phase transition, to explain all different phases of matter, known at the time, and transitions between them. The main idea underlying Landau's theory is the idea of *symmetry breaking*. Roughly speaking, this idea expresses that, in a phase transition from some disordered phase to a more ordered one, some symmetry is lost. In this theory, the notion of the *local* order parameter plays a crucial role. In the ordered phase, the order parameter takes a finite value, while its value is zero in the disordered phase. In the case of ferromagnetism, for example, the magnetization plays the role of the local order parameter.

Landau's theory was very successful in explaining different phases of matter and the transitions between them. However, by the discovery of the quantum Hall effects in the early 80s, it became clear that Landau's theory does not capture all phases of matter. In 1980, the German physicist Klaus von Klitzing found out that, at low temperatures and strong magnetic fields, the Hall resistance of a two-dimensional electron gas—in contrast to what one would expect classically as it is explained in Section 1.2—does not vary smoothly proportional to the strength of the magnetic field and changes in steps showing a pattern of plateaus [KDP80]. It turned out that the Hall resistance ρ_H of these plateaus can be expressed as $\rho_H = h/(\nu e^2)$, where e is the electric charge of the electron, h is the Planck constant, and ν, to a very high accuracy, is an integer. This phenomenon is known as the *integer quantum Hall effect* (IQHE). For this discovery, von Klitzing received the 1985 Nobel Prize in physics. Two years later, Horst L. Störmer and Daniel Tsui at Bell labs, doing essentially the same kind of experiments at a very low temperature of about 1 K and a very strong magnetic field of about 30 T and on a much cleaner sample, discovered

a new plateau [TSG82] corresponding to the fractional value 1/3 for ν in the relation above for the Hall resistance. As Fig. 1.1 shows, further experiments revealed the possibility of more fractional values for ν. This phenomenon is known as the *fractional quantum Hall effect* (FQHE).
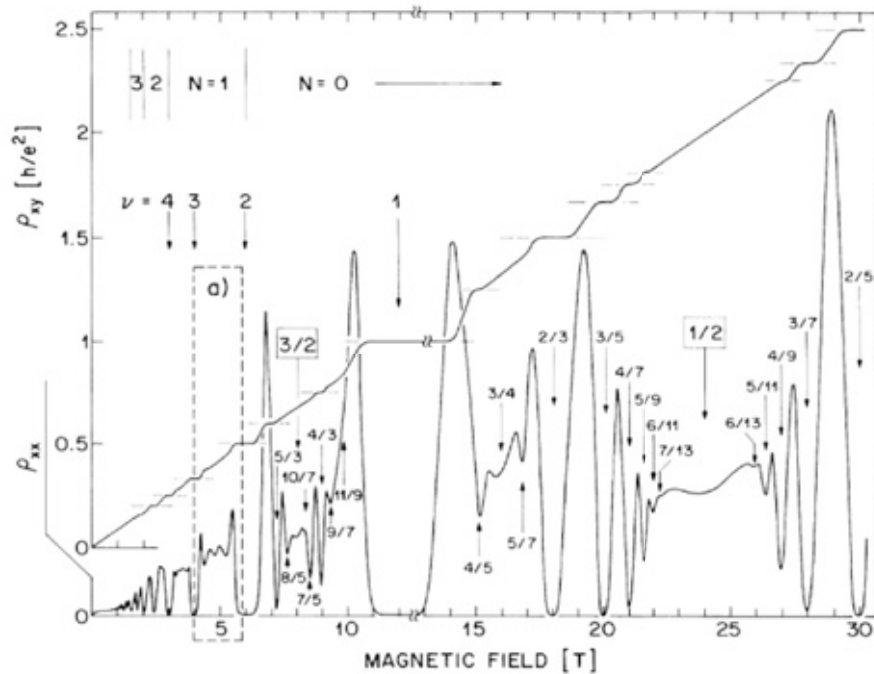
Figure 1.1: FQHE. This picture is taken from [Wil13].

Soon after its discovery, considering essentially the quantum-mechanical description of an electron moving in two dimensions in the presence of a perpendicular magnetic field, the IQHE was explained theoretically. This is explained in detail in Section 1.3. This simplicity stems from the fact that, in this case and at least to the first approximation, the Coulomb interaction between electrons can be ignored.

In contrast, the Coulomb interactions among electrons become important in the FQHE and the system is a strongly-correlated system. Interestingly, the internal order corresponding to a fractional quantum Hall (FQH) system does not allow for a description in terms of Landau's theory of phase transition. This is because the FQH states do not break any symmetry and there is no local order parameter. Instead, it was realized that the FQH system exhibits a totally new phase of matter, namely, a *topological* phase. The internal order describing

a topological phase of matter is called a *topological* order [Wen95]. Recognizing that a given phase is a topological phase is, in general, not easy. One manifestation of a topological phase is that the ground state of a topological phase is degenerate and the order of this degeneracy depends on *topological* properties, such as the genus, of the surface on which the system is set up [Wen95].

The first successful theoretical explanation of the FQHE was given by Robert Laughlin from the Stanford University in 1983 [Lau83]. As is explained in Section 1.4, his idea was based on introducing an approximate *trial* wavefunction that captured the important aspects of the physics underlying a FQH system.

1.2   From Classical to Quantum Hall Effect

In 1879 Edwin Hall, a graduate physics student at Johns Hopkins University, observed that if a thin strip of a conducting material that carries a longitudinal electric current is subject to a perpendicular uniform magnetic field $\boldsymbol{B}$, a transverse voltage appears [Hal79]. To explain this from the classical-physics point of view, consider a thin strip of a conducting material lying on the $x^1 O x^2$ plane and carrying a longitudinal electric current along the positive direction of the $O x^2$ axis. When a uniform magnetic field $\boldsymbol{B}$ in the positive direction of the $O x^3$ axis is turned on, the electrons in the strip are affected by the Lorentz force $\boldsymbol{F} = e\,\boldsymbol{v} \times \boldsymbol{B}$ that lies on the plane of the strip perpendicular to its length. Here, e ($e < 0$) is the electric charge of the electron and $\boldsymbol{v}$ is its velocity. Under this force, electrons begin to accumulate on one longitudinal edge of the strip, giving rise to a transverse voltage. This continues until the magnetic force on the electrons is balanced by the force exerted on them due to the so-called *Hall electric field* $\boldsymbol{E}_{\mathrm{H}}$, created by the transverse voltage. At this point, the electrons flow along the strip without being disturbed by any transverse acceleration and,

$$e\,\boldsymbol{v} \times \boldsymbol{B} + e\boldsymbol{E}_{\mathrm{H}} = 0. \tag{1.1}$$

In this context, the transverse resistivity ρ_{12} is known as *Hall resistivity* and it is denoted by ρ_{H}. To see how classical physics relates the Hall resistivity to the magnitude B of the magnetic field, consider the current density:

$$\boldsymbol{j} = ne\,\boldsymbol{v}, \tag{1.2}$$

where n is the number-density of the electrons in the strip. The two components $E_{\mathrm{H},1}$ and $E_{\mathrm{H},2}$ of the Hall electric field are related to the components of $\boldsymbol{j}$, through the resistivity tensor $\rho = [\rho_{\mu\nu}]_{2\times2}$, according to

$$E_{\mathrm{H},\mu} = \sum_{\nu=1}^{2} \rho_{\mu\nu} j_\nu. \tag{1.3}$$

For this problem it is straightforward to see that:

$$\rho = \frac{B}{ne} \begin{bmatrix} 0 & -1 \\ 1 & 0 \end{bmatrix}. \tag{1.4}$$

Therefore, classical physics predicts that ρ_{12} is proportional to the magnitude of the magnetic field according to the following equation:

$$\rho_{12} = \frac{B}{n|e|}, \tag{1.5}$$

and the *longitudinal resistivities* ρ_{11} and ρ_{22} vanish. By taking the inverse of the resistivity tensor in Eq (1.4), the conductivity tensor σ is found to be

$$\sigma = \frac{ne}{B} \begin{bmatrix} 0 & 1 \\ -1 & 0 \end{bmatrix}. \tag{1.6}$$

In contrast, by doing measurements on a silicon MOSFET (metal-oxide-semiconductor field effect transistor), von Klitzing found that the Hall resistance does not follow the classical predictions [KDP80]. It was revealed that increasing the magnetic field on some intervals does not affect the Hall resistivity ρ_{H} and the Hall resistivity remains constant on these intervals. In other words, the graph of ρ_{H} versus the magnetic field B shows plateaus. However, as in the classical case, on these plateaus the longitudinal resistivity is zero, as is shown in Fig. 1.1. It is also measured, to a very high accuracy, that the Hall resistance ρ_{H} on each plateau obeys the following simple relation:

$$\rho_{\mathrm{H}} = \frac{1}{\nu} \frac{h}{e^2}, \tag{1.7}$$

where h is the Planck constant and ν is either an integer or a simple fraction. The Hall conductance then is:

$$\sigma_{\mathrm{H}} = \nu \frac{e^2}{h}, \tag{1.8}$$

and, consequently, on the plateaus, Eqs. (1.4) and (1.6) must be corrected as follows:

$$\rho = \frac{1}{\nu} \frac{h}{e^2} \begin{bmatrix} 0 & -1 \\ 1 & 0 \end{bmatrix}, \qquad \sigma = \nu \frac{e^2}{h} \begin{bmatrix} 0 & 1 \\ -1 & 0 \end{bmatrix}. \tag{1.9}$$

As mentioned earlier, depending on ν being an integer or a simple fraction, the phenomenon is known as the integer or fractional quantum Hall effect, respectively.

1.3   Landau Levels and Quantum Hall Effects

As mentioned before, the corner stone of the theoretical understanding of the integer and fractional quantum Hall effects is the quantum-mechanical treatment of one single electron in two spatial dimensions and in a perpendicular magnetic field. Consider an electron of mass m_e and the electric charge e subject to a uniform strong[§] magnetic field of magnitude B along the positive direction of the Ox^3 axis. Assume also that the electron is somehow confined to move in the $x^1 O x^2$ plane[¶]. The corresponding Hamiltonian is

$$H = \frac{1}{2m_e} \left(\boldsymbol{p} - e\, \boldsymbol{A} \right)^2, \tag{1.10}$$

where c is the speed of light, $\boldsymbol{p} = -\mathrm{i}\hbar\boldsymbol{\nabla}$ is the momentum operator, and $\boldsymbol{A}$ is the vector potential related to the magnetic field through:[‡]

$$\varepsilon_{ij}\partial^i A^j = B. \tag{1.11}$$

The general solution of the equation above is:

$$A^i = -\frac{B}{2} \left(\varepsilon^{ij} x^j - \partial^i \xi \right), \tag{1.12}$$

where ξ is an arbitrary scalar function that fixes the gauge. It turns out that the allowed energy values for the electron are, as in the case of the harmonic oscillator, evenly spaced and are given by:

$$E_n = \hbar\omega_c \left(n + \frac{1}{2} \right), \tag{1.13}$$

where the quantum number n is a non-negative integer and the *cyclotron frequency* ω_c is given by

$$\omega_c = \frac{|e|B}{m_e}. \tag{1.14}$$

These energy levels are known as the *Landau levels* (LL)s in the honor of Lev Landau who, in 1930, solved the problem for the first time [Lan30]. The first energy level $E_0 = 1/2\hbar\omega_c$ is called the *lowest Landau level* (LLL). Although the energy levels are independent of the gauge chosen, but, in general, the form of the corresponding wave-functions does depend on the gauge.

[§]Strong magnetic field makes the chance of finding the electron with an anti-aligned spin so small that, in practice and at least to first approximation, one can safely ignore the spin degree of freedom of the electron.

[¶]In practice, this can be done, for example, by cooling a sample consisting of an interface of an insulator and a semi-conductor down to almost absolute zero.

[‡]$\varepsilon_{11} = \varepsilon_{22} = 0$, and $\varepsilon_{12} = -\varepsilon_{21} = 1$.

In the *symmetric gauge*, that is, the gauge for which ξ in Eq. (1.12) is chosen to be zero, the wave-functions corresponding to the nth Landau level expressed in complex coordinates are given by:

$$\psi_{l,n}(z) = \sqrt{\frac{n!}{2\pi 2^l (l+n)!}} \, z^l \, L_n^l \left(\frac{|z|^2}{2l_B^2} \right) \exp\left(-\frac{|z|^2}{4l_B^2} \right). \qquad (1.15)$$

In this equation, l is an integer not less than $-n$, L_n^l is the associated Laguerre polynomial, $z = x^1 + \mathrm{i}x^2$ where (x^1, x^2) are the Cartesian coordinates of the electron, and

$$l_B = \sqrt{\frac{\hbar}{|e|B}}. \qquad (1.16)$$

The number l_B has the dimension of length and it is called the *magnetic length*, which can be considered as the natural length scale of the system.

In the symmetric gauge, the third component L^3 of the angular momentum commutes with the Hamiltonian (1.10) and it turns out that for a given value of n the wave-function $\psi_{l,n}(z)$ in Eq. (1.15) is also an eigenstate of L^3 with the eigenvalue $l\hbar$. Note that in complex coordinates

$$L^3 = \hbar(z\partial - \bar{z}\bar{\partial}), \qquad (1.17)$$

where $\bar{z}$ is the complex conjugate of z and

$$\begin{aligned}
\partial &:= \frac{\partial}{\partial z} = \frac{1}{2}(\partial_1 - \mathrm{i}\partial_2), \\
\bar{\partial} &:= \frac{\partial}{\partial \bar{z}} = \frac{1}{2}(\partial_1 + \mathrm{i}\partial_2).
\end{aligned} \qquad (1.18)$$

Since l in Eq. (1.15) can take any integer value greater than or equal to $-n$, each LL is *infinitely* degenerate. This is a notable characteristic of this problem. This infinite degeneracy is the consequence of not considering any constraint on the electron except that it is limited to move in the x^1Ox^2 plane. However, in practice one always deals with a sample of finite size that confines the electron's motion to a finite region of the x^1Ox^2 plane. Finiteness of the sample, as the following argument shows, puts an upper bound on the degeneracy of the LLs.

For simplicity, we consider only the LLL, where the wave-functions correspond to $n = 0$ in Eq. (1.15), that is,

$$\psi_{l,0}(z) = \frac{1}{\sqrt{2\pi 2^l l!}} \, z^l \exp\left(-\frac{|z|^2}{4l_B^2} \right), \qquad l = 0, 1, 2, \dots. \qquad (1.19)$$

By calculating the derivative of $|\psi_{l,0}(z)|^2$ for a given non-negative integer l, it is seen that the maximum value of this function occurs at the points lying on the circle of radius $\sqrt{2l}\,l_B$ centered at the origin. Hence, for a circular sample

of radius R, one should not consider the states $\psi_{l,0}(z)$ with $\sqrt{2l}l_B > R$ and the degeneracy of LLL is

$$l_{\max} = \frac{R^2}{2l_B^2}. \tag{1.20}$$

This degeneracy can also be written as

$$l_{\max} = \frac{\pi R^2}{2\pi l_B^2} = \frac{\pi R^2 B}{2\pi l_B^2 B} = \frac{\Phi}{\Phi_0}. \tag{1.21}$$

Here Φ is the magnetic flux penetrating through the sample and Φ_0 is the *flux quantum* defined as

$$\Phi_0 = \frac{h}{|e|}. \tag{1.22}$$

The ratio Φ/Φ_0 is then the number of flux quanta and it is denoted by N_Φ ($N_\Phi = l_{\max}$). Another ratio of particular interest in the context of quantum Hall physics is the *filling factor* ν_f. It is defined by

$$\nu_f = \frac{N}{N_\Phi}, \tag{1.23}$$

where N denotes the number of electrons in the sample. This ratio can be expressed in a different way related to the geometry of the sample. From the discussion above, it is seen that to any value $l\hbar$ ($0 \leqslant l \leqslant l_{\max}$) of the angular momentum, one can associate a circle of radius $R_l = \sqrt{2l}l_B$ centered at the origin. The area ΔS encircled by the two concentric circles corresponding to two consecutive values l and $l+1$ of the angular momentum is:

$$\Delta S = \pi R_{l+1}^2 - \pi R_l^2 = 2\pi l_B^2. \tag{1.24}$$

Hence, from Equations (1.21) and (1.23), one gets:

$$\nu_f = \frac{N\Delta S}{S}. \tag{1.25}$$

It turns out that ν_f is equal to ν that appeared in the relation for the Hall resistivity and, therefore, from now on we denote it simply by ν.

Now let us look back at the integer and fractional quantum Hall effects. It is clear that, for an integer value of ν, the ground state of a quantum Hall system is the state corresponding to the case in which all the first ν Landau levels are completely filled[§] and, hence, the ground state is a non-degenerate state. In this case, since the system is gapped and the typical Coulomb repulsion between electrons is of order e^2/l_B, which is much less than the gap $\hbar\omega_c$, one

---

[§]Note that because of Pauli's exclusion principle, no more than one electron can be in the same state.

can neglect the Coulomb interaction, at least to first approximation. Therefore, a system in an integer quantum state is essentially a *non-interacting* system and this is why soon after its discovery it was explained theoretically. The many-body wave-function is just a single Slater determinant.

As an example, consider the simplest case $\nu = 1$ in which the number of electrons is exactly equal to the number of orbitals in the first LL and let $\Psi_{\nu=1}(z_1, \ldots, z_N)$ denote the unique ground state. This many-body ground state is the following Slater determinant:

$$\Psi_{\nu=1}(z_1, \ldots, z_N) = \frac{1}{\sqrt{N!}} \begin{vmatrix} \psi_{0,0}(z_1) & \ldots & \psi_{0,0}(z_N) \\ \psi_{1,0}(z_1) & \ldots & \psi_{1,0}(z_N) \\ \vdots & & \vdots \\ \psi_{N-1,0}(z_1) & \ldots & \psi_{N-1,0}(z_N) \end{vmatrix}. \tag{1.26}$$

Using Eq. (1.19) for the entries of this determinant, we come up with:

$$\Psi_{\nu=1}(z_1, \ldots, z_N) = \mathcal{N} \begin{vmatrix} 1 & \ldots & 1 \\ z_1 & \ldots & z_N \\ \vdots & & \vdots \\ z_1^{N-1} & \ldots & z_N^{N-1} \end{vmatrix} \exp\Big(- \frac{1}{4l_B^2} \sum_{k=1}^{N} |z_k|^2 \Big), \tag{1.27}$$

where $\mathcal{N}$ is a constant and the determinant above is the well-known *Vandermonde* determinant. Writing this determinant explicitly, one gets:

$$\Psi_{\nu=1}(z_1, \ldots, z_N) = \prod_{1 \leqslant i < j \leqslant N} (z_i - z_j) \exp\Big(- \frac{1}{4l_B^2} \sum_{k=1}^{N} |z_k|^2 \Big), \tag{1.28}$$

up to a normalization constant.

In contrast, FQHE is a whole new story. As mentioned earlier, the first substantial progress in theoretical explanation of this phenomenon was achieved by Laughlin through his introduction of a set of trial wave-functions, which is the topic of the next section.

1.4 Laughlin's Wave-Function

In a FQH system, that is, a two-dimensional quantum-mechanical system subject to a strong perpendicular magnetic field at a very low temperature whose Hall resistance corresponds to a fractional value of ν, only a fraction of orbitals in each LL is filled and, as mentioned earlier and the Fig. 1.1 shows, for a FQH system the graph of Hall resistance ρ_H versus the magnetic field B shows plateaus, which indicates that the system is gapped. This implies that the Coulomb repulsion between the electrons must definitely be taken into account, since in the absence of the Coulomb interaction any redistribution of

electrons within the same LL can be done at zero energy cost, giving rise to a large degeneracy. To explain that a gapped quantum Hall state can occur at the observed filling factors, one needs the Coulomb interaction to lift the degeneracy. In other words, a FQH system is a highly-correlated system and difficult to solve.

Robert Laughlin achieved a breakthrough in the theoretical explanation of the FQHE by proposing a set of quantum Hall states in the form of a set of trial wave-functions, which were shown to contain the basic features of this phenomenon. Laughlin proposed the ansatz wave-function:

$$\Psi_m(z_1, \ldots, z_N) = \prod_{1 \leqslant i < j \leqslant N} (z_i - z_j)^m \, \exp\Big(-\frac{1}{4l_B^2} \sum_{k=1}^{N} |z_k|^2\Big), \qquad (1.29)$$

to describe the ground state of the FQHE at filling factor $\nu = 1/m$, where m is an odd integer [Lau83]. Laughlin arrived to this wave-function arguing as follows:

(i) The suitable wave-function should be of the following form[§]:

$$\Upsilon(z_1, \ldots, z_N) = p(z_1, \ldots, z_N) \, \exp\Big(-\frac{1}{4l_B^2} \sum_{k=1}^{N} |z_k|^2\Big), \qquad (1.30)$$

where $p(z_1, \ldots, z_N)$ is a polynomial in z_1 till z_N. To write this, Laughlin was inspired by the form of the wave-function (1.19) for the LLL states.

(ii) Since this wave-function is to describe a system of electrons as fermions, it must be totally anti-symmetric. Therefore, the polynomial $p(z_1, \ldots, z_N)$ has to be totally anti-symmetric.

(iii) Because of the success of Jastrow-type wave-functions in describing the interacting systems with pairwise interactions like Coulomb interaction, as is the case here, Laughlin assumed the following form:

$$p(z_1, \ldots, z_N) = \prod_{1 \leqslant i < j \leqslant N} f(z_i - z_j), \qquad (1.31)$$

for the $p(z_1, \ldots, z_N)$ polynomial. Here f must be an odd polynomial-function so that $p(z_1, \ldots, z_N)$ be totally anti-symmetric.

(iv) Since the total angular momentum along the Ox^3 direction:

$$L^3 = \hbar \sum_{i=1}^{N} (z_i \partial_i - \bar{z}_i \bar{\partial}_i), \qquad (1.32)$$

[§]One should find out how Υ depends on the filling factor $\nu = 1/m$.

commutes with Coulomb term and, consequently, it commutes with the Hamiltonian, Laughlin required that the suitable wave-function to be an eigenstate of L^3 as well. A simple calculation shows that for this to happen, it is sufficient that the polynomial $p(z_1, \ldots, z_N)$ be an eigenstate of the operator $\hbar \sum_{i=1}^{N} z_i \partial_i$.

It is straightforward to see that, for any odd integer n, $f(z) = z^n$ is a suitable choice and gives rise to a polynomial $p(z_1, \ldots, z_N)$ that is an eigenstate of $\hbar \sum_{i=1}^{N} z_i \partial_i$ operator and, therefore,

$$\Upsilon(z_1, \ldots, z_N) = \prod_{1 \leqslant i < j \leqslant N} (z_i - z_j)^n \, \exp\Big(-\frac{1}{4l_B^2} \sum_{k=1}^{N} |z_k|^2 \Big). \qquad (1.33)$$

We now determine the appropriate exponent n as follows. This function is supposed to describe interacting electrons in the LLL at the filling factor $\nu = 1/m$. The maximum value $l_{\max}$ of the angular momentum that each electron in the state (1.33) can have is the maximum power $n(N-1)$ of any one of the variables z_1 till z_N in Υ. Thus according to Eq. (1.20), the area S of the sample described by (1.33) is:

$$S = 2\pi l_{\max} l_B^2 = 2\pi n(N-1) l_B^2. \qquad (1.34)$$

From Eqs. (1.24) and (1.25), the filling factor ν_f corresponding to the wave-function (1.33), for large values of N, is

$$\nu_f = \frac{N}{n(N-1)} \sim \frac{1}{n}, \qquad (1.35)$$

and, therefore, $n = m$.

At this stage, it is good to know that the wave-function above is an approximate eigenstate of the real Hamiltonian, that is, the Hamiltonian with Coulomb interaction as its interaction term. For small system sizes, namely, systems with only a few electrons, numerical calculations confirmed more than 99% overlap between Laughlin's trial wave-function (1.29) and the exact ground state wave-function. On the other hand, despite of being just an approximate eigenstate for the *real* Hamiltonian, Laughlin's wave-function is the exact solution of a contrived *model* Hamiltonian, namely, a Hamiltonian whose interaction term is engineered so that the Laughlin state (1.29) is the exact ground state[§] [Hal83]. This yet provides another explanation for the triumph of Laughlin's insight to explain the FQHE.

[§]This model interaction basically enforces that the wave-function should vanish at least as an mth power (instead of a first power, which is necessary because of the Pauli exclusion principle) when two electrons are at the same location.

Consider some "total" Hamiltonian H_{total} defined by:

$$H_{\text{total}} = \lambda\, H_{\text{model}} + (1 - \lambda)\, H_{\text{real}}, \tag{1.36}$$

where H_{model} is the model Hamiltonian mentioned above, H_{real} is the real Hamiltonian, and $0 \leqslant \lambda \leqslant 1$ is a real parameter. Numerical investigations confirm that, if one continuously varies the parameter λ from zero to one, no phase transition occurs. Therefore, the model Hamiltonian and its exact ground state, namely, the Laughlin wave-function, can be used to study interesting physical properties of FQH systems corresponding to filling factors of the form $\nu = 1/m$.

1.5   Abelian Quantum Hall States

Using his wave-function, Laughlin not only explained the $\nu = 1/3$ fractional quantum Hall effect but also predicted that *quasi-holes* with *fractional charge* and *statistics* can exist in FQH systems. The fractional charge of these quasi-holes was observed experimentally in 1997 [DPRH$^+$98, SGJE97]. Laughlin, Störmer, and Tsui were awarded the 1998 Nobel prize in physics for these contributions.

To understand the quasi-holes, consider a FQH system in the $x^1 O x^2$ plane subject to a magnetic field in the positive $O x^3$ direction that exhibits the fractional value $\nu = 1/m$. Suppose that its state is modeled by the Laughlin state Ψ_m given by Eq. (1.29). Following Laughlin, we locally increase the magnetic field at the origin by one flux quantum Φ_0. This can be thought to be done by considering an infinitesimally thin and infinitely long solenoid threading normally into the system at the origin, and adiabatically varying the current through it from zero (the initial value) to some appropriate value and in an appropriate direction. Such solenoid is referred to as a "*flux-tube.*" Variation of the magnetic field at the origin generates an electric field $\boldsymbol{E}$ curling around the origin in a direction resisting this change. This electric field in turn generates an electric current of density $\boldsymbol{j}$ that relates itself to the Hall conductivity tensor σ and the electric field $\boldsymbol{E}$ through the following relation:

$$\boldsymbol{j} = \sigma \boldsymbol{E}. \tag{1.37}$$

According to Eq. (1.9), for a FQH system on a plateau, the entries on the main diagonal of the conductivity tensor are zero and, therefore, $\boldsymbol{j}$ lies along the radial direction toward the origin, where the flux tube is located. Thus, Eq. (1.37) reduces to the following one:

$$j_r = \sigma_{\text{H}} E_\phi, \tag{1.38}$$

where j_r is the radial component of current density, E_ϕ is the azimuthal component of the electric field, and σ_{H} is as given in Eq. (1.9). This current density

indicates that the electrons flow out from a small region confined by a small circle centered at the origin, where the flux tube is located, making a "hole" behind them, known as a *quasi-hole*. During this adiabatic process, the ground state Ψ_m evolves to the ground state of the final Hamiltonian where the magnetic flux is now increased by one flux quantum Φ_0. This excess of magnetic flux can be gauged away with a *singular* gauge transformation and we are left with the new exact quasi-hole ground state of the Hamiltonian. It turns out that this small region can act as a particle in its own. Laughlin proposed the following trial wave-function:

$$\Psi_m^{\text{q.h.}}(z_1, \ldots, z_N) = \Psi_m(z_1, \ldots, z_N) \prod_{1 \leqslant k \leqslant N} z_k, \qquad (1.39)$$

for theoretical explanation of a FQH system with one quasi-hole at the origin. Though not an exact ground state for the Coulomb interaction, $\Psi_m^{\text{q.h.}}(z_1, \ldots, z_N)$ is an exact ground state for the model Hamiltonian. In general, if the magnetic flux is slowly changed from zero up to one flux quantum Φ_0 at n local points with complex coordinates w_1 till w_n, Eq. (1.39) then takes the following form:

$$\Psi_m^{\text{q.h.}}(z_1, \ldots, z_N) = \Psi_m(z_1, \ldots, z_N) \prod_{\substack{1 \leqslant k \leqslant N \\ 1 \leqslant l \leqslant n}} (z_k - w_l). \qquad (1.40)$$

Wave-functions $\Psi_m^{\text{q.h.}}(z_1, \ldots, z_N)$ are known as quasi-hole *excitations* of Laughlin states $\Psi_m(z_1, \ldots, z_N)$.

We now go back to the simple case of one quasi-hole at the origin to explore some interesting features of quasi-holes. The state (1.39) has a lack of charge of some magnitude Q at the origin. By Faraday's law:

$$\oint_\Gamma \boldsymbol{E} \cdot \mathrm{d}\boldsymbol{r} = -\frac{\mathrm{d}\Phi}{\mathrm{d}t}, \qquad (1.41)$$

where Γ is a small circle of radius R centered at the origin. This gives rise to

$$E_\phi = -\frac{1}{2\pi R} \frac{\mathrm{d}\Phi}{\mathrm{d}t}, \qquad (1.42)$$

and

$$Q = \int 2\pi R |j_r| \, \mathrm{d}t = \sigma_\text{H} \, \Phi_0 = \nu |e|. \qquad (1.43)$$

This means that this excitation can be regarded as the one with a *fractional* charge of magnitude $\nu|e|$. In a FQH system the quasi-holes obey fractional statistics in the sense that, if two of them are slowly interchanged, the wave-function picks up a phase factor $\mathrm{e}^{\mathrm{i}\alpha\pi}$, where α is a *fraction* strictly between zero and one. In other words, Laughlin's quasi-holes are Abelian anyons. It turns out that α is the same as the filling factor ν, as was shown by Arovas, Schrieffer and Wilczek [ASW84], by calculating the phase associated with the process of adiabatically exchanging two quasi-holes.

1.6   Non-Abelian Quantum Hall States

Although most of the quantum Hall plateaus occur at filling factors with odd denominators, plateaus occurring at filling factors with even denominators have been observed as well [Wil13]. Among the latter plateaus, the ones with filling factors $\nu = 5/2$ and $\nu = 7/2$ are the most well-known ones and have been observed very clearly in the laboratory. In the beginning, for a FQH system consisting of fermions such as electrons, the discovery of plateaus at filling factors with even denominators was not even expected. This was due to the fact that the Laughlin wave-function (1.29) was very successful in describing the plateaus at filling factors $\nu = 1/m$, and only for odd values of m this wave-function is totally anti-symmetric, which of course must be the case for a suitable wave-function describing a system consisting of fermions.

To explain the plateau at filling factor $\nu = 5/2$, following the same strategy as Laughlin, Moore and Read introduced a trial wave-function Ψ_{MR} that is supposed to describe a FQH state for fermions at filling factor $\nu = 1/m$, for *even* values of m [MR91]. To write down this wave-function, they used the notion of a *Pfaffian* of an anti-symmetric matrix, which we now introduce.

Let N be an even integer and let A be an $N \times N$ anti-symmetric matrix, namely, $A^T = -A$, where A^T is the transpose of A. The Pfaffian of A is denoted by $\mathrm{Pf}(A)$ and it is defined by:

$$\mathrm{Pf}(A) = \frac{1}{2^{N/2}(N/2)!} \sum_{\sigma} \Big(\mathrm{sgn}(\sigma) \prod_{i=1}^{N/2} a_{\sigma(2i-1),\sigma(2i)} \Big), \qquad (1.44)$$

where the sum is over all permutations σ of the set $\{1, 2, \ldots, N\}$, $\mathrm{sgn}(\sigma)$ is $+1$ or -1 according to whether σ is an even or odd permutation, respectively, and a_{kl} denotes the (kl)th entry of the matrix A. The Pfaffian and the determinant of an anti-symmetric matrix are related through the following relation:

$$\big(\mathrm{Pf}(A) \big)^2 = \det(A). \qquad (1.45)$$

Since the determinant of any anti-symmetric matrix of odd degree is zero, the Pfaffian of any such matrix is zero as well. As examples of non-trivial Pfaffians, one can mention the following ones:

$$\mathrm{Pf} \begin{bmatrix} 0 & a \\ -a & 0 \end{bmatrix} = a, \quad \mathrm{Pf} \begin{bmatrix} 0 & a & b & c \\ -a & 0 & d & e \\ -b & -d & 0 & f \\ -c & -e & -f & 0 \end{bmatrix} = af - be + dc. \qquad (1.46)$$

The Pfaffian of an $N \times N$ anti-symmetric matrix is a polynomial of degree $N/2$ with the matrix elements as its variables.

The Moore–Read state for an even number N of particles is now given as follows:

$$\Psi_{\mathrm{MR}}(z_1, \ldots, z_N) = \widetilde{\Psi}_{\mathrm{MR}}(z_1, \ldots, z_N) \exp\Big(-\frac{1}{4l_B^2} \sum_{k=1}^{N} |z_k|^2\Big), \qquad (1.47)$$

where

$$\widetilde{\Psi}_{\mathrm{MR}}(z_1, \ldots, z_N) := \mathrm{Pf}\Big(\frac{1}{z_i - z_j}\Big) \prod_{i<j}(z_i - z_j)^m. \qquad (1.48)$$

Here $\mathrm{Pf}(1/(z_i - z_j))$ denotes the Pfaffian of an $N \times N$ anti-symmetric matrix whose (ij)th entry is $1/(z_i - z_j)$, if $i \neq j$; and it is zero, otherwise. For example, for four particles, using the second part of (1.46), we have:

$$\mathrm{Pf}\Big(\frac{1}{z_i - z_j}\Big) = \frac{1}{z_1 - z_2} \frac{1}{z_3 - z_4} + \frac{1}{z_1 - z_3} \frac{1}{z_4 - z_2} + \frac{1}{z_1 - z_4} \frac{1}{z_2 - z_3}.$$

This Pfaffian is a totally anti-symmetric function and, therefore, for even values of m, the Moore–Read state is anti-symmetric and can indeed represent the wave-function for a system of fermions. On the other hand, the exponent of any variable in $\widetilde{\Psi}_{\mathrm{MR}}$ is $m(N-1) - 1$, in which $m(N-1)$ stems from the Laughlin-type factor in $\widetilde{\Psi}_{\mathrm{MR}}$ and -1 stems from the Pfaffian factor. Therefore, in thermodynamic limit, the exponent of any variable in $\widetilde{\Psi}_{\mathrm{MR}}$ is mN. Consequently, Ψ_{MR} describes a FQH system at filling factor $\nu = 1/m$, as is expected. Furthermore, although the Pfaffian above diverges when two particles come together, the Moore–Read state remains finite due to the compensation that the factor $\prod_{i<j}(z_i - z_j)^m$ causes. In addition, $\widetilde{\Psi}_{\mathrm{MR}}$ for $m = 1$ is the homogeneous polynomial with the lowest total degree, up to a numerical pre-factor, that does not vanish if two variables are identified but vanishes when any three variables are identified.

As in the case of the Laughlin state, the Moore–Read state is also the exact zero-energy ground state of a model Hamiltonian. We now look at the excitations of the Moore–Read state. Letting $\boldsymbol{z} := (z_1, \ldots, z_N)$, for any given complex number w, the wave-function:

$$\Psi_{\mathrm{MR}}^{\mathrm{q.h.}}(\boldsymbol{z}) = \widetilde{\Psi}_{\mathrm{MR}}^{\mathrm{q.h.}}(\boldsymbol{z}) \exp\Big(-\frac{1}{4l_B^2} \sum_{k=1}^{N} |z_k|^2\Big), \qquad (1.49)$$

where

$$\widetilde{\Psi}_{\mathrm{MR}}^{\mathrm{q.h.}}(\boldsymbol{z}) := \prod_{k}(z_k - w) \, \mathrm{Pf}\Big(\frac{1}{z_i - z_j}\Big) \prod_{i<j}(z_i - z_j)^m, \qquad (1.50)$$

is also a zero-energy state of the model Hamiltonian. Since the exponential factor is always present, in what follows we focus only on the non-exponential parts of the corresponding wave-functions, which are indicated with a tilde on

top. The exponent of each z variable in $\widetilde{\Psi}_{\mathrm{MR}}^{\mathrm{q.h.}}$ exceeds from the exponent of the corresponding variable in $\widetilde{\Psi}_{\mathrm{MR}}$ by one. Therefore, the angular momentum of this state is one unit larger than the angular momentum of $\widetilde{\Psi}_{\mathrm{MR}}$. The state $\widetilde{\Psi}_{\mathrm{MR}}^{\mathrm{q.h.}}$ is called the quasi-hole excitation of the Moore–Read state corresponding to one single quasi-hole sitting at w. As in the case of the Laughlin state, each quasi-hole carries a fractional charge e/m, but in this case more interesting things can happen.

Consider the following function with two independent parameters w_1 and w_2:

$$\widetilde{\Psi}_{\mathrm{MR}}^{2\mathrm{q.h.}}(\boldsymbol{z}) = \mathrm{Pf}\left(\frac{(z_i - w_1)(z_j - w_2) + (z_j - w_1)(z_i - w_2)}{z_i - z_j}\right)\prod_{i<j}(z_i - z_j)^m.$$

Note that the Pfaffian above is well-defined, since its argument is still an anti-symmetric matrix. This is also a state of the corresponding model Hamiltonian. Moreover, if $w_1 = w_2 = w$, then $\widetilde{\Psi}_{\mathrm{MR}}^{2\mathrm{q.h.}}(\boldsymbol{z})$ reduces to $\widetilde{\Psi}_{\mathrm{MR}}^{\mathrm{q.h.}}(\boldsymbol{z})$ given in (1.50). This would then mean that $\widetilde{\Psi}_{\mathrm{MR}}^{2\mathrm{q.h.}}(\boldsymbol{z})$ can be interpreted as a state with two quasi-hole at w_1 and w_2 of total charge e/m. Therefore, $\widetilde{\Psi}_{\mathrm{MR}}^{2\mathrm{q.h.}}(\boldsymbol{z})$ is an excitation of the Moore–Read state with two quasi-holes each of fractional charge $e/(2m)$.

Following the same idea as above, one can consider an excitation $\widetilde{\Psi}_{\mathrm{MR}}^{4\mathrm{q.h.}}(\boldsymbol{z})$ of the Moore–Read state consisting of four quasi-holes. This time we need a wave-function with four independent parameters w_1 till w_4 to locate the quasi-holes. A simple guess in this regard, splitting the quasi-holes into two parts in which the first and the second quasi-holes are grouped together and the third and the forth ones are grouped together, is the following:

$$\widetilde{\Psi}_{\mathrm{MR}}^{4\mathrm{q.h.}}(\boldsymbol{z}) = \mathrm{Pf}_{(12),(34)}(\boldsymbol{z})\prod_{i<j}(z_i - z_j)^m, \qquad (1.51)$$

where

$$\mathrm{Pf}_{(12),(34)}(\boldsymbol{z}) := \mathrm{Pf}\left(\frac{(z_i - w_1)(z_i - w_2)(z_j - w_3)(z_j - w_4) + (i \leftrightarrow j)}{z_i - z_j}\right).$$

Here $(i \leftrightarrow j)$ indicates the expression that is obtained by interchanging the indices i and j in the first term of the numerator. Apparently, there are two more states of this kind, namely, the one in which the quasi-holes are grouped as (13) and (24) and the one in which they are grouped as (14) and (23). However, it turns out that only two of these three states are indeed linearly independent. Therefore, the ground state corresponding to four quasi-holes is not not 3-fold degenerate but doubly degenerate. One can show that, for the general case of $2n$ quasi-holes, the ground state is 2^{n-1}-fold degenerate [NW96]. Hence, in general, if one starts from one of these degenerate states in the

corresponding 2^{n-1}-dimensional eigenspace and adiabatically follows a closed path in the configuration space of quasi-holes, one ends up with a state that still belongs to the the same eigenspace. Hence, the original and final states are related by a unitary transformation not just a simple phase. Quasi-hole excitations of the Moore–Read state are therefore non-Abelian anyons.

The Rank Saturation Conjecture

This chapter, which is based on [MG15], expands the main content of the first accompanied paper [GEA15]. This paper presents a new strategy toward a possible proof for a particular case of the rank saturation conjecture. The general statement of this conjecture is given in Section 2.1, but, in this thesis, we are only interested in a particular case of this conjecture in which the model state is the Laughlin state.

Sections 2.2 till 2.6 develop the mathematical tools necessary to formulate the rank saturation conjecture in a mathematical language and in terms of the properties of symmetric polynomials. These include the reduced density operator, Schmidt and weak-Schmidt decompositions, partition of non-negative integers, and finally a tiny part of the rich theory of symmetric polynomials. Based on what we gain in these sections, we state a theorem in Section 2.6 that is our main tool in writing the Laughlin state in a weak-Schmidt decomposed form. These notions are explained in more detail in [MG15]. For further studies in the theory of symmetric polynomials the reader is referred to [Mac95, Sta99].

Section 2.7 starts by delving more into the content of the rank saturation conjecture. It also mathematically formulates this conjecture, Eq. (2.35), for the special case of the Laughlin state Ψ_m, which we want to investigate in this thesis.

Section 2.8 is devoted to the problem of determining a possible way toward a weak-Schmidt decomposition of a generic Laughlin state Ψ_m corresponding to a FQH system that is subject to a bipartitioning scheme known as the *particle-cut*, explained in Section 2.1. In Section 2.8, to write the Laughlin state in a weak-Schmidt decomposed form, we do a mathematical trick and introduce a linear transformation, which we call the *clustering* transformation.

Finally, motivated by the results of Section 2.8, we study the properties of symmetric polynomials that vanish under the clustering transformation.

2.1 The Rank Saturation Conjecture, First Visit

As mentioned in the previous chapter, the physics of a system with topological order, like a FQH system, is very rich and it is important to study the non-local nature of these kind of systems. One way to probe systems with topological order is to partition the system into two subsystems in some way, and then

look at different properties of the reduced density operator corresponding to each part of the system [LW06, KP06]. In general, one can consider all the eigenvalues of the reduced density operator. In this thesis, however, we consider only the number of non-zero eigenvalues, that is, the *rank*, of the reduced density operator. In the FQH context, different ways of bipartitioning the total Hilbert space, namely, the *orbital-cut*, the *real-space-cut*, and the *particle-cut* have been proposed [ZHSR07, HZS07, LH08, DRR12, SCR⁺12, RSS12]. In this thesis, we focus on the particle-cut scheme in which one attaches numbers to N particles (electrons) in the system and declares the particles numbered 1 till N_A to belong to subsystem A and the remaining particles numbered $N_A + 1$ till N to belong to subsystem B.

In the context of fractional quantum Hall physics, it is conjectured that the rank of the reduced density operator for a model Hamiltonian describing the system is equal to the number of quasi-hole states. More precisely, for future reference, we formulate this conjecture as follows. The content of this conjecture is explained in more detail in Section 2.7.

Conjecture 2.1 (Rank Saturation Conjecture). *The rank of the reduced density operator corresponding to a particle-cut of a model state, such as a Laughlin or a Moore–Read state [MR91], is equal to the number of quasi-hole states in an appropriate number of flux quanta, that is, the number of ground states of the model Hamiltonian in an appropriate magnetic field.*

It is clear from Eq. (2.53) that the conjecture above is satisfied for the special case of the Laughlin state Ψ_1, with the filling factor equal to one. Numerical investigations, however, provide evidence that the above conjecture holds in general. Although we were not able to prove the above conjecture, we made progress in the case of the Laughlin states, which we explain briefly below. Detailed explanation in this regard is the subject of the next few sections.

We consider a FQH system in a pure Laughlin state $\Psi_m(z_1, \ldots, z_N)$, as the model state, and aim for determining the rank of the reduced density operator associated with a particle-cut of the system and then compare this rank with the number of independent quasi-hole wave-functions. The method pursued is to relate this conjecture, for the case of Laughlin state, to the properties of a few types of symmetric polynomials presented in Section 2.5, and then to use known results in this new context to determine the lowest total degree of the symmetric polynomials that vanish under some specific transformation referred to as the clustering transformation. Roughly speaking, this transformation, which is formally introduced in Section 2.7, partitions the variables of a symmetric polynomial into equally-sized parts and identifies the variables in each part. The main result needed from the theory of symmetric polynomials is Theorem 2.4 that enables us to decompose the double product $\prod_i \prod_j (1 + x_i y_j)$, in which the x and y variables are mixed, as a sum of terms where each term is a product of two symmetric polynomials, one of which depends only on x

variables and the other depends only on y variables. We then realize that, for a FQH system consisting of N electrons in a pure Laughlin state Ψ_m, Conjecture 2.1 is equivalent to the following conjecture, which is formulated in terms of the properties of a certain class of symmetric polynomials.

Conjecture 2.2. *There is no non-zero symmetric polynomial in mN variables with degree, in each variable, less than $N + 1$ that vanishes under the transformation that clusters the mN variables equally in m groups and identifies the variables in each group.*

The content of Conjecture 2.2 becomes clear during subsequent chapters.

For m greater than one, we were not able to find an analytic proof for the conjecture above, but we made progress. This observation led us to study the properties of symmetric polynomials, and in particular their properties under the clustering transformation. It turned out that proving Conjecture 2.2 is very hard and we did not succeed completely. However, we were able to prove that there are no non-zero symmetric polynomials in mN variables with *total degree* less than $N + 1$, that vanish under the clustering transformation. In addition, we determined a full characterization of the symmetric polynomials that vanish under this transformation.

2.2 Reduced Density Operator

Consider a composite system $\mathcal{S}$ that is composed of two subsystems A and B. If $\mathcal{H}$, $\mathcal{H}^A$, and $\mathcal{H}^B$ are Hilbert spaces corresponding to systems $\mathcal{S}$, A, and B, respectively, then one of the axioms of quantum mechanics asserts that $\mathcal{H} = \mathcal{H}^A \otimes \mathcal{H}^B$. In this chapter, it is assumed that $\mathcal{H}^A$ and $\mathcal{H}^B$, and, consequently, $\mathcal{H}$ are finite-dimensional Hilbert spaces.

Let the system $\mathcal{S}$ be described by a density operator ρ^{AB}. The *reduced density operator* ρ^A of subsystem A is defined by

$$\rho^A = \mathrm{tr}_B(\rho^{AB}), \tag{2.1}$$

where tr_B, called the *partial trace* over subsystem B, is a linear map that associates each linear map acting on $\mathcal{H}$ with a linear map acting on $\mathcal{H}^A$, according to the following rule:

$$\mathrm{tr}_B(|a_1\rangle\langle a_2| \otimes |b_1\rangle\langle b_2|) = |a_1\rangle\langle a_2| \, \mathrm{tr}(|b_1\rangle\langle b_2|). \tag{2.2}$$

Here $|a_1\rangle$ and $|a_2\rangle$ are two states in $\mathcal{H}^A$, and $|b_1\rangle$ and $|b_2\rangle$ are two states in $\mathcal{H}^B$. Note that Eq. (2.2) together with the linearity of tr_B suffice to know how tr_B acts on a generic Hermitian operator $A \otimes B$ that acts on $\mathcal{H}^A \otimes \mathcal{H}^B$. If $\mathcal{S}$ is in the pure state $|\Psi\rangle$, then Eq. (2.1) reduces to the following simple form:

$$\rho^A = \mathrm{tr}_B(|\Psi\rangle\langle\Psi|) \cdot \tag{2.3}$$

The reduced density operator ρ^B of subsystem B is defined similarly.

2.3   Schmidt and Weak-Schmidt Decompositions

Consider a composite system $\mathcal{S}$ composed of two subparts A and B. We know that, if $\left\{ |u_i\rangle \mid 1 \leqslant i \leqslant N_A \right\}$ is an orthonormal basis for the N_A-dimensional state space $\mathcal{H}^A$ of subsystem A and if $\left\{ |v_i\rangle \mid 1 \leqslant i \leqslant N_B \right\}$ is an orthonormal basis for the N_B-dimensional state space $\mathcal{H}^B$ of subsystem B, then the set

$$\left\{ |u_i\rangle \otimes |v_j\rangle \mid 1 \leqslant i \leqslant N_A \,,\, 1 \leqslant j \leqslant N_B \right\}, \tag{2.4}$$

is an orthonormal basis for the $(N_A N_B)$-dimensional state space $\mathcal{H}^A \otimes \mathcal{H}^B$ of the whole system $\mathcal{S}$. Therefore, if $|\Psi\rangle$ is a normalized pure state of the system $\mathcal{S}$, then,

$$|\Psi\rangle = \sum_{i=1}^{N_A} \sum_{j=1}^{N_B} c_{ij}\, u_i \otimes v_j, \tag{2.5}$$

for some complex numbers c_{ij} with $\sum_{i=1}^{N_A} \sum_{j=1}^{N_B} |c_{ij}|^2 = 1$. In other words, any pure state of the whole system $\mathcal{S}$ can be written as a *double* sum as is indicated in Eq. (2.5). However, the *Schmidt Decomposition* Theorem asserts that it is always possible to write $|\Psi\rangle$ as a *single* sum for an aptly chosen orthonormal subsets of the corresponding state spaces. More precisely, for a normalized pure state $|\Psi\rangle$ of the composite system $\mathcal{S}$, one can always find orthonormal states $\left\{ |\phi_i^A\rangle \right\}_i$ and $\left\{ |\phi_i^B\rangle \right\}_i$ in $\mathcal{H}^A$ and $\mathcal{H}^B$, respectively, such that

$$|\Psi\rangle = \sum_{i=1}^{r} \lambda_i\, |\phi_i^A\rangle \otimes |\phi_i^B\rangle, \tag{2.6}$$

where $r = \min\{N_A, N_B\}$ and λ_i's are non-negative real numbers such that $\sum_{i=1}^{r} \lambda_i^2 = 1$. The number of strictly positive λ_i's in (2.6) is called the *Schmidt number* of $|\Psi\rangle$. The interested reader can refer to [NC00] for a proof. One can also show that the rank of the reduced density operator of the subsystem with the Hilbert space of lower dimension is equal to the Schmidt number of $|\Psi\rangle$.

Schmidt's Theorem motivates Theorem 2.3, which we present here without proof. The proof can be found in [MG15]. This theorem asserts that if a pure state $|\Psi\rangle$ is decomposed as in (2.6), one can still conclude that the number r, that is, the number of summands in this sum, is the Schmidt number of $|\Psi\rangle$, even if, instead of being orthonormal, the states $\left\{ |\phi_i^A\rangle \right\}_i$ and $\left\{ |\phi_i^B\rangle \right\}_i$ are only known to be linearly independent in their corresponding Hilbert spaces. This theorem would be of interest in determining the desired rank in Section 2.8, *if*, of course, one can show that (2.49) is indeed a weak-Schmidt decomposition of the Laughlin state Ψ_m in the first place.

Theorem 2.3 (Weak-Schmidt Decomposition)**.** *Let $|\Psi\rangle$ be a normalized pure state of a composite system $\mathcal{S}$ composed of subsystems A and B with corresponding Hilbert spaces $\mathcal{H}^A$ and $\mathcal{H}^B$ of dimensions N_A and N_B, respectively.*

If the state $|\Psi\rangle$ has the following form:

$$|\Psi\rangle = \sum_{i=1}^{r} \xi_i |\varphi_i^A\rangle \otimes |\varphi_i^B\rangle, \tag{2.7}$$

where $r \leqslant \min\{N_A, N_B\}$, ξ_i's are non-zero numbers, and the following sets:

$$\{|\varphi_i^A\rangle \mid 1 \leqslant i \leqslant r\}, \quad \{|\varphi_i^B\rangle \mid 1 \leqslant i \leqslant r\}$$

are linearly independent subsets of $\mathcal{H}^A$ and $\mathcal{H}^B$, respectively, then the rank of the reduced density operators ρ^A and ρ^B is equal to r.

The sum in (2.7) is then called a weak-Schmidt decomposition of $|\Psi\rangle$.

2.4 Partitions of Non-Negative Integers

Let n be a positive integer. An infinite sequence

$$\boldsymbol{\lambda} = (\lambda_1, \ldots, \lambda_r, 0, 0, 0 \ldots), \tag{2.8}$$

consisting of positive integers λ_1 till λ_r together with infinite number of zeros at the end is said to be an *r-partition* of n, if

$$\lambda_1 \geqslant \cdots \geqslant \lambda_r, \tag{2.9}$$

and

$$\sum_{i=1}^{r} \lambda_i = n. \tag{2.10}$$

For simplicity in writing, one usually suppresses the infinite number of tail-zeros. Thus, the partition (2.8) is simply written as $\boldsymbol{\lambda} = (\lambda_1, \ldots, \lambda_r)$. For example, $(3, 1, 1, 0, 0, \ldots)$ is a partition of 5 that is usually written as $(3, 1, 1)$. We define that the infinite sequence $(0, 0, 0, \ldots)$ or, actually, the empty sequence $()$ after suppressing tail-zeros, is the only partition of zero. This partition is called the *empty* partition and it is denoted by $\emptyset$. In this thesis, although not a standard one, a partition is denoted by a bold Greek letter and its parts are denoted by the same non-bold letter and are subscripted by positive integers.

To indicate that $\boldsymbol{\lambda}$ is a partition of n, one writes $\boldsymbol{\lambda} \vdash n$. The number n is referred to as the *weight* of $\boldsymbol{\lambda}$ and it is denoted by $|\boldsymbol{\lambda}|$, so $|\emptyset| = 0$. Each (non-zero) λ_i is called a *part* of $\boldsymbol{\lambda}$. The number of parts of $\boldsymbol{\lambda}$ is defined to be its *length* and it is denoted by $l(\boldsymbol{\lambda})$, so $l(\emptyset) = 0$. The set of all partitions of n is denoted by $\mathrm{Par}(n)$. For instance,

$$\mathrm{Par}(5) = \{(5), (4, 1), (3, 2), (2, 2, 1), (2, 1, 1, 1), (1, 1, 1, 1, 1)\}. \tag{2.11}$$

The set of all partitions is denoted by $\mathscr{P}$ and it is defined by

$$\mathscr{P} = \bigcup_{n \geqslant 0} \mathrm{Par}(n). \tag{2.12}$$

The *multiplicity* of a positive integer i in a partition $\boldsymbol{\lambda}$ is denoted by $m_i(\boldsymbol{\lambda})$ or, when the partition $\boldsymbol{\lambda}$ is clear from the context, briefly by m_i and it is defined to be the the number of parts of $\boldsymbol{\lambda}$ that are equal to i. In other words,

$$m_i(\boldsymbol{\lambda}) = \mathrm{Card}\{\, j \mid \lambda_j = i \,\}, \tag{2.13}$$

where "Card" refers to the cardinality or the number of elements of a set. This provides still another useful notation for a partition. Using the notion of multiplicity, any partition $\boldsymbol{\lambda}$ can be written as

$$\boldsymbol{\lambda} = (1^{m_1} 2^{m_2} 3^{m_3} \cdots), \tag{2.14}$$

where i^{m_i}, for any $i \geqslant 1$, means that there are exactly m_i parts in $\boldsymbol{\lambda}$ that are equal to i. In this notation

$$\sum_{i \geqslant 1} i m_i = |\boldsymbol{\lambda}|. \tag{2.15}$$

For example, $\boldsymbol{\lambda} = (1^2 2^0 3^4 4^0 5^0 \cdots)$ is the partition $(3,3,3,3,1,1)$ of 14, which is usually written briefly as $\boldsymbol{\lambda} = (1^2 3^4)$.

To make working with partitions easier, one can associate a graphical representation with a partition in some way. For example, the gray squares in Fig. 2.1 represents the partition $\boldsymbol{\lambda} = (8,6,3,3,1)$.

The *complement* of a partition $\boldsymbol{\lambda}$ with respect to a rectangle of height n and width d, which we denote by $\bar{\boldsymbol{\lambda}}$, is defined as

$$\bar{\boldsymbol{\lambda}} = (d - \lambda_n, d - \lambda_{n-1}, \dots, d - \lambda_1). \tag{2.16}$$

For example, the complement of $\boldsymbol{\lambda} = (8,6,3,3,1)$ with respect to the rectangle shown in Fig. 2.1 is $\bar{\boldsymbol{\lambda}} = (10,9,7,7,4,2)$. It is clear that $l(\bar{\boldsymbol{\lambda}}) \leqslant n$ and $\bar{\lambda}_1 \leqslant d$.

Of particular interest in this thesis is the number of partitions with at most n parts such that each part is at most d. As is explained shortly, this number is equal to $\binom{n+d}{n}$ and, hence,

$$\mathrm{Card}\left\{\, \boldsymbol{\lambda} \in \mathscr{P} \mid \lambda_1 \leqslant d \,, l(\boldsymbol{\lambda}) \leqslant n \,\right\} = \binom{n+d}{n}. \tag{2.17}$$

One way to see this it to establish a one-to-one correspondence between the set of partitions that fit into a rectangle of height n and width d, and the set of polygon-lines consisting of n vertical (V) and d horizontal (H) segments, as is shown in Fig. 2.1 for a special case of $n = 6$ and $d = 10$. Therefore, one can count the number of these polygon-lines instead of counting the number of
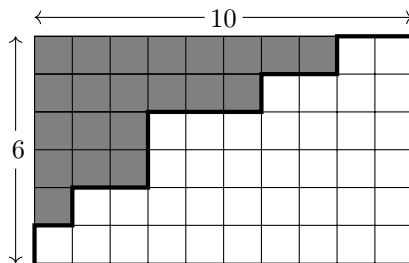
Figure 2.1: Gray squares represent $\boldsymbol{\lambda} = (8, 6, 3, 3, 1)$ and white squares represent $\bar{\boldsymbol{\lambda}} = (10, 9, 7, 7, 4, 2)$.

desired partitions. It is clear that each such polygon-line consists of n vertical and d horizontal segments. Consequently, the number of these polygon-lines is equal to the number of permutations of a string of letters consisting of n letters of V and d letters of H, which is $\binom{n+d}{n}$ by a simple combinatorial argument.

2.5 Symmetric Polynomials

A polynomial $s(x_1, \ldots, x_n)$ is said to be *symmetric* if interchanging any pair of its variables does not change the polynomial. For example, the polynomial

$$s(x_1, x_2, x_3) = x_1^2 x_2 + x_1 x_2^2 + x_2^2 x_3 + x_2 x_3^2 + x_3^2 x_1 + x_1 x_3^2, \qquad (2.18)$$

is a symmetric polynomial in three variables.

In this thesis, the highest exponent of anyone of the variables in a symmetric polynomial is referred to as the *degree* of the polynomial[§]. For instance, although the polynomial (2.18) is of total degree three, it is of degree two. The set of all symmetric polynomials in n variables x_1 till x_n is dentoed by $\Lambda_n[x_1, \ldots, x_n]$ and the set of all symmetric polynomials in these variables of degree at most m is denoted by $\Lambda_n^m[x_1, \ldots, x_n]$. If the variables are clear from the context, the mentioned sets are simply denoted by Λ_n and Λ_n^m.

2.5.1 Monomial Symmetric Polynomials

The *monomial* symmetric polynomial $m_{\boldsymbol{\lambda}}(x_1, \ldots, x_n)$, for a given partition $\boldsymbol{\lambda} = (\lambda_1, \ldots, \lambda_r)$, is defined to be the constant polynomial 1, if $\boldsymbol{\lambda} = \emptyset$; the zero polynomial, if $r > n$; and it is defined by

$$m_{\boldsymbol{\lambda}}(x_1, x_2, \ldots, x_n) = \text{Sym}(x_1^{\lambda_1} x_2^{\lambda_2} \cdots x_r^{\lambda_r} x_{r+1}^0 \cdots x_n^0), \qquad (2.19)$$

[§]This is not the same as in the mathematics literatures.

otherwise, where Sym stands for the symmetrization operation. For example,

$$m_{(2,1,1)}(x_1, x_2, x_3) = x_1^2 x_2 x_3 + x_1 x_2^2 x_3 + x_1 x_2 x_3^2,$$
$$m_{(2,1)}(x_1, x_2, x_3) = x_1^2 x_2 + x_1 x_2^2 + x_1^2 x_3 + x_1 x_3^2 + x_2^2 x_3 + x_2 x_3^2,$$
$$m_{(2,1,1)}(x_1, x_2) = 0.$$

The important property of these monomials for our purpose is that the set

$$\left\{ m_{\boldsymbol{\lambda}}(x_1, \ldots, x_n) \mid \lambda_1 \leqslant m \,,\, l(\boldsymbol{\lambda}) \leqslant n \right\}, \tag{2.20}$$

forms a basis for Λ_n^m and, therefore,

$$\dim \left(\Lambda_n^m \right) = \binom{m+n}{n}. \tag{2.21}$$

2.5.2 Elementary Symmetric Polynomials

Given a partition $\boldsymbol{\lambda}$, the *elementary symmetric* function corresponding to $\boldsymbol{\lambda}$ is denoted by $e_{\boldsymbol{\lambda}}$ and it is defined by

$$e_{\boldsymbol{\lambda}} = e_{\lambda_1} e_{\lambda_2} e_{\lambda_3} \cdots, \tag{2.22}$$

where,

$$e_0 := 1, \tag{2.23}$$

and, for any positive integer r, the rth elementary symmetric function e_r is defined by

$$e_r = \sum_{i_1 < \cdots < i_n} x_{i_1} \cdots x_{i_n}. \tag{2.24}$$

For instance, we have

$$e_1(x_1, x_2, x_3) = x_1 + x_2 + x_3,$$
$$e_2(x_1, x_2, x_3) = x_1 x_2 + x_2 x_3 + x_3 x_1,$$
$$e_3(x_1, x_2, x_3) = x_1 x_2 x_3,$$
$$e_n(x_1, x_2, x_3) = 0,$$

and

$$e_{(2,1,1)}(x_1, x_2) = e_2(x_1, x_2) e_1(x_1, x_2) e_1(x_1, x_2)$$
$$= x_1 x_2 (x_1 + x_2)^2.$$

It is easily seen that the total degree of $e_{\boldsymbol{\lambda}}$ is $|\boldsymbol{\lambda}|$ and its degree is $l(\boldsymbol{\lambda})$.

It is shown, for example, in [Sta99] that the set

$$\left\{ e_{\boldsymbol{\lambda}}(x_1, \ldots, x_n) \mid \lambda_1 \leqslant n \,,\, l(\boldsymbol{\lambda}) \leqslant m \right\}, \tag{2.25}$$

is a basis for Λ_n^m.

2.5.3   Power-Sum Symmetric Polynomials

Let $\boldsymbol{\lambda}$ be a partition. The *power-sum symmetric* polynomial corresponding to $\boldsymbol{\lambda}$ is denoted by $p_{\boldsymbol{\lambda}}$ and it is defined by

$$p_{\boldsymbol{\lambda}} = p_{\lambda_1} p_{\lambda_2} \cdots, \tag{2.26}$$

where,

$$p_0 := n, \tag{2.27}$$

and, for any positive integer r, the rth power-sum symmetric function p_r is defined by

$$p_r = \sum_{i \geqslant 1} x_i^r. \tag{2.28}$$

The total degree and the degree of $p_{\boldsymbol{\lambda}}$ are both equal to $|\boldsymbol{\lambda}|$.

2.6   The Main Tool to Decompose the Laughlin State

In this section, without proof, we state the theorem that is used in the next chapter to decompose the Laughlin state Ψ_m as sum of a number of terms in which each term is a product of a symmetric polynomial depending only on one group of variables with a symmetric polynomial depending only on another group of variables. The proof is given in [Mac95, Sta99, MG15].

Theorem 2.4. *For a finite number of variables x_1 till x_n and y_1 till y_m, we have the following identities:*

$$\prod_{i=1}^{n} \prod_{j=1}^{m} (1 + x_i y_j) = \sum_{\boldsymbol{\lambda}} m_{\boldsymbol{\lambda}}(x_1, \ldots, x_n) e_{\boldsymbol{\lambda}}(y_1, \ldots, y_m), \tag{2.29}$$

$$= \sum_{\boldsymbol{\lambda}} e_{\boldsymbol{\lambda}}(x_1, \ldots, x_n) m_{\boldsymbol{\lambda}}(y_1, \ldots, y_m), \tag{2.30}$$

where the sum in Eq. (2.29) is over all partitions $\boldsymbol{\lambda}$ for which $l(\boldsymbol{\lambda}) \leqslant n$ and $\lambda_1 \leqslant m$, and the sum in Eq. (2.30) is over all partitions $\boldsymbol{\lambda}$ for which $l(\boldsymbol{\lambda}) \leqslant m$ and $\lambda_1 \leqslant n$.

Note that the number of summands on the right hand sides of each one of the above identities is $\binom{m+n}{m}$.

2.7   The Rank Saturation Conjecture, Second Visit

In this section, we first expand the content of the rank saturation conjecture stated in Section 2.1 in more detail. We then, considering the Laughlin state as the model state, determine the number of quasi-hole states and mathematically formulate the conjecture for this special case.

Consider a FQH system consisting of a number of electrons that is described by a model state like a Laughlin or a Moore–Read state at a generic filling factor. As mentioned in Chapter 1, these model states are exact ground states of some model Hamiltonians. Any ground state of the corresponding model Hamiltonian is called a *quasi-hole state*. It was also mentioned in Chapter 1 that, for the special case of the Laughlin state, quasi-hole states are suitable trial wave-functions that describe the system $\mathcal{S}$ with some number of flux quanta added locally to the system. These states are usually referred to as quasi-hole excitations of the corresponding model state. In this context, the model state itself can be regarded as a quasi-hole state corresponding to zero number of additional flux quanta or quasi-holes. The number of quasi-hole states #q.h.(N, N_Φ) for a FQH system with N number of electrons and N_Φ number of additional flux quanta can often be obtained exactly [RR96, GR00, ARRS01, Ard02, Rea06].

Suppose now that $\mathcal{S}$ is a FQH system consisting of N electrons, described by a model state at filling factor ν, and subject to a particle-cut that divides $\mathcal{S}$ into two subsystems A and B with N_A and N_B number of electrons, respectively, such that $N_A \leqslant N_B$, and let $\mathcal{R}_\nu^A(N_A, N_B)$ denote the rank of the reduced density operator ρ^A. The rank saturation conjecture then claims that

$$\mathcal{R}_\nu^A(N_A, N_B) = \#\text{q.h.}(N_A, \nu^{-1}N_B). \tag{2.31}$$

Let us now consider the special case of the Laughlin state Ψ_m at the filling factor $\nu = 1/m$, which is of interest in this thesis, and determine the right hand side of the Eq. (2.31). Consider a FQH system consisting of N_A number of electrons and $\nu^{-1}N_B = mN_B$ number of flux quanta located at unspecified points with complex coordinates w_1 till w_{mN_B}. It turns out that the ground state $\Psi_m^{\text{q.h.}}$ of the corresponding model Hamiltonian takes the following form:

$$\Psi_m^{\text{q.h.}}(z_1, \ldots, z_{N_A}) = \Psi_m(z_1, \ldots, z_{N_A})P_{\boldsymbol{w}}(z_1, \ldots, z_{N_A}), \tag{2.32}$$

where Ψ_m is the Laughlin wave-function at filling factor $1/m$ and $P_{\boldsymbol{w}}$, with $\boldsymbol{w} = (w_1, \ldots, w_{mN_B})$ being the coordinates of the added flux quanta, is a symmetric polynomial in z variables. On the other hand, the degree of Ψ_m is $m(N_A-1)$ and the degree of $\Psi_m^{\text{q.h.}}$ is $m(N_A-1)+mN_B$. Thus $P_{\boldsymbol{w}}$ is a symmetric polynomial in N_A variables and the degree at most mN_B and, therefore, $P_{\boldsymbol{w}}$ belongs to $\Lambda_{N_A}^{mN_B}$. Therefore, by Eq. (2.21), for the special case that the system $\mathcal{S}$ is described by the Laughlin state Ψ_m, we have

$$\#\text{q.h.}(N_A, \nu^{-1}N_B) = l_m, \tag{2.33}$$

where

$$l_m := \binom{N_A + mN_B}{N_A}. \tag{2.34}$$

Therefore, the rank saturation conjecture, when Laughlin state Ψ_m is considered as the model state, reads simply as follows:

$$\mathcal{R}^A_{1/m}(N_A, N_B) = l_m. \tag{2.35}$$

In the next section, we explain our strategy toward a possible proof of this relation.

2.8 Toward a Possible Proof of $\mathcal{R}^A_{1/m}(N_A, N_B) = l_m$

Consider a FQH system $\mathcal{S}$ consisting of N electrons with coordinates z_1 till z_N in a pure state that can be modeled by the following Laughlin state:

$$\Psi_m(z_1, \ldots, z_N) = \prod_{1 \leqslant i < j \leqslant N} (z_i - z_j)^m \, \exp\left(-\frac{1}{4l_B^2} \sum_{k=1}^{N} |z_k|^2 \right), \tag{2.36}$$

at filling factor $\nu = 1/m$, with m an odd integer. As mentioned in Section 2.1, one way to probe the properties of $\mathcal{S}$ is to look at the rank of the reduced density operator corresponding to a particle-cut associated with $\mathcal{S}$. Consider the particle-cut in which we declare the electrons numbered 1 till N_A to constitute subsystem A and electrons numbered $N_A + 1$ till N to constitute subsystem B. Note that, in what follows, x_j and y_j are complex numbers and they are no longer used as the real and imaginary part of z_j. Here $N_B = N - N_A$ is the number of electrons in subsystem B and, without the loss of generality, one can assume that $N_A \leqslant N_B$. Let x_1 till x_{N_A} indicate the coordinates of particles in A and y_1 till y_{N_B} indicate the coordinates of particles in B. One should note that $\mathcal{H}^A$ is the space of all physically acceptable totally anti-symmetric functions in variables x_1 till x_{N_A} and $\mathcal{H}^B$ is the space of all physically acceptable totally anti-symmetric functions in variables y_1 till y_{N_B}. The goal is to determine the rank of the reduced density operator ρ^A corresponding to the pure state $\Psi_m(z_1, \ldots, z_N)$. To this end, according to Theorem 2.3, it suffices to find a weak-Schmidt decomposition of $\Psi_m(z_1, \ldots, z_N)$ and count the number of summands in that decomposition. Letting $\boldsymbol{x} = (x_1, \ldots, x_{N_A})$, $\boldsymbol{y} = (y_1, \ldots, y_{N_B})$, and $\boldsymbol{z} = (z_1, \ldots, z_N)$, Ψ_m in (2.36) can be written as

$$\Psi_m(\boldsymbol{z}) = F_m(\boldsymbol{x})\Phi_m(\boldsymbol{x}, \boldsymbol{y})G_m(\boldsymbol{y}), \tag{2.37}$$

where

$$\Phi_m(\boldsymbol{x}, \boldsymbol{y}) := \prod_{i=1}^{N_A} \prod_{j=1}^{N_B} (x_i - y_j)^m, \tag{2.38}$$

and

$$
F_m(\boldsymbol{x}) := \prod_{i_1 < i_2} (x_{i_1} - x_{i_2})^m \, \exp\Big(-\frac{1}{4l_B^2}\sum_{k=1}^{N_A}|x_k|^2\Big),
$$

$$
G_m(\boldsymbol{y}) := \prod_{j_1 < j_2} (y_{j_1} - y_{j_2})^m \, \exp\Big(-\frac{1}{4l_B^2}\sum_{k=1}^{N_B}|y_k|^2\Big).
$$
(2.39)

We now define the clustering transformation $\mathcal{C}_m$ from Λ_{mN_B} to Λ_{N_B} such that, for any symmetric polynomial s with mN_B variables in Λ_{mN_B},

$$
\mathcal{C}_m(s) = t,
$$
(2.40)

where t is a polynomial with N_B variables in Λ_{N_B} such that

$$
t(y_1, y_2 \ldots, y_{N_B}) = s(\underbrace{y_1, \ldots, y_1}_{m}, \underbrace{y_2, \ldots, y_2}_{m}, \ldots, \underbrace{y_{N_B}, \ldots, y_{N_B}}_{m}).
$$
(2.41)

It is straightforward to see that, if $\boldsymbol{w} = (w_1, \ldots, w_{mN_B})$, the effect of $\mathcal{C}_m$ on

$$
\Omega(\boldsymbol{x}, \boldsymbol{w}) := \prod_{i=1}^{N_A} \prod_{j=1}^{mN_B} (x_i - w_j),
$$
(2.42)

considered as a symmetric polynomial in Λ_{mN_B} with w variables, is as follows:

$$
\mathcal{C}_m(\Omega)(\boldsymbol{x}, \boldsymbol{w}) = \Phi_m(\boldsymbol{x}, \boldsymbol{y}).
$$
(2.43)

Pulling the x variables out on the right hand side of (2.42) yields

$$
\Omega(\boldsymbol{x}, \boldsymbol{w}) = \Big[\prod_{i=1}^{N_A} x_i^{mN_B}\Big]\Big[\prod_{i=1}^{N_A}\prod_{j=1}^{mN_B}\Big(1 - \frac{1}{x_i}\,w_j\Big)\Big],
$$
(2.44)

or, equivalently, by the first identity in Theorem 2.4, we get

$$
\Omega(\boldsymbol{x}, \boldsymbol{w}) = \Big[\prod_{i=1}^{N_A} x_i^{mN_B}\Big] \sum_{\boldsymbol{\lambda}} m_{\boldsymbol{\lambda}}(-1/\boldsymbol{x})e_{\boldsymbol{\lambda}}(\boldsymbol{w}),
$$
(2.45)

where $(-1/\boldsymbol{x})$ is a shorthand for $(-1/x_1, \ldots, -1/x_{N_A})$. In addition, again by Theorem 2.4, the sum in (2.45) is over all partitions that fit into a rectangle of height N_A and width mN_B. Hence, according to (2.17), this sum consists of l_m number of terms, where l_m is given in (2.34). It is straightforward to check that

$$
\Big[\prod_{i=1}^{N_A} x_i^{mN_B}\Big] m_{\boldsymbol{\lambda}}(-1/\boldsymbol{x}) = (-1)^{|\boldsymbol{\lambda}|} m_{\bar{\boldsymbol{\lambda}}}(\boldsymbol{x}),
$$
(2.46)

where $\bar{\boldsymbol{\lambda}}$, defined in (2.16), is the complement of $\boldsymbol{\lambda}$ with respect to the rectangle of height N_A and width mN_B. Hence, (2.44) reduces to

$$\Omega(\boldsymbol{x}, \boldsymbol{w}) = \sum_{\boldsymbol{\lambda}} (-1)^{|\boldsymbol{\lambda}|} m_{\bar{\boldsymbol{\lambda}}}(\boldsymbol{x}) e_{\boldsymbol{\lambda}}(\boldsymbol{w}), \tag{2.47}$$

with l_m number of summands on the right hand side. Acting $\mathcal{C}_m$ on both sides of (2.47) and considering (2.43), one gets

$$\Phi_m(\boldsymbol{x}, \boldsymbol{y}) = \sum_{\boldsymbol{\lambda}} (-1)^{|\boldsymbol{\lambda}|} m_{\bar{\boldsymbol{\lambda}}}(\boldsymbol{x}) \mathcal{C}_m(e_{\boldsymbol{\lambda}})(\boldsymbol{y}). \tag{2.48}$$

Finally, substituting the above relation for Φ_m back into (2.37), yields

$$\Psi_m(\boldsymbol{z}) = \sum_{\boldsymbol{\lambda}} \big(F_m(\boldsymbol{x})(-1)^{|\boldsymbol{\lambda}|} m_{\bar{\boldsymbol{\lambda}}}(\boldsymbol{x})\big)\big(\mathcal{C}_m(e_{\boldsymbol{\lambda}})(\boldsymbol{y}) G_m(\boldsymbol{y})\big), \tag{2.49}$$

where the sum runs through l_m number of partitions $\boldsymbol{\lambda}$. Note at this stage that, if one could show (2.49) is indeed a weak-Schmidt decomposition of $\Psi_m(\boldsymbol{z})$, then Theorem 2.3 implies Eq. (2.35) and, as desired, the rank saturation conjecture for the special case of the Laughlin state is proven. To prove that Eq. (2.49) provides a weak-Schmidt decomposition for $\Psi_m(\boldsymbol{z})$, one only needs to show that the set

$$\big\{\mathcal{C}_m(e_{\boldsymbol{\lambda}}) \mid \lambda_1 \leqslant mN_B\,,\, l(\boldsymbol{\lambda}) \leqslant N_A\big\}, \tag{2.50}$$

forms a linearly independent subset of Λ_{N_B}. Note that, since the symmetric monomials form a basis, the set $\big\{(-1)^{|\boldsymbol{\lambda}|} F_m m_{\bar{\boldsymbol{\lambda}}}\big\}_{\boldsymbol{\lambda}}$ is already linearly independent. On the other hand the set

$$\big\{e_{\boldsymbol{\lambda}}(w_1, \ldots, w_{mN_B}) \mid \lambda_1 \leqslant mN_B\,,\, l(\boldsymbol{\lambda}) \leqslant N_A\big\}, \tag{2.51}$$

is linearly independent, since, as we saw in (2.25), this set forms a basis for $\Lambda^{N_A}_{mN_B}$. Hence, if one could show that the restriction of $\mathcal{C}_m$ to $\Lambda^{N_A}_{mN_B}$, which is a linear map to $\Lambda^{mN_A}_{N_B}$, is injective as long as $N_A \leqslant N_B$, it proves that the set (2.50) is linearly independent, since injective linear maps respect linear independence of vectors. Moreover, a linear map is injective if and only if its kernel is trivial. Thus, one needs to show that, besides the zero polynomial, no symmetric polynomial in mN_B variables and maximum degree N_A vanish under $\mathcal{C}_m$. This is in fact the content of Conjecture 2.2 that motivates the study of the class of symmetric polynomials that vanish under $\mathcal{C}_m$ and is discussed in Section 2.9.

Before ending this section, to have a signal indicating that we are actually on a right track, it would be instructive to check two points. Firstly, we present a proof of Eq. (2.35), along the lines described above, for the special case where $m = 1$. Secondly, we show that l_m in (2.34) is an upper bound for the rank of

the reduced density operator for the Laughlin state (2.36), when the system is subject to a particle-cut as described earlier.

For the first point, note that the clustering transformation $\mathcal{C}_1$, corresponding to $m = 1$, is just the identity map on Λ_{N_B} and, therefore, the set (2.50) reduces to the following set:

$$\left\{ e_{\boldsymbol{\lambda}}(y_1, \ldots, y_{N_B}) \mid \lambda_1 \leqslant N_B \,,\, l(\boldsymbol{\lambda}) \leqslant N_A \right\}. \tag{2.52}$$

Comparing the set above with the set given in (2.25), one realizes that the set in (2.52) forms a basis for $\Lambda_{N_B}^{N_A}$ and, consequently, it is linearly independent. Thus, the rank of the reduced density operator in this simple case is, by (2.21), equal to

$$\binom{N_A + N_B}{N_A} = l_1. \tag{2.53}$$

For the second point, consider a Schmidt decomposition of $\Psi_m(\boldsymbol{z})$ as follows[§]:

$$\Psi_m(\boldsymbol{z}) = \sum_{i=1}^{r} \lambda_i \, \phi_i^A(\boldsymbol{x}) \phi_i^A(\boldsymbol{y}). \tag{2.54}$$

Since $\Psi_m(\boldsymbol{z})$ vanishes as mth power when two variables coincide, this implies that $\phi_i^A(\boldsymbol{x})$ vanishes as mth power when two x coordinates coincide. Therefore,

$$\phi_i^A(\boldsymbol{x}) = P_i^A(\boldsymbol{x}) \prod_{1 \leqslant i < j \leqslant N_A} (x_i - x_j)^m, \tag{2.55}$$

where $P_i^A(\boldsymbol{x})$ is a symmetric polynomial in N_A variables of some degree d. Since the degree of the symmetric polynomial expressed as a product on the right hand side of (2.55) is $m(N_A - 1)$ and the degree of Ψ_m is $m(N - 1)$, one should have $d + m(N_A - 1) \leqslant m(N - 1)$ or, equivalently, $d \leqslant mN_B$. Hence, the polynomials $P_i^A(\boldsymbol{x})$ belongs to $\Lambda_{N_A}^{mN_B}$ and, by (2.21), the number of linearly independent such polynomials is at most l_m. Consequently, the number of linearly independent $\phi_i^A(\boldsymbol{x})$'s, which is an upper bound for the rank of the reduced density operator of Ψ_m, is also at most l_m.

One should note that if one could prove Conjecture 2.2, this would then mean that the rank of the reduced density operator of a FQH system modeled by the Laughlin state and subject to a particle-cut always reaches this upper bound. In other words the rank of the reduced density operator is "saturated".

2.9   New Generating Set for Λ_{mN}

In this section, motivated by the results of the previous section regarding symmetric polynomials that vanish under the clustering transformation introduced

---

[§]In the rest of this section, the exponential term of the Laughlin wave-function has no effect and it is suppressed.

in (2.40) and (2.41), we probe some characteristic features of these kind of symmetric polynomials. In this section, however, we suppress the subscript B and simply write N instead of N_B. Moreover, in what follows, we assume that m and N are given positive integers.

From all algebraically independent sets of generators introduced for Λ_{mN} in Section 2.5, only the elements of the set $\{p_1, \ldots, p_{mN}\}$, consisting of power-sum symmetric polynomials p_i, have a simple behavior under $\mathcal{C}_m$, namely,

$$\mathcal{C}_m(p_i)(w_1, \ldots, w_{mN}) = m\, p_i(y_1, \ldots, y_N). \tag{2.56}$$

Despite this simple behavior, in order to describe the property of the polynomials in Λ_{mN} that vanish when acted on by $\mathcal{C}_m$, these polynomials are not convenient to work with. Therefore, we construct a new set of generators for Λ_{mN} that are suitable in this regard. The strategy is to introduce a family of polynomials in Λ_{mN} depending on a single real parameter, and show that any member of this family, corresponding to a non-zero value of the parameter, constitutes an algebraically independent generating set for Λ_{mN}.

Let x be a real parameter and let n be a non-negative integer. The polynomial $r_n^{(x)}$ in Λ_{mN} is defined, in terms of power-sum symmetric polynomials, by

$$r_n^{(x)} = n! \sum_{\boldsymbol{\lambda} \vdash n} (-x)^{l(\boldsymbol{\lambda})} \frac{p_{\boldsymbol{\lambda}}}{z_{\boldsymbol{\lambda}}}, \tag{2.57}$$

where

$$z_{\boldsymbol{\lambda}} := \prod_{i \geqslant 1} i^{m_i(\boldsymbol{\lambda})}\, m_j(\boldsymbol{\lambda})!, \tag{2.58}$$

and $m_i(\boldsymbol{\lambda})$ is the multiplicity defined in (2.13). It is clear that $r_n^{(x)}$ is a symmetric polynomial of total degree n. It is shown in [MG15] that the degree of this polynomial is also n. The first five of these polynomials are listed below:

$$
\begin{aligned}
r_0^{(x)} &= 1, \\
r_1^{(x)} &= -xp_1, \\
r_2^{(x)} &= x^2 p_1^2 - xp_2, \\
r_3^{(x)} &= -x^3 p_1^3 + 3x^2 p_1 p_2 - 2xp_3, \\
r_4^{(x)} &= x^4 p_1^4 - 6x^3 p_1^2 p_2 + 3x^2 p_2^2 + 8x^2 p_1 p_3 - 6xp_4.
\end{aligned}
\tag{2.59}
$$

From Eq. (2.57), it is clear that for a given positive integer n, the term corresponding to $\boldsymbol{\lambda} = (n)$ in $r_n^{(x)}$ is the product of a monomial in x with p_n. Therefore, iterative computation shows that, for a non-zero value of the parameter x and any positive integer n, the power-sum p_n can be written as a polynomial in $r_1^{(x)}$ till $r_n^{(x)}$ with functions of x as coefficients. Thus, since $\{p_1, \ldots, p_{mN}\}$ is an algebraically independent generating set for Λ_{mN}, so does $\{r_1^{(x)}, \ldots, r_{mN}^{(x)}\}$, for any non-zero x. Therefore we proved the following lemma:

Lemma 2.5. *The set $\left\{r_1^{(x)}, \ldots, r_{mN}^{(x)}\right\}$, for any non-zero value of the parameter x, forms an algebraically independent generating set for Λ_{mN}.*

The key property of the polynomials $r_n^{(x)}$ is that they behave nicely under the action of $\mathcal{C}_m$, namely,

$$\mathcal{C}_m\left(r_n^{(x)}\right) = r_n^{(mx)}. \tag{2.60}$$

This is readily seen by applying $\mathcal{C}_m$ on both sides of Eq. (2.57) and using

$$\mathcal{C}_m(p_{\boldsymbol{\lambda}}) = m^{l(\boldsymbol{\lambda})} p_{\boldsymbol{\lambda}}, \tag{2.61}$$

which, in turn, is a consequence of Equation (2.56).

For a non-negative integer n, we now define the nth *modified power-sum symmetric polynomial* $\widetilde{p}_n$, as an element in Λ_{mN}, by

$$\widetilde{p}_n = \frac{(-1)^n}{n!} r_n^{(1/m)}. \tag{2.62}$$

The total degree of $\widetilde{p}_n$ is n and, by Lemma 2.5, the set $\left\{\widetilde{p}_1, \ldots, \widetilde{p}_{mN}\right\}$ is an algebraically independent generating set for Λ_{mN}. Actually, these polynomials are engineered to enjoy the following property:

$$\mathcal{C}_m(\widetilde{p}_n) = e_n, \tag{2.63}$$

where e_n is the nth symmetric polynomial defined in (2.24). Eq. (2.63) can be obtained by applying $\mathcal{C}_m$ on both sides of Eq. (2.62), using Eq. (2.60), and the fact that $r_n^{(1)} = (-1)^n n! e_n$. The proof of the latter can be found in [MG15]. We remind the reader that $\widetilde{p}_n$ in Eq. (2.63) contains mN variables, while e_n in that equation contains N variables. Hence, we have the following lemma:

Lemma 2.6. *The set $\mathcal{G} = \left\{\widetilde{p}_1, \ldots, \widetilde{p}_{mN}\right\}$ is an algebraically independent generating set for Λ_{mN} and $\mathcal{C}_m(\widetilde{p}_n) = e_n$, for all integers n with $1 \leqslant n \leqslant mN$.*

Based on the fact that, for $n > N$, $e_n = 0$ and what Lemma 2.6 teaches us, we conclude the following statement:

Corollary 2.7. *For any integer n with $N + 1 \leqslant n \leqslant mN$, $\mathcal{C}_m(\widetilde{p}_n) = 0$.*

The polynomials $\widetilde{p}_n$ have the exact right property that enables us to prove the following theorem:

Theorem 2.8. *A non-zero symmetric polynomial in Λ_{mN} vanishes under $\mathcal{C}_m$ if and only if, when expressed as a polynomial in $\widetilde{p}_1$ till $\widetilde{p}_{mN}$, each monomial term contains some power of at least one of the polynomials $\widetilde{p}_{N+1}$ till $\widetilde{p}_{mN}$.*

Proof. First, Let s be a symmetric polynomial in Λ_{mN} such that $\mathcal{C}_m(s) = 0$. By Lemma 2.5, there exists a polynomial r in mN variables such that

$$s(w_1, \ldots, w_{mN}) = r(\widetilde{p}_1, \ldots, \widetilde{p}_{mN}). \tag{2.64}$$

In general, there are two kinds of monomials on the right hand side of the equation above: those that do contain some power of at least one of the polynomials $\widetilde{p}_{N+1}$ till $\widetilde{p}_{mN}$, and those that don't. Thus, $s(w_1, \ldots, w_{mN})$ can be decomposed uniquely into two parts as follows:

$$s(w_1, \ldots, w_{mN}) = a(\widetilde{p}_1, \ldots, \widetilde{p}_N) + b(\widetilde{p}_1, \ldots, \widetilde{p}_{mN}). \tag{2.65}$$

Here $a(\widetilde{p}_1, \ldots, \widetilde{p}_N)$ consists of the monomials on the right side of Eq. (2.64) that do not depend on any of the polynomials $\widetilde{p}_{N+1}$ till $\widetilde{p}_{mN}$, and $b(\widetilde{p}_1, \ldots, \widetilde{p}_{mN})$ consists of the rest. Based on its construction and Corollary 2.7, $b(\widetilde{p}_1, \ldots, \widetilde{p}_{mN})$ vanishes under $\mathcal{C}_m$.

Applying $\mathcal{C}_m$ on both sides of (2.65) and using (2.63) yields:

$$\mathcal{C}_m(s)(y_1, \ldots, y_N) = a(e_1, \ldots, e_N), \tag{2.66}$$

and, therefore, $a(e_1, \ldots, e_N)$ vanishes. We know that the set $\{e_1, \ldots, e_N\}$, whose elements are considered as polynomials in Λ_N, are algebraically independent. Therefore, a is the zero polynomial and, by (2.65), we have:

$$s(w_1, \ldots, w_{mN}) = b(\widetilde{p}_1, \ldots, \widetilde{p}_{mN}). \tag{2.67}$$

The converse is obviously true. $\qquad\square$

Since, for all positive integers n, the total degree of $\widetilde{p}_n$ is equal to n, the following two corollaries are immediate consequences of Theorem 2.8.

Corollary 2.9. *In Λ_{mN}, the polynomial $\widetilde{p}_{N+1}$ is the unique (up to an overall factor) symmetric polynomial of total degree $N + 1$ that vanishes under $\mathcal{C}_m$.*

Corollary 2.10. *In Λ_{mN}, there is no non-zero symmetric polynomial with total degree less than $N + 1$ that vanishes under $\mathcal{C}_m$.*

In other words the kernel of the restriction of $\mathcal{C}_m$ to $\Lambda_{mN,N}$ is trivial. At this stage it would be instructive to state a brief new version of Conjecture 2.2 here again to compare it with the statement in Corollary 2.10.

Conjecture 1.2. *In Λ_{mN}, there is no non-zero symmetric polynomial with degree less than $N + 1$ that vanishes under $\mathcal{C}_m$.*

Example 2.11. Consider the simplest non-trivial case where $m = 2$ and $N = 1$. We want to describe all non-zero polynomials in Λ_2 that vanish under clustering transformation $\mathcal{C}_2$. Assume that s is such a polynomial. As in Eq. (2.67),

$$s(w_1, w_2) = b\big(\widetilde{p}_1(w_1, w_2), \widetilde{p}_2(w_1, w_2)\big), \tag{2.68}$$

for some polynomial b that each term in $b(\widetilde{p}_1, \widetilde{p}_2)$ contains some power of $\widetilde{p}_2$. From Eqs. (2.59) and (2.62),

$$\widetilde{p}_2(w_1, w_2) = \frac{1}{8}\left(p_1^2(w_1, w_2) - 2p_2(w_1, w_2)\right)$$

$$= \frac{1}{8}(w_1 - w_2)^2. \tag{2.69}$$

Thus

$$s(w_1, w_2) = (w_1 - w_2)^2 q(w_1, w_2), \tag{2.70}$$

where q is some symmetric polynomial in Λ_2.

Example 2.12. As another example, consider the case in which $m = N = 2$. Let s be a symmetric polynomial in Λ_4 such that $\mathcal{C}_2(s) = 0$. As in the previous example,

$$s = b(\widetilde{p}_1, \widetilde{p}_2, \widetilde{p}_3, \widetilde{p}_4). \tag{2.71}$$

where b is a polynomial such that each term in $b(\widetilde{p}_1, \widetilde{p}_2, \widetilde{p}_3, \widetilde{p}_4)$ contains at least some power of $\widetilde{p}_3$ or $\widetilde{p}_4$ (or both). So

$$s = \widetilde{p}_3 q_1 + \widetilde{p}_4 q_2 + \widetilde{p}_3 \widetilde{p}_4 q_3, \tag{2.72}$$

where q_1, q_2, and q_3 are some symmetric polynomials in Λ_4 such that q_1 does not involve $\widetilde{p}_4$ and q_2 does not involve $\widetilde{p}_3$. Moreover

$$\widetilde{p}_3 = \frac{1}{48}(p_1^3 - 6p_2 p_1 + 8p_3), \tag{2.73}$$

and

$$\widetilde{p}_4 = \frac{1}{384}(p_1^4 - 12p_1^2 p_2 + 12p_2^2 + 32p_1 p_3 - 48p_4), \tag{2.74}$$

each in four variables.

Before ending this section a comment on the Conjecture 2.2, rephrased as the one on page 43, seems in order. Despite the apparent similarity between statements of the Corollary 2.10 and the Conjecture 2.2, it turned out that the proof for Conjecture 2.2 is much harder and highly non-trivial. This is due to the fact that upon taking linear combinations of symmetric polynomials the *total* degree does not change, as long as the resulting polynomial does not vanish, while the *degree* can be lowered.

Chapter 3

General Theory of Anyons

An anyon model is an abstract physical theory involving particles living in $(2 + 1)$-dimensional space-time. To characterize an anyon model, one has to specify three pieces of information [Kit06].

- The first is to specify a finite set $\mathcal{L}$, known as the *label set*, whose elements are to label the different *type*s of anyons present in the model. Elements of $\mathcal{L}$ are usually called *charge*s or simply *label*s.

- The second is to specify a set of rules between any two labels. These are known as *fusion* rules and they specify the possible total charge(s) when two anyons of given charges come close and combine (fuse) as well as the charges of each of the two anyons when one anyon of a given charge *split*s into two.

- The third is to specify a set of rules, known as *braiding* rules, to specify what occurs when two particular anyons are interchanged.

This chapter contains three sections. Each one of the items above is explained in more detail in a separate section below.

3.1   The Label Set

This section is about the required structures for the label set $\mathcal{L}$. As mentioned above, elements of $\mathcal{L}$, which we generically denote by small Roman letters a, b, etc., label the type of anyons in the theory. Analogy with the more familiar three-dimensional case makes using the word "type" for anyons more tangible. In three dimensions, we know that particles come in two different types, namely, boson-type or fermion-type. Electrons and protons, for example, are fermions and photons and gluons are bosons. In two dimensions, the situation is similar except that there are, in principle, infinite number of particle types that could exist, depending on the phase factor appearing in the wave-function of the system when two particles are exchanged. Despite this, each anyon model is required to deal with only finitely many anyon-types. In what comes, we use the words anyons, particles, and anyon-types interchangeably.

In $\mathcal{L}$, there is exactly one distinguished label, known as the *vacuum*, which we denote by $\mathbf{1}$. The vacuum represents the state of the model corresponding

to no particle at all. Moreover, for any label a in $\mathcal{L}$, there is a unique associated label $\widehat{a}$ in $\mathcal{L}$, called the *dual* to a. Physically, $\widehat{a}$ is the charge of the anti-particle of the particle with charge a. Particles of charges a and $\widehat{a}$ can be annihilated to the vacuum or can be created, as a pair, out of the vacuum. The dual to the vacuum is the vacuum itself, $\widehat{\mathbf{1}} = \mathbf{1}$. For any anyon a, the dual $\widehat{a}$ may or may not be equal to a itself, but is required that $\widehat{\widehat{a}} = a$.

3.2   Fusion Rules

Let a and b be labels in $\mathcal{L}$. The *fusion* of a with b is denoted by $a \otimes b$, and it is defined to be a map that assigns, to each label c in $\mathcal{L}$, a non-negative integer denoted by N_{ab}^c, such that these integers satisfy the axioms that are given below. The integers N_{ab}^c are called fusion *coefficient*s. The fusion $a \otimes b$ is usually written as follows:

$$a \otimes b = \bigoplus_{c \in \mathcal{L}} N_{ab}^c \, c. \tag{3.1}$$

The reader should note that this is just a symbolic equation and it is just another way to state the same thing, namely, the number associated with label c by the fusion $a \otimes b$ is N_{ab}^c. Thus, the symbol $\oplus$ in Eq. (3.1) does not stand for a direct sum.

If N_{ab}^c is non-zero, the triple (a, b, c) is said to be *admissible*. For any two given labels a and b, labels c for which (a, b, c) is admissible are called fusion *channel*s of a and b. Moreover, if the outcome of the fusion of a with b turns out to be c, then c is *the* fusion channel of a and b. In this case, N_{ab}^c is interpreted as the number of distinct ways that an anyon of charge c can be produced when two anyons of charges a and b are fused. If $N_{ab}^c > 0$, usually a diagram as the one depicted in Fig. 3.1a, known as a *fusion-tree*, is drawn to show that two anyons of types a and b are fused and an anyon of type c is produced in the μth possibility, $\mu = 1, 2, \ldots, N_{ab}^c$, among N_{ab}^c number of distinct possibilities. With the time axis going vertically *downward*, this diagram is to be interpreted

(a) $|ab; c(\mu)\rangle$ (b) $\langle ab; c(\mu)|$

Figure 3.1: Time axis points downward, and $\mu = 1, 2, \ldots, N_{ab}^c$.

as a process in $(2 + 1)$ space-time in which anyons a and b are fused to anyon

c. In analogy, Fig. 3.1b represents splitting, in time, of anyon c to anyons *a* and *b*. Sometimes the ket notation $|ab; c(\mu)\rangle$ is used to denote the fusion-tree in Fig. 3.1a and the corresponding bra $\langle ab; c(\mu)|$ is used to denote the one in Figure 3.1b. If, on the other hand, $N_{ab}^c = 0$, this then means that there is no way that an anyon of charge *c* be an outcome of the fusion of anyons of charges *a* and *b* and, similarly, there is no way that an anyon of charge *c* can be split into two anyons of charges *a* and *b*.

If for all labels *a*, *b*, and *c*, the numbers N_{ab}^c are either zero or one, the model corresponding to the fusion rules is said to be a *multiplicity-free* model. For multiplicity-free models, the index μ in any fusion-tree of the model is always equal to one and, as Figs. 3.2a and 3.2b show, is suppressed. In this case, the corresponding ket and bra are simply denoted by $|ab; c\rangle$ and $\langle ab; c|$, respectively.

(a) $|ab; c\rangle$ (b) $\langle ab; c|$

Figure 3.2: Time axis points downward, and $\mu = 1$.

A model of anyons whose corresponding fusion rule has the property that $\sum_{c \in \mathcal{L}} N_{ab}^c > 1$, for some *a* and *b* in $\mathcal{L}$, is said to be *non-Abelian*. Otherwise, it is said to be *Abelian*.

We now turn our attention to the axioms demanded for the fusion coefficients. To make these axioms physically more accessible, let us first see how physicists interpret fusion rules. When two anyons of charges *a* and *b* are fused to an anyon of charge *c*, it is interpreted that, if one brings the two anyons close, then the outcome object, seen from afar, looks as an anyon of charge *c*. To see the point, we consider an analogy in three dimensions once more.

Let *b* stand for a boson and let *f* stand for a fermion. Consider now a box including a bunch of electrons and protons and assume that they are well-separated, do not interact, and are pinned in their positions. Recall that both proton and electron are fermions, that is, both are of type *f*. Now take one electron and one proton and bring them slowly very close. Viewed from distant, this then would seem as a collective particle—actually a hydrogen atom—which is a boson. One can imagine that two *f*-type particles has fused to a *b*-type particle.

Another analogy that is also helpful and is very often used in the literature, is comparing Eq. (3.1) with the corresponding decomposition equation when adding two angular momenta in quantum mechanics. For example, consider

bringing two spin-1/2 particles together. The Hilbert space of the total system is the tensor product of the Hilbert spaces corresponding to each individual particle and, therefore, is of dimension four. This Hilbert space decomposes into two Hilbert spaces, one that corresponds to the spin-singlet and one that corresponding to the spin-triplet. All this can actually be summarized in the following equation:

$$\mathbf{2} \otimes \mathbf{2} = \mathbf{1} \oplus \mathbf{3}, \tag{3.2}$$

comparable to Eq. (3.1). Of course, one should not push this analogy too far. In contrast to a particle with spin, which has its position-coordinates as its external degrees of freedom and its spin as its internal degree of freedom, a single anyon has no degrees of freedom beyond its (external) degrees of freedom due to taking into account the coordinates of its position in the two dimensional plane it lives on. Therefore, setting the degrees of freedom due to its position aside, a single anyon does not possess any degrees of freedom and, consequently, there is no Hilbert space associated with a single anyon. Hence, the Hilbert space of a system consisting of two anyons can no longer be considered as the tensor product of the Hilbert spaces of each individual anyon. However, as is discussed later, due to fusion rules, one can still associate a Hilbert space with a collection of *two* or *more* anyons, to describe the internal degrees of freedom associated with this collection.

Here we itemize the axioms demanded for fusion rules. These are somehow the reflection of our physical intuition about the model.

(i) For any two labels a and b in $\mathcal{L}$, $a \otimes b = b \otimes a$, that is, the fusion is *commutative*. Therefore, $N_{ab}^c = N_{ba}^c$, for any label c in $\mathcal{L}$.

   This is physically plausible, we do not want the final charge depends on whether we take a close to b or b close to a.

(ii) For any label a in $\mathcal{L}$, $a \otimes \mathbf{1} = a$, that is, the vacuum $\mathbf{1}$ is the *identity* of the fusion. Therefore, for any label c, $N_{\mathbf{1}a}^c = \delta_{ac}$, where δ is the Kronecker delta.

   Physically, it means that if an anyon is combined with the vacuum, its charge is not expected to change.

(iii) For any label a in $\mathcal{L}$,

$$a \otimes \widehat{a} = 1\,\mathbf{1} \oplus (\text{possibly other terms}), \tag{3.3}$$

   and, therefore, $N_{a\widehat{a}}^{\mathbf{1}} = 1$. Moreover, we also demand that $N_{ab}^{\mathbf{1}} = \delta_{b\widehat{a}}$, that is, $\widehat{a}$ is the only label with this property.

   This can also be understood, if one allows for the possibility of particle-antiparticle annihilation.

(iv) For any three labels a, b, and c in $\mathcal{L}$, $(a \otimes b) \otimes c = a \otimes (b \otimes c)$, that is, fusion is *associative*. What is actually meant by this relation is that the set of all possible fusion outcomes of the expression on the left is equal to the set of all possible fusion outcomes of the expression on the right. This translates itself to the following equation among the fusion coefficients:

$$\sum_{u \in \mathcal{L}} N_{xw}^u \, N_{uy}^z = \sum_{u \in \mathcal{L}} N_{wy}^u \, N_{xu}^z, \tag{3.4}$$

for all labels x, w, y, and z in $\mathcal{L}$.

This is also physically sound. We demand that the actual outcome of fusing three anyons does not depend on the order in which the particles are combined.

One can deduce more relations among the fusion coefficients. For example, letting $x \to a$, $w \to b$, $y \to \widehat{c}$, and $z \to \mathbf{1}$ in Eq. (3.4), invoking property (iii) above, and considering the fact that $\widehat{\widehat{c}} = c$, one gets $N_{ab}^c = N_{a\widehat{c}}^{\widehat{b}}$. Similarly one can show $N_{ab}^c = N_{\widehat{a}b}^{\widehat{c}}$.

3.2.1 Examples of Fusion Rules

Example 3.1 (Fibonacci Fusion Rules). Consider the two-element set $\mathcal{L} = \{a, b\}$ as the label set together with the following relations:

$$a \otimes a = a,$$
$$a \otimes b = b \otimes a = b,$$
$$b \otimes b = a \oplus b.$$

It is straightforward to check the properties of a fusion rule for $\otimes$ defined above. Here a is the vacuum $\mathbf{1}$ and b is its own dual. Anyon b is usually denoted by τ in the literature and is called the *Fibonacci* anyon. This fusion rule corresponds to a multiplicity-free and non-Abelian anyon model. $\diamondsuit$

Example 3.2 (Ising Fusion Rules). Consider the three-element set $\mathcal{L} = \{\mathbf{1}, \sigma, \psi\}$. Then $\otimes$ defined by

$$\psi \otimes \psi = \mathbf{1},$$
$$\sigma \otimes \sigma = \mathbf{1} \oplus \psi,$$
$$\sigma \otimes \psi = \sigma,$$

along with other trivial relations, defines a fusion rule on $\mathcal{L}$. Every particle is its own dual, it is multiplicity-free, and non-Abelian. $\diamondsuit$

Example 3.3 ([Wan10]). Let G be a finite group with the identity element e and let, for any $g \in G$, g^{-1} denote the group inverse of g. It is straightforward to see that

$$g \otimes h = \bigoplus_{k \in G} N_{gh}^k \, k, \qquad (\forall g, h \in G),$$

with $N_{gh}^k := \delta_{gh,k}$, defines a fusion rule on G (as the label set) in which $\mathbf{1} = e$ and $\widehat{g} = g^{-1}$, for every $g \in G$. It is multiplicity-free and Abelian.

Now let $\mathcal{L} = G \bigcup \{m\}$, where $m \notin G$ [Tam00]. Then $\otimes$ defined by

$$g \otimes h = gh,$$
$$m \otimes g = g \otimes m = m,$$
$$m \otimes m = \bigoplus_{g \in G} g,$$

for ever g and h in G, is a multiplicity-free fusion rule on $\mathcal{L}$ with vacuum e. The dual of every element in G is its group inverse and m is its own dual. It is Abelian if and only if G is a group of order one. The reader notes that if the group G is taken to be $\mathbb{Z}_2$, then this reproduces the Ising fusion rules in the previous example. $\diamondsuit$

Example 3.4 ($\frac{1}{2} E_6$ Fusion Rules). Consider the label set $\mathcal{L} = \{a, b, c\}$ with $\otimes$ defined by

$$a \otimes a = a,$$
$$b \otimes b = a \oplus 2\,b \oplus c,$$
$$c \otimes c = a,$$
$$b \otimes c = c \otimes b = b.$$

This defines a fusion rule on $\mathcal{L}$ where a is the vacuum, both b and c are self-duals, it is non-Abelian, and it is not multiplicity-free. For details, the reader is referred to [HH09]. $\diamondsuit$

Example 3.5 ($\mathfrak{su}(2)_k$ Fusion Rules). Let k be a positive integer. For any labels a, b, and c in the set $\mathcal{L}_k := \{0, 1/2, 1, 3/2, \ldots, k/2\}$, define the fusion coefficient N_{ab}^c as follows:

$$N_{ab}^c = \begin{cases} 1, & |a - b| \leqslant c \leqslant \min\{a + b, k - a - b\} \\ 0, & \text{othewise.} \end{cases}$$

In other words, for any a and b in $\mathcal{L}_k$, we have

$$a \otimes b := |a - b| \oplus (|a - b| + 1) \oplus \cdots \oplus \min\{a + b, k - a - b\}. \qquad (3.5)$$

Eq. (3.5) defines a multiplicity-free fusion rule on $\mathcal{L}_k$ in which 0 is the vacuum and every element is self-dual. This is Abelian if and only if $k = 1$. This fusion rule is the building block of the model that is considered in Chapter 4. Note that $k = 2$ corresponds to the Ising case. $\diamondsuit$

3.2.2   Fusion Matrix and Quantum Dimension

With each anyon type a in $\mathcal{L}$ is associated a non-negative number d_a, called the *quantum dimension* of anyon a. To define d_a, we introduce the notion of the *fusion matrix* N_a first. By definition, N_a is a square matrix of dimension $|\mathcal{L}|$ whose rows and columns are labeled by elements of $\mathcal{L}$, in some order, and for every b and c in $\mathcal{L}$, its (bc)th entry $(N_a)_{bc}$ equals to the fusion coefficient N^c_{ab}. Hence, any fusion matrix N_a is composed of only non-negative (integer) numbers. Then, by Perron–Frobenius theorem for matrices with non-negative entries, N_a has a real non-negative eigenvalue that is larger than the absolute value of all other eigenvalues of N_a. The quantum dimension d_a is defined to be this eigenvalue.

Example 3.6. For the Fibonacci anyon τ of Example 3.1, the corresponding fusion matrix is

$$N_\tau = \begin{bmatrix} 0 & 1 \\ 1 & 1 \end{bmatrix}. \tag{3.6}$$

Henceforth, $d_\tau = \phi$, where ϕ denotes the *golden ratio* $(1 + \sqrt{5})/2$. $\qquad\diamond$

Example 3.7. Consider, in the same order, the label set given in Example 3.2. We have the following fusion matrices:

$$N_{\mathbf{1}} = \begin{bmatrix} 1 & 0 & 0 \\ 0 & 1 & 0 \\ 0 & 0 & 1 \end{bmatrix}, \quad N_\sigma = \begin{bmatrix} 0 & 1 & 0 \\ 1 & 0 & 1 \\ 0 & 1 & 0 \end{bmatrix}, \quad N_\psi = \begin{bmatrix} 0 & 0 & 1 \\ 0 & 1 & 0 \\ 1 & 0 & 0 \end{bmatrix}. \tag{3.7}$$

Simple calculations show $d_{\mathbf{1}} = d_\psi = 1$ and $d_\sigma = \sqrt{2}$. $\qquad\diamond$

Example 3.8. For $\mathfrak{su}(2)_k$ anyons introduced in Example 3.5, for any j in $\mathcal{L}_k$, the corresponding quantum dimension d_j obeys the following formula:

$$d_j = \frac{\sin\left(\frac{2j+1}{k+2}\,\pi\right)}{\sin\left(\frac{1}{k+2}\,\pi\right)}. \tag{3.8}$$

It is shown, for example, in [Kit06] that the quantum dimensions form a one-dimensional representation of the fusion algebra, namely, we have the following key equation:

$$d_a d_b = \sum_{c \in \mathcal{L}} N^c_{ab}\, d_c, \qquad (\forall a, b \in \mathcal{L}). \tag{3.9}$$

Using Eq. (3.9), one can see that a $|\mathcal{L}|$-dimensional vector $\boldsymbol{d}$, whose components are quantum dimensions of the labels in $\mathcal{L}$, is a common eigenvector of all fusion matrices with an eigenvalue equal to the quantum dimension corresponding to that label. In other words:

$$N_a\, \boldsymbol{d} = d_a\, \boldsymbol{d}, \qquad (\forall a \in \mathcal{L}). \tag{3.10}$$

The norm of the vector $\boldsymbol{d}$ is called the *total* quantum dimension and it is denoted by $\mathcal{D}$. More explicitly,

$$\mathcal{D} = \sqrt{\sum_{a \in \mathcal{L}} d_a^2}. \tag{3.11}$$

It is straightforward to see that the associativity of fusion rules is equivalent to

$$N_a N_b = N_b N_a, \qquad (\forall a, b \in \mathcal{L}). \tag{3.12}$$

Therefore, all fusion matrices can be simultaneously diagonalized. Furthermore, associativity together with the commutativity of fusion rules give rise to the following equation:

$$N_a N_b = \sum_{c \in \mathcal{L}} N_{ab}^c N_c, \qquad (\forall a, b \in \mathcal{L}), \tag{3.13}$$

among the fusion matrices. Eq. (3.13) actually expresses the fact that fusion matrices can be considered as a representation of the fusion algebra.

3.2.3   Hilbert Space of Anyon Models and F-symbols

To be able to construct a model of anyons, the first step is to address the question of how one can associate a Hilbert space with a number of anyons under consideration. Actually, this is briefly discussed when we talked about fusion-trees. We now investigate this in a greater detail. We ignore all external degrees of freedom that a single anyon may have and concentrate ourselves only on internal degrees of freedom.

To this end, consider a system of two or more anyons. As mentioned earlier, no internal degrees of freedom is associated with just a *single* anyon. Consider two anyons a and b with fusion channel c. The corresponding Hilbert space is denoted by $\mathcal{H}_{ab}^c$ and it is defined to be the space for which the following set consisting of fusion kets (or trees):

$$\mathcal{B}_{ab}^c := \big\{ |ab; c(\mu)\rangle \mid \mu = 1, 2, \ldots, N_{ab}^c \big\}, \tag{3.14}$$

forms an orthonormal basis. For the dimension of this Hilbert space we therefore have $\dim(\mathcal{H}_{ab}^c) = N_{ab}^c$. In other words, any state in $\mathcal{H}_{ab}^c$ is a linear combination of the elements of the set above and

$$\langle ab; c(\mu) | ab; d(\nu) \rangle = \delta_{cd} \delta_{\mu\nu}, \tag{3.15}$$

$$\sum_{\mu=1}^{N_{ab}^c} |ab; c(\mu)\rangle \langle ab; c(\mu)| = I_{ab}^c, \tag{3.16}$$

where I_{ab}^c denotes the identity on $\mathcal{H}_{ab}^c$. The full Hilbert space $\mathcal{H}_{ab}$ corresponding to the pair (a,b), which describes the internal states of these anyons, is defined to be the direct sum of the partial Hilbert spaces, that is,

$$\mathcal{H}_{ab} = \bigoplus_c \mathcal{H}_{ab}^c, \tag{3.17}$$

where the sum is over all fusion channels c of anyons a and b and, consequently,

$$\dim(\mathcal{H}_{ab}) = \sum_c N_{ab}^c. \tag{3.18}$$

Since the models that are considered in this thesis are multiplicity-free models, we continue the discussion in this section only for multiplicity-free models.

Consider now three anyons a, b, and c with overall charge d, and let $\mathcal{H}_{abc}^d$ denote the associated Hilbert space. Two different bases can be imagined for this space. One is the set consisting of all fusion-trees as the one shown in Fig. 3.3a. Note that the intermediate label e must be a fusion channel for b and c and, in the same time, d must be a fusion channel for a and e. The other one is the set consisting of all fusion-trees as the one shown in Fig. 3.3b. Here f must be a fusion channel of a and b, and d must be in the fusion channel of f and c.

Figure 3.3: In (a), b fuses with c first, then a fuses with e to give d. In (b), a fuses with b first, then f fuses with c to give d.

One should note that the associativity of fusion rules guarantees the consistency that one needs here regarding the dimension of $\mathcal{H}_{abc}^d$ determined through each one of the bases described above. Counting the number of fusion-trees in Fig. 3.3a gives

$$\dim(\mathcal{H}_{abc}^d) = \sum_e N_{ab}^e N_{ec}^d, \tag{3.19}$$

and counting the number of fusion-trees in Fig. 3.3b gives

$$\dim(\mathcal{H}_{abc}^d) = \sum_f N_{bc}^f N_{af}^d. \tag{3.20}$$

These two are the same because of Eq. (3.4).

As is always the case, two different bases of the Hilbert space of a physical theory are related by a unitary matrix. Here, the basis-transformation matrix from the basis in Fig. 3.3a to the basis in Fig. 3.3b, is called the F-*matrix* and it is denoted by F_d^{abc}. Therefore,

$$
\begin{array}{c}
\text{[fusion tree diagram with } a,b,c \text{ fusing through } f \text{ to } d\text{]}
\end{array}
= \sum_e F_{d;ef}^{abc}
\begin{array}{c}
\text{[fusion tree diagram with } a,b,c \text{ fusing through } e \text{ to } d\text{]}
\end{array}
\quad ,
\tag{3.21}
$$

where $F_{d;ef}^{abc}$ indicates the (ef)th of the F-matrix and is called an F-*symbol*. One notes that Eq. (3.21) is meaningful only if the triples (a,b,f), (f,c,d), (b,c,e), and (a,e,d) are all admissible. If this is not the case, the F-symbol $F_{d;ef}^{abc}$ is defined to be zero. Eq. (3.21), which is called an F-*move*, is merely a symbolic equation and does not provide any information about the actual numerical values of F-symbols. To get that information, one needs some constraints among the F-symbols themselves. To this end, we consider four anyons a, b, c, and d, with overall charge e, and look at different configurations of the fusion-trees corresponding to these anyon charges. Fig. 3.4 shows two of these possible configurations.

Figure 3.4: Two possible fusion-trees in which anyons a, b, c, and d fuse to anyon e.

As Figs. 3.5 and 3.6 show, there are two different ways, using F-moves, that one can go from the fusion-tree in Fig. 3.4a to the fusion-tree in Fig. 3.4b.
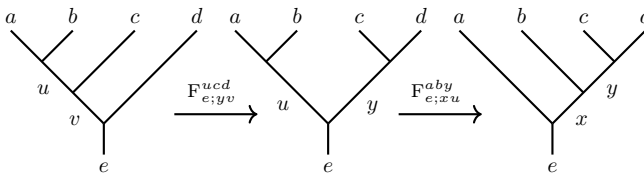
Figure 3.5: Two F-moves
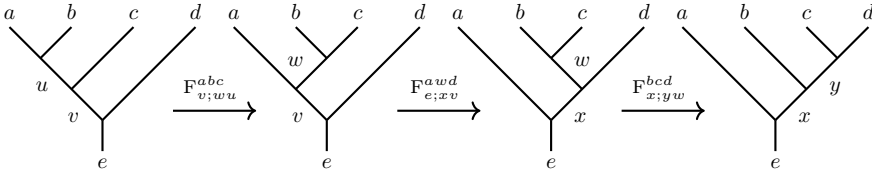
Figure 3.6: Three F-moves

To have a consistent theory, these two ways have to be equivalent. This gives rise to the following equations:

$$\mathrm{F}^{aby}_{e;xu}\,\mathrm{F}^{ucd}_{e;yv} = \sum_{w\in\mathcal{L}} \mathrm{F}^{abc}_{v;wu}\,\mathrm{F}^{awd}_{e;xv}\,\mathrm{F}^{bcd}_{x;yw}. \tag{3.22}$$

These are the *Pentagon* equations. Before going further, some points about Pentagon equations worth being mentioned explicitly. For detail, the reader is encouraged to consult [Bon07].

First, one notes that these equations are actually multivariate *polynomial* equations. The Pentagon equations either have no solution at all or they have infinitely many of them. The latter is due to the *gauge freedom* of these symbols. It is straightforward to check that if a set of F-symbols satisfy the Pentagon equations, then the new set of F-symbols defined by

$$\widetilde{\mathrm{F}}^{abc}_{d;ef} = \frac{k^{af}_d\,k^{bc}_f}{k^{ab}_e\,k^{ec}_d}\,\mathrm{F}^{abc}_{d;ef}, \tag{3.23}$$

where the k's with scripts are just complex numbers, satisfy the same Pentagon equations as well. However, it is shown [Kit06, ENO05] that all the solutions fall into only finitely many equivalence classes.

Determining the F-symbols for a given set of fusion rules, even with the help of computers, is a formidable task. In practice, one uses the freedom mentioned in Eq. (3.23) to, a priori, fix some of the F-symbols. The one that is widely used in physics literature is to set the matrix F^{abc}_d equal to the identity matrix, which acts on the Hilbert space $\mathcal{H}^d_{abc}$, whenever one of the labels a, b, or c is the vacuum. This is of course a natural convention for physical theories since any branch of a fusion-tree labeled by vacuum can simply be ignored. Furthermore, as mentioned earlier, each F-matrix, being a basis-transformation matrix for a physical Hilbert space, is invertible and unitary in the first place. To give a flavor of how to calculate the F-symbols, let us consider the following examples.

Example 3.9 (F-symbols for the Fibonacci anyon model). In this example we determine the F-symbols corresponding to Fibonacci fusion rules introduced in Example 3.1. From the fusion rules and the convention mentioned above, we

have:

$$\mathrm{F}^{\mathbf{111}}_{\mathbf{1};\mathbf{11}} = \mathrm{F}^{\tau\mathbf{11}}_{\tau;\mathbf{1}\tau} = \mathrm{F}^{\mathbf{1}\tau\mathbf{1}}_{\tau;\tau\tau} = \mathrm{F}^{\mathbf{11}\tau}_{\tau;\tau\mathbf{1}} = \mathrm{F}^{\tau\tau\mathbf{1}}_{\mathbf{1};\tau\mathbf{1}} = \mathrm{F}^{\tau\tau\mathbf{1}}_{\tau;\tau\tau}$$
$$= \mathrm{F}^{\tau\mathbf{1}\tau}_{\mathbf{1};\tau\tau} = \mathrm{F}^{\tau\mathbf{1}\tau}_{\tau;\tau\tau} = \mathrm{F}^{\mathbf{1}\tau\tau}_{\mathbf{1};\mathbf{1}\tau} = \mathrm{F}^{\mathbf{1}\tau\tau}_{\tau;\tau\tau} = 1.$$

There are only five more F-symbols, namely, $\mathrm{F}^{\tau\tau\tau}_{\tau;\mathbf{11}}$, $\mathrm{F}^{\tau\tau\tau}_{\tau;\mathbf{1}\tau}$, $\mathrm{F}^{\tau\tau\tau}_{\tau;\tau\mathbf{1}}$, $\mathrm{F}^{\tau\tau\tau}_{\tau;\tau\tau}$, and $\mathrm{F}^{\tau\tau\tau}_{\mathbf{1};\tau\tau}$, that might be non-zero and yet to be determined. For simplicity, we denote them by m, n, p, q, and r, respectively. The first four of these are actually entries of the 2×2 unitary matrix $\mathrm{F}^{\tau\tau\tau}_{\tau}$:

$$\mathrm{F}^{\tau\tau\tau}_{\tau} = \begin{bmatrix} m & n \\ p & q \end{bmatrix}, \tag{3.24}$$

and the last one is the only entry of the 1×1 unitary matrix $\mathrm{F}^{\tau\tau\tau}_{\mathbf{1}}$:

$$\mathrm{F}^{\tau\tau\tau}_{\mathbf{1}} = \begin{bmatrix} r \end{bmatrix}. \tag{3.25}$$

The unitarity of $\mathrm{F}^{\tau\tau\tau}_{\tau}$ implies that

$$q = \xi\,\overline{m}, \quad p = -\xi\,\overline{n}, \quad |m|^2 + |n|^2 = 1, \tag{3.26}$$

for some phase factor ξ. Similarly, we have

$$\mathrm{F}^{\tau\tau\tau}_{\mathbf{1};ab} = r\,\delta_{a\tau}\delta_{b\tau}, \quad |r| = 1, \tag{3.27}$$

for any labels a and b, with δ standing for the Kronecker delta. To determine these F-symbols we now invoke the Pentagon equations. Letting, for example, $a = b = c = d = e = v = y = \tau$ and $x = u = \mathbf{1}$ in Eq. (3.22) and using the first part of Eq. (3.27), we get:

$$m = rpn. \tag{3.28}$$

It turns out that considering all other possible labelings in Eq. (3.22) gives rise to only 11 more non-trivial and independent equations. All the 12 equations are listed below:

$$
\begin{array}{lll}
n(1 - q^2 - m) = 0, & n(m + qr) = 0, & np - mr^2 = 0, \\
p(1 - q^2 - m) = 0, & p(m + qr) = 0, & m^2 + npr = 1, \\
r^2 - rq^2 - np = 0, & nq(1 + r) = 0, & m^2 + npq = 0, \\
q^3 - q^2 + np = 0, & pq(1 + r) = 0, & m - npr = 0.
\end{array}
$$

It is straightforward to see that the above system of equations gives rise to two different family of solutions for the unknowns. These are

$$m = -\phi, \quad np = -\phi, \quad q = \phi, \quad r = 1, \tag{3.29}$$

and

$$m = \phi^{-1}, \quad np = \phi^{-1}, \quad q = -\phi^{-1}, \quad r = 1. \tag{3.30}$$

The result $m = -\phi$, which appears in (3.29), is incompatible with the last equation in (3.26) and, therefore, it is not unitary. It is readily seen that, if $\xi = -1$, then Eqs. (3.30) are consistent with Eqs. (3.26) and one finally gets

$$\mathrm{F}^{\tau\tau\tau}_{\mathbf{1};\tau\tau} = 1, \quad \mathrm{F}^{\tau\tau\tau}_{\tau} = \begin{bmatrix} \phi^{-1} & \eta\,\sqrt{\phi^{-1}} \\ \bar{\eta}\,\sqrt{\phi^{-1}} & -\phi^{-1} \end{bmatrix}, \tag{3.31}$$

where η is an *arbitrary* phase. Thus, we still have one degree of gauge freedom η left. One can fix the gauge by setting η equal to, say, one. $\diamondsuit$

Example 3.10 (F-symbols for the Ising anyon model). The same strategy as the one followed in the last example can be used to determine the F-symbols of the Ising anyon model as well. By the convention mentioned earlier, F^{abc}_d is the identity matrix of appropriate order, if at least one of the labels a, b, or c is the vacuum. Of course, in this case, all these identity matrices are actually of order one. Setting these trivial F-symbols aside, there are 14 more F-symbols to be determined. Four of them, namely, $m := \mathrm{F}^{\sigma\sigma\sigma}_{\sigma,\mathbf{11}}$, $n := \mathrm{F}^{\sigma\sigma\sigma}_{\sigma,\mathbf{1}\psi}$, $p := \mathrm{F}^{\sigma\sigma\sigma}_{\sigma,\psi\mathbf{1}}$, and $q := \mathrm{F}^{\sigma\sigma\sigma}_{\sigma,\psi\psi}$, are the entries of the following 2×2 unitary matrix:

$$\mathrm{F}^{\sigma\sigma\sigma}_{\sigma} = \begin{bmatrix} m & n \\ p & q \end{bmatrix}. \tag{3.32}$$

We have the same relations as the ones given in (3.26) for the entries of this matrix to guarantee the unitarity of this matrix. The following items list particular assignments to the labels of the Pentagon equations (3.22) together with the corresponding outcome equations. The assignments are made in a manner so that the outcome equations involve the entries of the matrix above, which we want to determine.

- $a = b = c = d = v = x = \sigma$ and $e = u = y = \mathbf{1}$:

$$m^2 + np\,\mathrm{F}^{\sigma\psi\sigma}_{\mathbf{1};\sigma\sigma} = 1, \tag{3.33}$$

- $a = b = c = d = v = x = \sigma$, $e = u = \mathbf{1}$, and $y = \psi$:

$$mp + pq\,\mathrm{F}^{\sigma\psi\sigma}_{\mathbf{1};\sigma\sigma} = 0, \tag{3.34}$$

- $a = b = c = d = v = x = \sigma$, $e = \mathbf{1}$, and $u = y = \psi$:

$$np + q^2\,\mathrm{F}^{\sigma\psi\sigma}_{\mathbf{1};\sigma\sigma} = \mathrm{F}^{\sigma\sigma\psi}_{\mathbf{1};\sigma\psi}\,\mathrm{F}^{\psi\sigma\sigma}_{\mathbf{1};\psi\sigma}, \tag{3.35}$$

- $a = \psi$, $b = c = d = e = u = x = \sigma$, and $v = y = \mathbf{1}$:

$$m = n\,\mathrm{F}^{\psi\sigma\sigma}_{\mathbf{1};\psi\sigma}\,\mathrm{F}^{\psi\psi\sigma}_{\sigma;\sigma\mathbf{1}}, \tag{3.36}$$

- $a = \psi$, $b = c = d = e = u = x = \sigma$, $v = \mathbf{1}$, and $y = \psi$:

$$p\,\mathrm{F}_{\sigma;\sigma\sigma}^{\psi\sigma\psi} = q\,\mathrm{F}_{\mathbf{1};\psi\sigma}^{\psi\sigma\sigma}\,\mathrm{F}_{\sigma;\sigma\mathbf{1}}^{\psi\psi\sigma}. \qquad (3.37)$$

The above equations give rise to the following two solutions:

$$\mathrm{F}_{\sigma}^{\sigma\sigma\sigma} = \pm\frac{1}{\sqrt{2}}\begin{bmatrix} 1 & 1 \\ 1 & -1 \end{bmatrix}, \qquad (3.38)$$

for the F-matrix in (3.32).

Example 3.11 (F-symbols for the $\mathfrak{su}(2)_k$ anyon model). The standard F-symbols of $\mathfrak{su}(2)_k$ anyon models, which is used in physics literature, is given by the following formula. Note that this formula expresses only non-zero F-symbols. For the proof, the reader can refer to [Kac89].

$$\mathrm{F}_{d;ef}^{abc} =$$

$$(-1)^{a+b+c+d}\Delta(a,b,e)\Delta(c,d,e)\Delta(b,c,f)\Delta(a,d,f)\sqrt{\lfloor 2e+1\rfloor_q}\sqrt{\lfloor 2f+1\rfloor_q}$$

$$\times \sum_{n=m}^{M}\left(\frac{(-1)^n\,\lfloor n+1\rfloor_q!}{\lfloor a+b+c+d-n\rfloor_q!\lfloor a+c+e+f-n\rfloor_q!\lfloor b+d+e+f-n\rfloor_q!}\right.$$

$$\left.\times\frac{1}{\lfloor n-a-b-e\rfloor_q!\lfloor n-c-d-e\rfloor_q!\lfloor n-b-c-f\rfloor_q!\lfloor n-a-d-f\rfloor_q!}\right),$$

for all labels in the set $\{0, 1/2, \ldots, k/2\}$. Here for any real number r, the so-called *q-number* $\lfloor r\rfloor_q$, is defined by

$$\lfloor r\rfloor_q = \frac{q^{r/2} - q^{-r/2}}{q^{1/2} - q^{-1/2}}, \quad q := \exp\left(\frac{2\pi\,\mathrm{i}}{k+2}\right), \qquad (3.39)$$

and for a non-negative integer n, the *q-factorial* $\lfloor n\rfloor_q!$ is defined by

$$\lfloor n\rfloor_q! = \lfloor n\rfloor_q\lfloor n-1\rfloor_q\cdots\lfloor 1\rfloor_q, \quad \lfloor 0\rfloor_q! := 1. \qquad (3.40)$$

Moreover, for labels a, b, and c from $\{0, 1/2, \ldots, k/2\}$, with $a \leqslant b+c$, $b \leqslant c+a$, $a \leqslant b+c$, and $a+b+c = 0 \pmod 1$,

$$\Delta(a,b,c) := \sqrt{\frac{\lfloor a+b-c\rfloor_q!\lfloor a-b+c\rfloor_q!\lfloor -a+b+c\rfloor_q!}{\lfloor a+b+c+1\rfloor_q!}}. \qquad (3.41)$$

Finally, summation-limits m and M are defined by

$$\begin{aligned} m &= \max\{a+b+e, c+d+e, b+c+f, a+d+f\}, \\ M &= \min\{a+b+c+d, a+c+e+f, b+d+e+f\}. \end{aligned} \qquad (3.42)$$

It should be mentioned that the F-matrices with entries given by the formula on the previous page are their own inverses. Moreover, employing this formula, we get

$$\mathrm{F}_a^{a\frac{1}{2}\frac{1}{2}} = \frac{1}{\sqrt{d_{1/2}d_a}} \begin{bmatrix} -\sqrt{d_{a-1/2}} & \sqrt{d_{a+1/2}} \\ \sqrt{d_{a+1/2}} & \sqrt{d_{a-1/2}} \end{bmatrix}, \tag{3.43}$$

for any label $0 < a < k/2$. The rows of the matrix above correspond to $e = a - 1/2, a + 1/2$ and the columns correspond to $f = 0, 1$, respectively. The F-symbols given in (3.43) are the only ones that we need for the anyon models discussed in Chapter 4

As the final point of this example, using the q-number notation introduced above, we have

$$d_j = \lfloor 2j + 1 \rfloor_q, \tag{3.44}$$

for the quantum dimensions given by Eq. (3.8). $\diamondsuit$

3.3 R-Symbols

Since the models investigated in this thesis do not involve exchange or braiding of anyons, we keep this section short and just mention some basic properties only for multiplicity-free models.

Consider two anyons a and b sitting on a given plane. Being exchanged in time, the world-lines of these anyons form a braid in three-dimensional space. As depicted on the left and right panels of Fig. 3.7, depending on which direction the anyons move during the exchange, two topologically inequivalent braid can be formed out of their world-lines. We use R_{ab} and R_{ab}^{-1} to denote the situations in Figs. 3.7a and 3.7b, respectively.
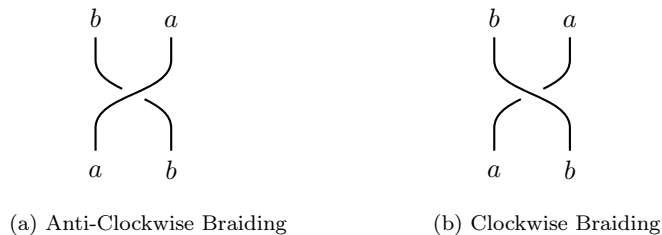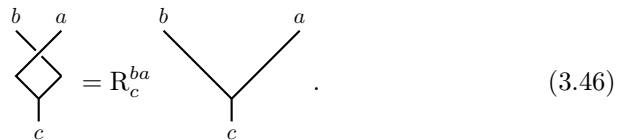

(a) Anti-Clockwise Braiding (b) Clockwise Braiding

Figure 3.7: World-lines of anyons a and b being braided in different directions.

Consider now two anyons a and b with total charge c. As mentioned before, this state is denoted by $|ab; c\rangle$ and it is an element of the Hilbert space $\mathcal{H}_{ab}^c$.

Recall that, since the model is assumed to be multiplicity-free, this is a one-dimensional Hilbert space. In this context, R_{ab} can be viewed as a (unitary) linear operator from the Hilbert space $\mathcal{H}_{ab}^c$ to the Hilbert space $\mathcal{H}_{ba}^c$. In other words, $R_{ab}|ab;c\rangle$ belongs to $\mathcal{H}_{ba}^c$. On the other hand, $|ba;c\rangle$ is a state in the Hilbert space $\mathcal{H}_{ba}^c$, which is also one-dimensional. Therefore,

$$R_{ab}|ab;c\rangle = R_c^{ba}\,|ba;c\rangle, \tag{3.45}$$

for some phase factor R_c^{ba}, called R-*symbol*. Of course, in general, R_c^{ab} is not just a phase but an $N_{ab}^c \times N_{ab}^c$ unitary matrix. Eq. (3.45) is usually visualized as below:

$$\begin{array}{c} b \quad a \\ \diamondsuit \\ c \end{array} = R_c^{ba} \begin{array}{c} b \qquad a \\ \diagdown\diagup \\ c \end{array}. \tag{3.46}$$

Going from the right fusion-tree in the equation above to the braided fusion-tree on the left is called an R-*move*.

As Figs. 3.8 and 3.9 show, there are two different combinations consisting of F-moves and R-moves that take us from the state on the left to the state on the right. To have a consistent theory though, these two combinations have to be equivalent, giving rise to the following set of consistency equations known as the *'anti-clockwise' Hexagon* equations for obvious reason:

$$R_p^{yx}\,F_{u;qp}^{yxz}\,R_q^{zx} = \sum_r F_{u;rp}^{xyz}\,R_u^{rx}\,F_{u;qr}^{yzx}. \tag{3.47}$$

Similarly, considering the clockwise braidings, we get the following *'clockwise' Hexagon* equations:

$$\left(R_p^{xy}\right)^{-1} F_{u;qp}^{yxz} \left(R_q^{xz}\right)^{-1} = \sum_r F_{u;rp}^{xyz} \left(R_u^{xr}\right)^{-1} F_{u;qr}^{yzx}. \tag{3.48}$$
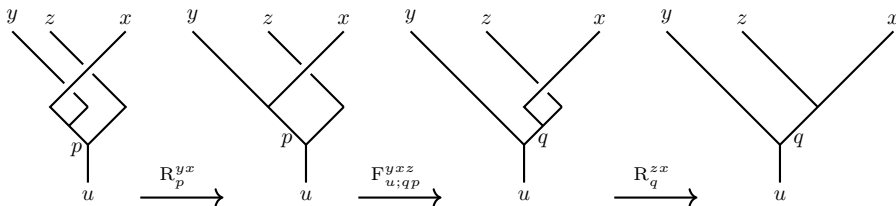

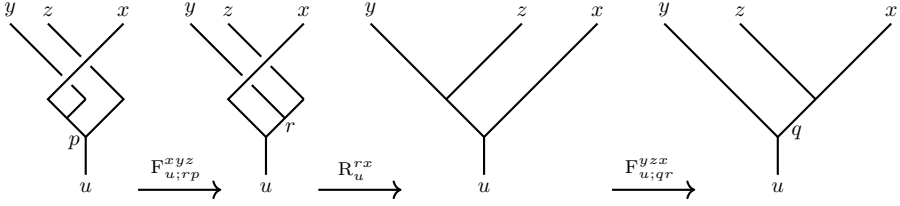Figure 3.8: Going from the state on the left to the one one the right, RFR

Figure 3.9: Going from the state on the left to the one one the right, FRF

For a consistent anyon model with a given set of fusion rules, the Pentagon equations and both versions of the Hexagon equations must be satisfied.

Example 3.12. In this example we determine the R-symbols for the Fibonacci anyon model. As for the F-symbols, braiding with vacuum is also considered to be trivial, namely, we have

$$\mathrm{R}_{\mathbf{1}}^{\mathbf{11}} = \mathrm{R}_{\tau}^{\tau\mathbf{1}} = \mathrm{R}_{\tau}^{\mathbf{1}\tau} = 1. \tag{3.49}$$

Therefore, there are only two undetermined R-symbols $\mathrm{R}_{\mathbf{1}}^{\tau\tau}$ and $\mathrm{R}_{\tau}^{\tau\tau}$ left. We determine them using the Hexagon equations and the corresponding F-symbols determined in Example 3.9. Letting $x = y = z = p = q = u = \tau$ in Eq. (3.47) and using (3.31), we get the following equation:

$$\left(\mathrm{R}_{\tau}^{\tau\tau}\right)^2 + \phi^{-1}\,\mathrm{R}_{\tau}^{\tau\tau} + 1 = 0. \tag{3.50}$$

Considering other possibilities in Eq. (3.47), one gets the following three more equations:

$$\left(\mathrm{R}_{\tau}^{\tau\tau}\right)^2 - \mathrm{R}_{\mathbf{1}}^{\tau\tau} = 0, \tag{3.51}$$

$$\phi\left(\mathrm{R}_{\mathbf{1}}^{\tau\tau}\right)^2 - \phi\,\mathrm{R}_{\tau}^{\tau\tau} - 1 = 0, \tag{3.52}$$

$$\phi\,\mathrm{R}_{\tau}^{\tau\tau}\,\mathrm{R}_{\mathbf{1}}^{\tau\tau} + \mathrm{R}_{\tau}^{\tau\tau} - 1 = 0. \tag{3.53}$$

This system of equations have two sets of solutions, namely,

$$\left\{\mathrm{R}_{\mathbf{1}}^{\tau\tau} = \mathrm{e}^{\frac{4\pi\mathrm{i}}{5}}, \mathrm{R}_{\tau}^{\tau\tau} = \mathrm{e}^{-\frac{3\pi\mathrm{i}}{5}}\right\}, \quad \left\{\mathrm{R}_{\mathbf{1}}^{\tau\tau} = \mathrm{e}^{-\frac{4\pi\mathrm{i}}{5}}, \mathrm{R}_{\tau}^{\tau\tau} = \mathrm{e}^{\frac{3\pi\mathrm{i}}{5}}\right\}. \tag{3.54}$$

It is straightforward to see that the equations obtained from the clockwise Hexagon equations for R-symbols have the same form with one difference that, instead of $\mathrm{R}_{\tau}^{\tau\tau}$, we have $\left(\mathrm{R}_{\tau}^{\tau\tau}\right)^{-1}$ and, instead of $\mathrm{R}_{\mathbf{1}}^{\tau\tau}$, we have $\left(\mathrm{R}_{\mathbf{1}}^{\tau\tau}\right)^{-1}$. Despite this difference, it turns out that the new equations have still the same solutions given in (3.54). $\diamondsuit$

A Non-Abelian Anyon-Chain Model

This chapter, which is based on the second accompanied paper [GA17], introduces a one-dimensional model of a chain of $\mathfrak{su}(2)_k$ anyons, with the special feature that the number of spin-1/2 anyons in the model can fluctuate, and then investigates some of the properties of this model.

First, for odd values of k and at a point in the parameter space for which the Hamiltonian becomes a sum of projectors, we realize that the model possesses zero-energy ground states and determine these states explicitly, both for open and closed chains. Numerical computations reveal that, for even values of k, there are no zero-energy ground states.

Then, by an investigation based on the *transfer matrix* idea and the *Yang–Baxter* equation, and a two-dimensional model in statistical mechanics, introduced by Warnaar et al in 1992 [WNS92], we specify four other points in the parameter space for which the system is integrable. That the anyon models are closely related to a special type of two-dimensional models of statistical mechanics, known as RSOS (restricted-solid-on-solid) models [ABF84], had already been observed in [FTL$^+$07].

4.1 Introduction

To increase our understanding about topological phases of matter, a good starting point is to study some reasonably simple so-called toy-models that reveal various aspects of the underlying physics of the more complicated real systems of interest. This kind of studies has already been proven to be fruitful to shed light on capturing the physics of interacting quantum many-body systems during early days of condensed matter physics. Quantum one-dimensional spin chains, namely, $SU(2)$ spins sitting on the sites of a one-dimensional lattice, are prototype examples in this regard. For instance, the Heisenberg one-dimensional spin-1/2 model played an important role in our quantum-mechanical understanding of magnetism and, in particular, phase transition between the ferromagnet and anti-ferromagnet phases of matter. The Hamiltonian H of this model, in its simplest incarnation, is

$$H = J \sum_i \boldsymbol{S}_i \cdot \boldsymbol{S}_{i+1}, \tag{4.1}$$

where $\boldsymbol{S}_i$ and $\boldsymbol{S}_{i+1}$ are *local* spin operators actings on sites i and $i+1$, respectively, and J is the only coupling constant. Here only the nearest-neighbor interactions are taken into account. The interaction term $\boldsymbol{S}_i \cdot \boldsymbol{S}_{i+1}$ assigns energy J, if the spins on sites i and $i+1$ are aligned, and assigns energy $-J$, if they are anti-aligned. The Hilbert space upon which H acts is the tensor product of l copies, l being the number of sites, of the Hilbert space corresponding to one single site. The second accompanied paper introduces one of these toy-models for non-Abelian $\mathfrak{su}(2)_k$ anyons, in which each site is either empty or occupied with a spin-1/2 anyon, and investigate some of its physical aspects.

4.1.1   Hilbert Space of $\mathfrak{su}(2)_k$ Anyon Chains

To cook up model-Hamiltonians for one-dimensional anyon chains, the first thing to be addressed is how to keep track of anyon degrees of freedom. In other words, one should identify the Hilbert space upon which a particular anyon model-Hamiltonian acts. We consider only the $\mathfrak{su}(2)_k$ anyons introduced in Example 3.5 together with the fusion rules given by (3.5). In the context of anyon chains, considering this class of anyons seems to be a natural choice due to the following two-fold resemblance that this class of anyons share with $SU(2)$ spins. This class of anyons have 'generalized spins'

$$j = 0, \frac{1}{2}, 1, \frac{3}{2}, \cdots, \frac{k}{2}, \tag{4.2}$$

comparable to $SU(2)$ spins

$$s = 0, \frac{1}{2}, 1, \frac{3}{2}, \cdots, \tag{4.3}$$

and their fusion rule (3.5) is also comparable to the following combination rule

$$s_1 \otimes s_2 = |s_1 - s_2| \oplus (|s_1 - s_2| + 1) \oplus \cdots \oplus (s_1 + s_2), \tag{4.4}$$

for spins s_1 and s_2. Actually these similarities provide an analogy as a guideline from spin-chain physics toward anyon-chain physics. Of course, one should be careful not to push this analogy too far. As mentioned in Chapter 3, in contrary to the spin-chain case, the Hilbert space of a number of anyons is not the tensor product of the Hilbert spaces corresponding to each individual anyon. As a consequence, there are no analogs of spin local operators $\boldsymbol{S}_i$ for anyons.

Consider now a one-dimensional lattice whose l sites are either empty or filled with any j-type anyon, where j is any non-zero label chosen from the list (4.2). In the context of anyon chains, the common language is to represent the anyon degrees of freedom by drawing a tree-like object, known as a fusion-*chain* or a fusion-*tree*, depicted in Fig. 4.1. If none of the y labels is zero,

the corresponding chain is called a *dense* chain, otherwise, it is called a *dilute* chain.
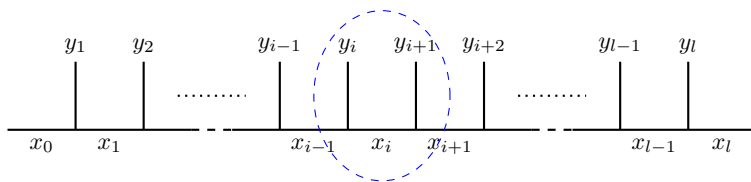

Figure 4.1: A typical fusion-tree.

The vertical segments in the fusion-tree represent sites of the lattice. Hence, based on the lines above, y labels assigned to these vertical segments are either zero, interpreted as the site is empty, or a non-zero number from the list (4.2), interpreted as the site is occupied by an anyon of that particular spin. The values that the x labels can take are, on the other hand, constrained by the fusion rules (3.5) in the sense that, for all $1 \leqslant i \leqslant l$, x_i can take only those values from the list (4.2) for which it is a fusion channel of $x_{i-1} \otimes y_i$. Besides, for future reference, we agree to refer the part of the fusion-tree in Fig. 4.1 that is highlighted by the blue dashed-line as the *i*th *part* of the fusion-tree.

We now require that the set of all fusion-trees described above constitutes an orthonormal basis for the Hilbert space associated with the one-dimensional *l*-sited lattice of anyons outlined in the last paragraph. Orthonormality is interpreted in the sense that the inner product of two fusion-trees is defined to be $\prod_{i=0}^{l} \delta_{x_i x_i'} \prod_{i=1}^{l} \delta_{y_i y_i'}$, where primed and unprimed labels denote the corresponding labels of each one of the fusion-trees, respectively.

4.1.2 Toward the Anyon Chain Hamiltonians

Suppose we want to contrive a Hamiltonian analogous to the one in Eq. (4.1), but this time for a dense chain of spin-1/2 anyons, that is, a chain for which all y labels in Fig. 4.1 are 1/2. Since there is no analog of local spin operators $\boldsymbol{S}_i$ for spin-1/2 anyons, we first rewrite the Hamiltonian in a form that is suitable to model anyon chains. As the calculations below show, in its new dress, the Hamiltonian (4.1) is a sum of projectors so that each one of the projectors projects onto a specified and fixed-for-all-sites *total* spin channel. In its new form, the Hamiltonian (4.1) would inspire how to write a model Hamiltonian for spin-1/2 anyons with nearest-neighbor interactions.

Let $\boldsymbol{S}_{i,T} := \boldsymbol{S}_i + \boldsymbol{S}_{i+1}$ denote the total spin of interacting spins on sites i and $i+1$. Since each site is filled with a spin-1/2, $s_{i,T}$ is either zero or one and, consequently, the eigenvalues of $\boldsymbol{S}_{i,T}^2$ are either zero or two. Hence

$$\boldsymbol{S}_{i,T}^2 = 0\,P_i^{(0)} + 2\,P_i^{(1)}, \tag{4.5}$$

where $P_i^{(0)}$ is the projection onto the spin-singlet and $P_i^{(1)}$ is the projection onto the spin-triplet. Moreover, we have

$$P_i^{(0)} + P_i^{(1)} = I, \tag{4.6}$$

where I is the identity operator. On the other hand,

$$
\begin{aligned}
\boldsymbol{S}_i \cdot \boldsymbol{S}_{i+1} &= \frac{1}{2}\left(\boldsymbol{S}_{i,T}^2 - \boldsymbol{S}_i^2 - \boldsymbol{S}_{i+1}^2\right) \\
&= \frac{1}{2}\left(2\,P_i^{(1)} - \frac{3}{4}\,I - \frac{3}{4}\,I\right) \\
&= P_i^{(1)} - \frac{3}{4}\,I.
\end{aligned} \tag{4.7}
$$

Therefore, ignoring an unimportant overall shift, the Hamiltonian in Eq. (4.1) can be written as a sum of projectors, namely,

$$H = J\sum_i P_i^{(1)}. \tag{4.8}$$

Operator $P_i^{(1)}$ acts locally and, as far as this operator is concerned, only spins at sites i and $i+1$ contribute.

The above Hamiltonian can indeed be considered as a Hamiltonian that models the spin-1/2 anyon chain, with nearest-neighbor interactions, provided that one finds a suitable way to interpret consistently how the projection operator $P_i^{(1)}$ should act in the case of spin-1/2 anyons. Following the analogy with the spin-chain case, we let $P_i^{(1)}$ act only on the ith part of the fusion-tree in Fig. 4.1. The problem is then that the fusion channel of anyons at sites i and $i+1$ is not explicit, but we want to assign energy $E = J$, when anyons at sites i and $i+1$ fuse to one, and to assign energy $E = 0$, otherwise. To deal with this problem, we can do a local basis transformation on the ith part of the fusion-tree using an F-move introduced in Chapter 3 and is shown in Fig. 4.2.
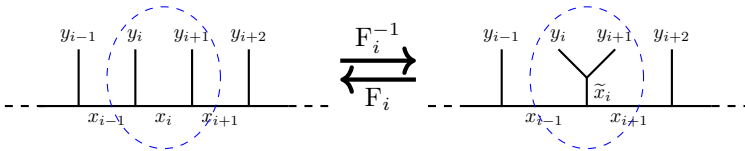

Figure 4.2: Local basis transformation.

4.2   Our Anyon-Chain Model

In this section, we introduce the models investigated in the second accompanied paper [KMG17] for a one-dimensional anyon chain, with l sites, consisting of $\mathfrak{su}(2)_k$ anyons. First, the Hilbert space of the models is introduced and then the model-Hamiltonian is discussed.

4.2.1 The Hilbert Space

The general aspects of the Hilbert spaces associated with anyon-chain models were discussed in Section 4.1.1. In our model, among other possibilities, we want to allow for the possibility of anyons to hop to the next-nearest site, provided the latter is empty. We consider the simplest model in which every site of the chain is either empty or occupied by a spin-1/2 anyon. We also rule out the possibility that a site is doubly occupied. Hence, for the models we study, the y labels of the fusion-tree in Fig. 4.1 are either zero or 1/2. This in turn allows for the simpler ket notation for a fusion-tree in our case. In other words, knowing x labels suffices to recognize a fusion-tree—because of the corresponding fusion rules, for any $1 \leqslant i \leqslant l$, $y_i = 1/2$ only if $x_{i-1} \neq x_i$. Therefore, in our case, the fusion-tree in Fig. 4.1 can be simply denoted by the ket $|x_0, x_1, \ldots, x_{l-1}, x_l\rangle$. Of course, we use this ket notation and the fusion-tree notation in Fig. 4.1 interchangeably, depending which is suitable for the particular purpose being considered. For positive integers k and l, we now declare that the set

$$\mathcal{B}(k,l) := \left\{ |x_0, x_1, \ldots, x_{l-1}, x_l\rangle \mid x_i \in \mathcal{L}_k, \text{for every } i \right\}, \tag{4.9}$$

with $\mathcal{L}_k := \left\{ 0, 1/2, 1, 3/2, \cdots, k/2 \right\}$, constitutes an orthonormal basis for the Hilbert space $\mathscr{H}(k,l)$ of the models we study. The orthonormality here means:

$$\langle x_0, x_1, \ldots, x_l | x_0', x_1', \ldots, x_l' \rangle = \prod_{i=0}^{l} \delta_{x_i x_i'}. \tag{4.10}$$

In the models discussed in the second paper, the subspace $\mathscr{H}_{\mathrm{cl}}(k,l)$ of $\mathscr{H}(k,l)$, whose basis $\mathcal{B}_{\mathrm{cl}}(k,l)$ is composed of those elements of $\mathcal{B}(k,l)$ with the *periodic* boundary condition, $x_0 = x_l$, imposed on them, is considered as well. An anyon chain satisfying the periodic boundary condition is called a *closed* chain, otherwise, it is called an *open* chain. For an open chain with l sites, the lth part of the chain is not defined whereas Fig. 4.3 shows what we refer to as the lth part of a closed chain.
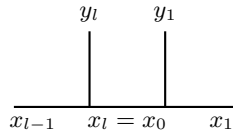

Figure 4.3: The lth part of a closed chain.

4.2.2 The Hamiltonian of the Model

We consider two Hamiltonians, although having the same form, one of them, denoted by $H(k,l)$, acts on the whole Hilbert space $\mathscr{H}(k,l)$ and one of them,

denoted by $H_{\mathrm{cl}}(k,l)$, acts only on the subspace $\mathscr{H}_{\mathrm{cl}}(k,l)$. In what follows we consider l and k to be given constants. Thus, we suppress them from the subsequent notations and we denote both Hamiltonians, whether it acts on $\mathscr{H}$ or $\mathscr{H}_{\mathrm{cl}}$, simply by H, and use the subscript "cl" only when necessary.

The Hamiltonians we consider are of the following form:

$$H = \sum_{i=0}^{\nu} h_i. \tag{4.11}$$

Here, ν is either $l-1$ or l, depending on whether the Hamiltonian acts on $\mathscr{H}$ or $\mathscr{H}_{\mathrm{cl}}$, respectively, and h_i, which we call the ith *local* Hamiltonian, is itself a sum of nine terms as follows:

$$\begin{aligned} h_i := h_{i,\mu_{00}} + h_{i,\mu_{0\frac{1}{2}}} &+ h_{i,\mu_{\frac{1}{2}0}} + h_{i,\mu_{\frac{1}{2}\frac{1}{2}}} \\ &+ h_{i,J} + h_{i,t} + h'_{i,t} + h_{i,\Delta} + h'_{i,\Delta}. \end{aligned} \tag{4.12}$$

Here, we briefly describe how each term acts on a typical element of the basis $\mathcal{B}$ in (4.9). We should first mention that the index i on each term indicates that the corresponding term acts only on the ith part of the fusion-tree, leaving other parts of the tree intact. In other words, it acts as the identity operator on all parts of the fusion-tree except the ith part. In other words, as far as an operator with index i is concerned, only x_{i-1}, x_i, and x_{i+1} labels in the basis ket $|x_0, x_1, \ldots, x_{i-1}, x_i, x_{i+1}, \ldots, x_{l-1}, x_l\rangle$ play a role. Therefore, in what follows we use the shorter notation $|u, v, w\rangle$ to denote this ket without explicitly referring to the index i.

Diagonally-Acting Terms The first term in (4.12) assigns energy μ_{00} only if sites i and $i+1$ are both empty, namely,

$$h_{\mu_{00}}|u, v, w\rangle := \delta_{uv}\delta_{vw}\mu_{00}|u, v, w\rangle. \tag{4.13}$$

The next two terms, accordingly, assign energies $\mu_{0\frac{1}{2}}$ and $\mu_{\frac{1}{2}0}$ if site i is empty and site $i+1$ is occupied and the other way around, respectively. This can be written in the following form:

$$h_{\mu_{0\frac{1}{2}}}|u, v, w\rangle := \delta_{uv}\mu_{0\frac{1}{2}}|u, v, w\rangle, \tag{4.14}$$

$$h_{\mu_{\frac{1}{2}0}}|u, v, w\rangle := \delta_{vw}\mu_{\frac{1}{2}0}|u, v, w\rangle. \tag{4.15}$$

Each of these three terms act as a chemical potential term.

The fourth term assigns energy $\mu_{\frac{1}{2}\frac{1}{2}}$ if both site i and site $i+1$ are occupied, namely,

$$h_{\mu_{\frac{1}{2}\frac{1}{2}}}|u, v, w\rangle := (1 - \delta_{uv})(1 - \delta_{vw})\mu_{\frac{1}{2}\frac{1}{2}}|u, v, w\rangle. \tag{4.16}$$

This term can be viewed as an interaction term.

Explicit Interaction Term The fifth term in (4.12) models a non-trivial interaction based on the fusion channel of the two anyons sitting on sites i and $i + 1$. This is somehow analogous to the interaction term described in the introduction for the Heisenberg spin-1/2 chain model (4.1). We require that this term assigns energy J only if sites i and $i + 1$ are occupied and the spin-1/2 anyons at these sites fuse to zero. To achieve this, as discussed in Section 4.1.2, we switch to a basis in which the fusion channel of the sites i and $i + 1$ is explicit and the define h_J as follows:

$$
h_J\left(\begin{array}{c} \frac{1}{2} \quad \frac{1}{2} \\ \searrow z \\ u \quad w \end{array} \right) := J\ \delta_{uw}\delta_{z0} \begin{array}{c} \frac{1}{2} \quad \frac{1}{2} \\ \searrow z \\ u \quad w \end{array} . \tag{4.17}
$$

To express how h_J acts on a local fusion-tree, as was done for all previous terms, we use Eq. (3.21) to write

$$
\begin{array}{c} \frac{1}{2} \quad \frac{1}{2} \\ | \quad | \\ u \quad v \quad w \end{array} = \sum_z \mathrm{F}^{u\frac{1}{2}\frac{1}{2}}_{w;zv} \begin{array}{c} \frac{1}{2} \quad \frac{1}{2} \\ \searrow z \\ u \quad w \end{array} , \tag{4.18}
$$

and then act both sides of this equation by h_J. Using definition (4.17), we now obtain

$$
h_J\left(\begin{array}{c} \frac{1}{2} \quad \frac{1}{2} \\ | \quad | \\ u \quad v \quad w \end{array} \right) = J\delta_{uw}\, \mathrm{F}^{u\frac{1}{2}\frac{1}{2}}_{w;0v} \begin{array}{c} \frac{1}{2} \quad \frac{1}{2} \\ \searrow 0 \\ u \quad w \end{array} . \tag{4.19}
$$

To express everything in terms of the original basis of local fusion-trees, we use the inverse of an F-move to switch back to the original basis. As mentioned in Example 3.11, every F-matrix corresponding to these F-symbols is an orthogonal matrix. Therefore, the right side of the last equation can be expressed in terms of the original basis and this equation will then read as follows:

$$
h_J\left(\begin{array}{c} \frac{1}{2} \quad \frac{1}{2} \\ | \quad | \\ u \quad v \quad w \end{array} \right) = J\delta_{uw} \sum_s \left(\mathrm{F}^{u\frac{1}{2}\frac{1}{2}}_{w,0v}\, \mathrm{F}^{u\frac{1}{2}\frac{1}{2}}_{w;0s} \begin{array}{c} \frac{1}{2} \quad \frac{1}{2} \\ | \quad | \\ u \quad s \quad w \end{array} \right). \tag{4.20}
$$

Finally, using (3.43) to replace for the F-symbols, one obtains,

$$
h_J \left(\underset{u\ \ v\ \ w}{\overset{\frac{1}{2}\ \ \frac{1}{2}}{\big|\ \ \big|}} \right) = J\delta_{uw} \sum_s \left(\frac{\sqrt{d_v d_s}}{d_u d_{1/2}} \ \underset{u\ \ s\ \ w}{\overset{\frac{1}{2}\ \ \frac{1}{2}}{\big|\ \ \big|}} \right), \tag{4.21}
$$

which we can take as the definition of the interaction term h_J.

Hopping Terms One feature of the anyon model considered in this thesis is that it takes into account the possibility of an anyon to hop onto the nearest site provided the latter is empty. The terms h_t and h'_t in (4.12) represents hopping of an anyon one site to the right and one site to the left, respectively. This kind of process for anyons was first discussed in [FTL$^+$07]. In the model considered here, both these hopping processes are assigned the same energy t. Formally, we have

$$
h_t|u,v,w\rangle := \delta_{vw}t\,|u,u,w\rangle, \tag{4.22}
$$
$$
h'_t|u,v,w\rangle := \delta_{uv}t\,|u,w,w\rangle. \tag{4.23}
$$

Creation and Annihilation Terms The main feature of the anyon model considered here is that, by a simple mechanism, it allows for the number of anyons to increase or decrease. This fluctuation in the number of anyons is taken care of by the last two terms h_Δ and h'_Δ in (4.12). This mechanism is as follows that, through the term h_Δ, it allows for the possibility that at sites i and $i+1$ a pair of spin-1/2 anyons be created out of the vacuum and, through the term h'_Δ, it allows for the possibility that a pair of spin-1/2 anyons at sites i and $i+1$ be annihilated into the vacuum. For these to be consistent, the fusion channel of the two anyons has to be zero. In the models considered, the strength of these creation and annihilation processes are given the same value Δ. This, of course, guarantees the Hermiticity, or better to say being symmetric in our case, of the model Hamiltonian in the first place. Formally, the creation process is defined as follows:

$$
h_\Delta \left(\underset{u\ \ u\ \ u}{\overset{0\ \ \ 0}{\big|\ \ \big|}} \right) := \Delta\ \underset{u\ \ \ u}{\overset{\frac{1}{2}\ \ \frac{1}{2}}{\diagdown 0 \diagup}}. \tag{4.24}
$$

Moreover, h_Δ is defined to act by zero on any other configuration of a fusion-tree whose ith part differs from the one on the left hand side of the equation above. Once more, we use the inverse of an F-move to write the term on the right of Eq. (4.24) in terms of the original basis elements, and

use information in Eq. (3.43) to reach at the following explicit relation for the creation term:

$$h_\Delta\left(\overset{0\quad 0}{\underset{u\quad u\quad u}{|\quad |}}\right) = \Delta \sum_s \left(\sqrt{\frac{d_s}{d_u d_{1/2}}}\ \overset{\frac{1}{2}\quad \frac{1}{2}}{\underset{u\quad s\quad u}{|\quad |}}\right).$$

(4.25)

We define the annihilation term as the conjugate of the creation term in the following sense:

$$h'_\Delta\left(\overset{\frac{1}{2}\quad \frac{1}{2}}{\underset{u\quad w}{\underset{z}{\vee}}}\right) := \Delta\,\delta_{uw}\delta_{z0}\ \overset{0\quad 0}{\underset{u\quad u\quad u}{|\quad |}}.$$

(4.26)

To write both sides of the above defining equation in terms of the same basis elements, we apply h'_Δ on both sides of Eq. (4.18) and employ Eq. (4.26). Substituting the explicit form of the F-symbols encountered, we then get:

$$h'_\Delta\left(\overset{\frac{1}{2}\quad \frac{1}{2}}{\underset{u\quad v\quad w}{|\quad |}}\right) = \delta_{uw}\Delta\,\sqrt{\frac{d_v}{d_u d_{1/2}}}\ \overset{0\quad 0}{\underset{u\quad u\quad u}{|\quad |}}.$$

(4.27)

This concludes introducing the model. From the next section, we start analyzing the model by studying it at some special points of the parameter space.

4.3 Analysis of the Model

We now start to analyze the dilute anyon model introduced in the previous section. A full analysis of the model is not possible due to, on one hand, the rather large number of parameters and, on the other hand, the quick growth of the size of the corresponding Hilbert space with both k and system size l. Hence, we limit our analysis to certain points in the parameter space.

4.3.1 The Hamiltonian as a Sum of Porjectors

In this subsection we choose, among only a few number of choices, a particular set of values for the parameters of the model Hamiltonians H and H_{cl} introduced in the previous section so that, for the values chosen, each local hamiltonian h_i in (4.12) turns into a projector and, consequently, the model Hamiltonians become a sum of projectors. We first discuss how writing a

Hamiltonian as a sum of projectors can be helpful in determining the zero-energy ground states (if any) of the model.

For a Hamiltonian that is a sum of projectors the *zero*-energy states, if they exist, are certainly the ground states of the Hamiltonian. This is due to the fact that eigenvalues of such Hamiltonian are all non-negative. Another property of practical importance when working with a Hamiltonian H that is expressed as a sum of projectors is as follows. If $H = \sum_i P_i$, where each P_i is a projector in the sense that $P_i^2 = P_i$, then a state $|\psi\rangle$ is a zero-energy ground state if and only if $P_i|\psi\rangle = 0$, for all i. The latter property translates itself to the following relation among the kernels of the corresponding operators:

$$\ker(H) = \bigcap_i \ker(P_i). \tag{4.28}$$

Therefore, if the Hamiltonian H expressed above does indeed possess zero-energy ground states, these states can be explored by looking into the kernel of the constituent projectors P_i, one at a time. To explain this in more detail, let $|\psi_0\rangle$ be a zero-energy ground state of H and let $\{|e_i\rangle\}_i$ be an orthonormal basis for the corresponding Hilbert space upon which the Hamiltonian H acts. Generally, $|\psi_0\rangle = \sum_i c_i |e_i\rangle$, for complex numbers c_i. As mentioned above, $|\psi_0\rangle$ must be annihilated by all projectors P_i. The first constraint $P_1|\psi_0\rangle = 0$ gives rise to a number of equations among the coefficients c_i and, generically, decreases the number of independent coefficients. In other words, this enables us to express some of these coefficients in terms of the rest. We now rewrite the linear combination for $|\psi_0\rangle$ so that the dependent coefficients are eliminated in favor of independent ones and, consequently, we get a new form for $|\psi_0\rangle$. Despite the fact that this new form expresses the same ket $|\psi_0\rangle$, to keep track of the steps, we designate this new form by $|\psi_0^{(1)}\rangle$. We now go to the second step by looking at the second constraint $P_2|\psi_0^{(1)}\rangle = 0$. This new constraint in turn gives rise to a number of new equations among the coefficients that survived the previous step and this typically decreases the number of independent coefficients even more. We then continue in the same manner and take care of all constraints one after the other. Applying the last constraint and writing the linear combination for $|\psi_0\rangle$ in terms of the final independent coefficients, the generic structure of a typical zero-energy ground state $|\psi_0\rangle$ reveals itself. The degeneracy of the zero energy is, due to normalization, one less than the number of final independent coefficients.

Investigating a model at a single point in the parameter space in which the Hamiltonian can be expressed as a sum of projectors, provided that it indeed possesses zero-energy ground sates, is more fruitful than it might seem at the beginning. This stems from the fact that, generically, the existence of zero-energy ground states for the Hamiltonians that can be expressed as a sum of projectors is a signature of the system being gapped. Because of the gap, these zero-energy ground states capture the underlying physics of the system, not

only at the points $\mathcal{P}$ in the parameter space in which the Hamiltonian can be expressed as a sum of projectors but also at the points close to $\mathcal{P}$. In other words, by probing the behavior of the model at point $\mathcal{P}$ we could, in principle, know about the behavior of the system close to $\mathcal{P}$.

One should note that the method described above to determine the ground states is helpful only if the ground state(s) are of *zero* energy. The above strategy has already been employed to determine the zero-energy ground states of a number of models and has been proven to be valuable in those models. As an example, one can mention the spin-1 AKLT model [AKLT87].

Now that we know the benefit of writing a Hamiltonian as a sum of projectors, we employ it for our model. To determine the values for the parameters so that each local Hamiltonian becomes a projector, one should note that the outer labels x_{i-1} and x_{i+1} of the ith part $|x_{i-1}, x_i, x_{i+1}\rangle$ of any fusion ket are not affected when acted upon by h_i. This makes the determination of the parameters straightforward, since this allows for considering the local subspaces spanned by

$$\big\{|x_{i-1}, x_{i-1}, x_{i-1} \pm 1/2\rangle, |x_{i-1}, x_{i-1} \pm 1/2, x_{i-1} \pm 1/2\rangle\big\},$$

and

$$\big\{|x_{i-1}, x_{i-1}, x_{i-1}\rangle, |x_{i-1}, x_{i-1} - 1/2, x_{i-1}\rangle, |x_{i-1}, x_{i-1} + 1/2, x_{i-1}\rangle\big\},$$

separately. Of course, each of the states $|x_{i-1}, x_{i-1} - 1/2, x_{i-1} - 1\rangle$ and $|x_{i-1}, x_{i-1} + 1/2, x_{i-1} + 1\rangle$ individually forms a one-dimensional subspace in its own. Moreover, in the model considered, we are interested in non-zero values for J, t, and Δ. Out of a few possible choices left, we picked the following values:

$$\mu_{00} = \mu_{0\frac{1}{2}} = \mu_{\frac{1}{2}0} = t = \frac{1}{2} \;,\; \mu_{\frac{1}{2}\frac{1}{2}} = 0 \;,\; J = \frac{1}{2} \;,\; \Delta = \frac{1}{2}, \qquad (4.29)$$

which, due to assigning the same value $1/2$ to all of the first four parameters, has the benefit that the investigation of the model is simpler.

Doing analytics supported by numerical computations for small system sizes, we realized that, for the above values for parameters and *odd* values of k, both of the Hamiltonians H and H_{cl} indeed possess zero-energy ground states for sufficiently large l. More explicitly, H has $(k+1)(k+2)(k+3)/6$ zero-energy ground states for $l \geqslant k$ and H_{cl} has $(k+1)/2$ zero-energy ground states for $l \geqslant k+1$. Numerical computations reveal that, for system sizes smaller than the ones mentioned in each case, the number of zero-energy ground states can be larger than the numbers given above. We also determined, for odd values of k, the explicit form of all these zero-energy ground states in each case. These explicit forms are expressed in the subsequent two subsections, respectively.

For *even* values of k, numerical computation indicates that, for sufficiently large system sizes, there are no zero-energy ground states. The difference arising between the behavior of the model for even values of k and its behavior for odd values of k should be sought in the difference between the structure of the fusion rules corresponding to even and odd values of k. As an example of this difference, we consider the generic relation $j \otimes k/2 = k/2 - j$. When k is even, the anyon type $j = k/4$ satisfies this relation whereas, when k is odd, there is no anyon type satisfying this relation.

Zero-energy Ground States of H, Open Chain

In this subsection, we assume that k is a given odd positive integer and the parameters of the model have the values given in (4.29). Numerical calculations already support the existence of zero-energy ground states for the Hamiltonian H, which is given by (4.11) for $\nu = l - 1$, and acts on the Hilbert space $\mathscr{H}$ introduced in Subsection 4.2.1. We employ the strategy mentioned in the beginning of Subsection 4.3.1, to probe these ground states. This can be done more easily if one decomposes $\mathscr{H}$ as the direct sum of $(k+1)^2$ mutually disjoint subspaces:

$$\mathscr{H} = \bigoplus_{a,b \in \mathcal{L}_k} \mathscr{H}^{ab}, \tag{4.30}$$

where $\mathscr{H}^{ab}$ denotes the subspace whose basis is the following set:

$$\mathcal{B}^{ab} := \big\{ |x_0, x_1, \ldots, x_l\rangle \in \mathcal{B} \mid x_0 = a, x_l = b \big\}, \tag{4.31}$$

with $\mathcal{B}$ introduced in (4.9), and look for zero-energy ground states in each one of the individual sectors $\mathscr{H}^{ab}$ of the total Hilbert space $\mathscr{H}$. This way of determining all zero-energy ground states by probing them separately in each one of these individual sectors of the Hilbert space is valid, because the outer labels x_0 and x_l of any ket $|x_0, x_1, \ldots, x_l\rangle$ do not alter when acted upon by the Hamiltonian H. In other words, all subspaces $\mathscr{H}^{ab}$ are invariant under the action of the Hamiltonian H.

Before giving the general explicit formula for the zero-energy ground states for a generic odd k and a system of size $l \geqslant k$, it would be instructive to describe the mathematical structure of these states for the special cases of $k = 1$ and $k = 3$ first.

Let $k = 1$ first and, consequently, let $\mathcal{L}_1 = \{0, 1/2\}$ be the label set. For any two labels a and b in $\mathcal{L}_1$, let $|\psi^{ab}\rangle$ denote a generic zero-energy ground state in the sector $\mathscr{H}^{ab}$. Thus, $|\psi^{ab}\rangle$ can be written in the following form:

$$|\psi^{ab}\rangle = \sum_{\{x_i\}} C^{ab}(x_1, \ldots, x_{l-1}) \, |a, x_1, \ldots, x_{l-1}, b\rangle. \tag{4.32}$$

Here $C^{ab}(x_1, \ldots, x_{l-1})$'s are, in general, complex numbers and the sum runs over all states in $\mathcal{B}^{ab}$.

Following the strategy outlined in Subsection 4.3.1, it turns out that for any given pair of labels a and b there exists a unique zero-energy ground state in $\mathscr{H}^{ab}$, whose explicit form is given by

$$|\psi^{ab}\rangle = \sum_{\{x_i\}} (-1)^{\#(1/2)} |a, x_1, \ldots, x_{l-1}, b\rangle, \tag{4.33}$$

where $\#(1/2)$ denotes the number of $1/2$ labels in $|a, x_1, \ldots, x_{l-1}, b\rangle$ (including a and b). Hence, for $k = 1$, there exists a total of four zero-energy ground states, one in each sector of the total Hilbert space. The distribution of the number of these states in each sector, is tabulated in the following matrix:

$$M^{(k=1)} = \begin{array}{c} \\ 0 \\ \frac{1}{2} \end{array} \begin{array}{cc} 0 & \frac{1}{2} \\ \left[\begin{array}{cc} 1 & 1 \\ 1 & 1 \end{array} \right]. \end{array} \tag{4.34}$$

Consider now $k = 3$ and $l \geqslant 3$ and the label set $\mathcal{L}_3 = \{0, 1/2, 1, 3/2\}$. Following the same strategy along the lines above and making use of the results of numerical computations for small system sizes as a guide, enabled us to determine the explicit form of all twenty zero-energy ground states in this case. Looking into the structure of these ground states reveals that, in contrast to $k = 1$ case in which all four ground states have the same structure expressed by a single formula (4.32), the twenty ground states in this case fall in two different classes and can be expressed by two formulas, which we discuss in the next few lines.

It turns out that, for any two labels a and b in $\mathcal{L}_3$, there exists a zero-energy ground state $|\psi^{ab}\rangle$ in $\mathscr{H}^{ab}$ with the property that in the expansion of $|\psi^{ab}\rangle$ in terms of the basis states, all basis states in $\mathcal{B}^{ab}$ have a non-zero coefficient. Moreover, the coefficient of $|a, x_1, \ldots, x_{l-1}, b\rangle$ in the expansion of $|\psi^{ab}\rangle$ is

$$(-1)^{[\#(1/2)+\#(3/2)]} d_{1/2}^{-\frac{3}{2} \times \#(1,1/2)},$$

where $\#(3/2)$ is interpreted similar to $\#(1/2)$, and $\#(1, 1/2)$ denotes the number of ordered pairs in the list below

$$(a, x_1), (x_1, x_2), \ldots, (x_{l-2}, x_{l-1}), (x_{l-1}, b)$$

that are equal to the ordered pair $(1, 1/2)$. Here $d_{1/2}$ is the quantum dimension of an anyon of type $1/2$. From Eq. (3.8), it is readily seen that, for $k = 3$, $d_{1/2}$ equals the golden ratio $(1 + \sqrt{5})/2$. We call this type of ground states, *type-one* ground states.

There is also another type of ground states that appear in some, but not all, sectors of the Hilbert space. These are the ones with the property that in their

expansions in terms of basis states, only those basis states $|a, x_1, \ldots, x_{l-1}, b\rangle$ contribute that the set $\{a, x_1, \ldots, x_{l-1}, b\}$ is a subset of $\{1/2, 1\}$ or, in other words, the labels of $|a, x_1, \ldots, x_{l-1}, b\rangle$ are either $1/2$ or 1. Moreover, the coefficient of this basis state is

$$(-1)^{\#(1/2)} \, d_{1/2}^{\frac{1}{2} \times \#(1, 1/2)}.$$

We call these ground states, *type-two* ground states.

From what mentioned above regarding type-one and type-two ground states, in a subspace $\mathscr{H}^{ab}$, if both labels a and b belong to the set $\{1/2, 1\}$, there are two ground states, one of each type, and, if at least one of these labels belongs to the set $\{0, 3/2\}$, there exists only one ground state and it is of the first type. The last statements can be tabulated in the following matrix:

$$M^{(k=3)} = \begin{array}{c c} & \begin{array}{cccc} 0 & \frac{1}{2} & 1 & \frac{3}{2} \end{array} \\ \begin{array}{c} 0 \\ \frac{1}{2} \\ 1 \\ \frac{3}{2} \end{array} & \left[\begin{array}{cccc} 1 & 1 & 1 & 1 \\ 1 & 2 & 2 & 1 \\ 1 & 2 & 2 & 1 \\ 1 & 1 & 1 & 1 \end{array} \right] \end{array}. \tag{4.35}$$

We finalize this subsection by outlining the results regarding the explicit form of the zero-energy ground states for a generic odd k and for a system of size $l \geqslant k$. In the general case, as mentioned earlier, there are $(k+1)(k+2)(k+3)/6$ number of zero-energy ground states and it turns out that they fall into $(k+1)/2$ different types. Let n, $1 \leqslant n \leqslant (k+1)/2$, be given and let a and b be labels in $\mathcal{L}_k$. If both a and b belong to the following set:

$$\mathcal{A} = \left\{ \frac{n-1}{2}, \frac{n+1}{2}, \ldots, \frac{k-(n+1)}{2}, \frac{k-(n-1)}{2} \right\}, \tag{4.36}$$

then there exists a unique zero-energy ground state $|\psi^{ab}\rangle$ in $\mathscr{H}^{ab}$, which we call a *type-n* ground state, with the property that in the expansion of $|\psi^{ab}\rangle$ in terms of elements of $\mathcal{B}^{ab}$, only those basis states $|a, x_1, \ldots, x_{l-1}, b\rangle$ have non-zero coefficients for which the set $\{a, x_1, \ldots, x_{l-1}, b\}$ is a subset of $\mathcal{A}$. To express these coefficients explicitly in an efficient way, we introduce some notation first. Let k be an odd positive integer and let n be an integer such that $1 \leqslant n \leqslant (k+1)/2$. For $i = n, n+1, \ldots, (k+1)/2$,

$$D(k, n, i) := d_{1/2}^{1/2} \, d_{(k-1)/4}^{-1} \, d_{(i-1)/2}^{-1/2} \, d_{i/2}^{-1/2} \, d_{(i-n-1)/4} \, d_{(k-n-i)/4}, \tag{4.37}$$

if $i - n$ is odd; and

$$D(k, n, i) := d_{1/2}^{1/2} \, d_{(k-1)/4}^{-1} \, d_{(i-1)/2}^{-1/2} \, d_{i/2}^{-1/2} \, d_{(n+i-2)/4} \, d_{(k-n+i+1)/4}, \tag{4.38}$$

if $i - n$ is even. The coefficient of $|a, x_1, \ldots, x_{l-1}, b\rangle$ in the expansion of the type-n ground state $|\psi^{ab}\rangle$ then is

$$(-1)^m \prod_{i=n}^{(k+1)/2} [D(k, n, i)]^{\theta_i}, \tag{4.39}$$

where m is the number of half-integers in $|a, x_1, \ldots, x_{l-1}, b\rangle$,

$$\theta_i := \#\left(\frac{i}{2}, \frac{i-1}{2}\right) + \#\left(\frac{k-i+1}{2}, \frac{k-i}{2}\right), \tag{4.40}$$

for $n \leqslant i \leqslant (k-1)/2$, and

$$\theta_{(k+1)/2} := \#\left(\frac{k+1}{4}, \frac{k-1}{4}\right). \tag{4.41}$$

Here $\#(r, s)$, for any numbers r and s, refers to the number of ordered pairs in the following list:

$$(a, x_1), (x_1, x_2), \ldots, (x_{l-2}, x_{l-1}), (x_{l-1}, b)$$

that are equal to (r, s). In addition, the matrix $M^{(k)}$, analogous to matrices (4.34) and (4.35), that tabulates how different types of ground states distribute over various sectors of the Hilbert space has entries m_{ij} accessible by the following relation:

$$m_{ij} = \frac{1}{2} \left[k + 2 - \max\{|k - 4i|, |k - 4j|\} \right], \tag{4.42}$$

where i and j run over the values $0, 1/2, \ldots, k/2$.

Zero-energy Ground States of H_{cl}, The Periodic Chain

In this subsection, k is again assumed to be a given odd integer and the parameters, as before, have the values given in (4.29). The Hamiltonian H_{cl}, which again is given by (4.11), has one term h_l more than the Hamiltonian H investigated in the previous subsection and it acts on $\mathscr{H}_{cl}$ instead of $\mathscr{H}$. Let us recall that this additional term in the Hamiltonian acts on the lth part of the fusion-tree and affects the label $x_0 = x_l$. Therefore, any zero-energy ground state $|\psi\rangle$ of $\mathscr{H}_{cl}$, which again numerical computations indicate the existence of such states for $l \geqslant k + 1$, has to satisfy one more constraint, namely, $h_l|\psi\rangle = 0$. Hence, one would expect that the degeneracy of such states to be smaller than the degeneracy of such states in the previous case. It turns out that the zero-energy ground state of the Hamiltonian H_{cl} can be labeled by an integer n, $1 \leqslant n \leqslant (k+1)/2$. We call this the ground state of type n and denote it by $|GS_n\rangle$. In the expansion of $|GS_n\rangle$ in terms of elements of the basis $\mathcal{B}_{cl}$, only

those basis states contribute whose labels are from the set $\mathcal{A}$ in (4.36). Moreover, if $|x_0, x_1, \ldots, x_{l-1}, x_l\rangle$ is a state in $\mathcal{B}_{\text{cl}}$, that is, if $x_0 = x_l$, and if all the labels of this state belong to the set $\mathcal{A}$, then the coefficient of this state in the expansion of $|\text{GS}_n\rangle$ is given exactly by the same expression (4.39) with slight change in how it should be interpreted. This time m refers to the number of half-integers in the list x_0 till x_{l-1} and θ_i, $i = n, n+1, \ldots, (k+1)/2$, although given by the same relations (4.40) and (4.41), but this time $\#(r, s)$ refers to the number of ordered pairs in the list $(x_0, x_1), (x_1, x_2), \ldots, (x_{l-2}, x_{l-1})$ that are equal to the ordered pair (r, s).

4.3.2   Integrability of the Model

This section is devoted to the discussion around the integrability of the introduced model. Roughly speaking, a quantum system is said to be *integrable* if it accommodates "sufficient" number of commuting quantum operators (conserved charges) so that each one of them commutes with the Hamiltonian of the system as well. By the sufficient number here, one would mean the number of conserved charges that is sufficient to enable one to calculate some quantities of physical interest regarding the system, like the energy spectrum of the system.

The route that is followed in this subsection to study the integrability issue of the model passes through the notions of *Temperley–Lieb* algebra, *Yang–Baxter* equation, and the closely related notion of *transfer* matrices. Based on these, we explore four points in the parameter space at which the model is integrable.

Consider a family of matrices $\{R_i(u)\}_{i\in\mathbb{N}}$, called R-matrices, depending on a parameter u, called the *spectral* parameter, which is, in general, a complex number. Moreover, suppose that these matrices fulfill the equation

$$R_i(u)R_{i+1}(u+v)R_i(v) = R_{i+1}(v)R_i(u+v)R_{i+1}(u), \qquad (4.43)$$

known as the Yang–Baxter equation. Using the R-matrices, we now define a new one-parameter family of matrices $\{T(u)\}_u$, known as transfer matrices, as follows:

$$T(u) := \prod_i R_i(u). \qquad (4.44)$$

It follows from Eq. (4.43) that

$$[T(u), T(v)] = 0, \qquad (4.45)$$

for all values of the parameters u and v. If now one defines the Hamiltonian H_R through the transfer matrix $T(u)$ according to

$$T(u) = \mathrm{e}^{-u\,H_R + o(u^2)}, \qquad (4.46)$$

then clearly

$$[H_R, T(u)] = 0, \tag{4.47}$$

for all values of u. Therefore, we have a large number of commuting observables $T(u)$, one for each value of u, that all of them commute with H_R and, consequently, one can expect that the system described by the Hamiltonian H_R is integrable. In addition, with the aid of Eq. (4.44), the explicit form of the Hamiltonian H_R defined in (4.46) is

$$H_R = -\frac{\mathrm{d}\ln T(u)}{\mathrm{d}u}\bigg|_{u=0} = -\sum_i R_i^{-1}(u=0)\,\frac{\mathrm{d}R_i(u)}{\mathrm{d}u}\bigg|_{u=0}. \tag{4.48}$$

Before applying the above recipe to our model, which turns out to be more complicated, we consider first the simpler case of the dense anyon chain. We recall that a dense anyon chain is the one in which all sites of the chain are filled with spin-1/2 anyons.

Example 4.1 (Integrability of the dense $\mathfrak{su}(2)_k$ anyon chain). Consider an anyon chain with l sites where each site is occupied with a spin-1/2 anyon. The Hilbert space corresponding to this chain is then the space whose basis consists of all fusion-trees in Fig. 4.1 for which the labels are from $\mathcal{L}_k$ and, in particular, y labels are equal to 1/2. We look at a model for this chain in which only next-nearest neighbor interactions are taken into account. We require that this interaction assigns energy $+1$ when two neighboring anyons fuse to zero and assigns zero energy, otherwise. In other words, the Hamiltonian H_{dense} that we consider for this system is

$$H_{\mathrm{dense}} = \sum_{i=1}^{l-1} h_{i,J=1}, \tag{4.49}$$

where $h_{i,J=1}$ is given by Eq. (4.17) for $J = 1$. We now show that the above Hamiltonian, up to a shift and an overall scaling factor, can be obtained from Eq. (4.46) for an aptly chosen set of R matrices and, consequently, according to what mentioned, the model is integrable.

Consider the operators e_i defined by

$$e_i = d_{1/2}\,h_{i,J=1}, \qquad (i = 1, 2, \ldots, l-1), \tag{4.50}$$

and the one-parameter family of operators $R_i(u)$ defined by

$$R_i(u) = \sin\left(\frac{\pi}{k+2} - u\right) I + \sin(u)\,e_i. \tag{4.51}$$

Here $d_{1/2}$ is the quantum dimension of spin-1/2, k is the same as in $\mathfrak{su}(2)_k$, I is the identity operator, and the subscript i indicates the part of the fusion-tree on which the corresponding operator acts. Using Eq. (4.21) for $J = 1$,

it is straightforward to check that the operators e_i satisfy the Temperley–Lieb algebra

$$
\begin{aligned}
e_i^2 &= d_{1/2}\, e_i, &&\text{for all } i,\\
e_i e_{i\pm 1} e_i &= e_i, &&\text{for all } i,\\
[e_i, e_j] &= 0, &&\text{for } |i-j| \geqslant 2.
\end{aligned}
\tag{4.52}
$$

Using only these algebraic properties, one can show that R_i operators, introduced in (4.51), satisfy the Yang–Baxter equation. These R-matrices then can be used in (4.48) to produce a Hamiltonian corresponding to an integrable system. Using (4.51), the Hamiltonian H_R obtained from (4.48) is

$$
H_R = 2\cot\frac{\pi}{k+2}\sum_{i=1}^{l-1}\Big(\frac{1}{2}\,I - \frac{1}{d_{1/2}}\,e_i\Big) = 2\cot\frac{\pi}{k+2}\sum_{i=1}^{l-1}\Big(\frac{1}{2}\,I - h_{i,J=1}\Big).
$$

Hence, the Hamiltonian of the dense anyon chain can be written as:

$$
H_{\text{dense}} = \alpha\, H_R + \beta\, I,
\tag{4.53}
$$

where $\alpha = -\tan(\frac{\pi}{k+2})/2$ and $\beta = (l-1)/2$ and, hence, the dense anyon chain model introduced above is integrable. For further details regarding this example, the reader is referred to [FTL$^+$07]. $\diamondsuit$

The reader notes that the triumph of the method described above to show the integrability of the dense anyon chain model is, to large extent, indebted to the smart specification of R-matrices given in (4.51) and also the educated identification made in (4.50). In the case of the dense anyon-chain model, these were relatively simple due to the fact that there is only one type of term, namely, the interaction term, present in the Hamiltonian. Our goal is to adopt the same strategy to investigate the integrability of the dilute anyon-chain model introduced earlier. Due to the existence of a fairly large number of terms involved in the Hamiltonian of the dilute anyon-chain model, determining the correct expression for the corresponding R-matrices and recognizing identifications similar to the ones given in (4.50) for dilute anyon-chain model, becomes more complicated in this case. We realized similarities between a restricted solid-on-solid (RSOS) model introduced in [WNS92] and the dilute anyon model we are interested in. This similarity is based on the graphical representation introduced in [WNS92] to investigate the corresponding RSOS model.

To describe the idea of this kind of graphical representations, we start with a simple case first. This is the graphical representation of the Temperley–Lieb algebra. We introduce some pictures to serve as operators and describe the graphical rules to multiply them together. Consider l sites and draw a vertical line segment out of each site as depicted in Fig. 4.4 and call it the identity operator I.

$$I = \Big| \quad \Big|_{\cdots} \Big| \quad \Big| \quad \Big| \quad \Big|_{\cdots} \Big| \quad \Big|$$

$$\quad\; 1 \quad\;\; 2 \quad i-1 \quad i \quad\; i+1 \; i+2 \; l-1 \quad l$$
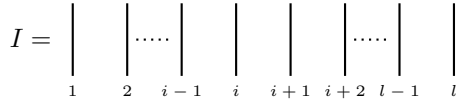
Figure 4.4: Graphical representation of the identity operator.

In addition, consider the operator e_i, $i = 1, \ldots, l-1$, as the one given in Fig. 4.5 in which the sites i and $i+1$ are connected by semicircles at the top and the bottom.

$$e_i = \Big| \quad \Big|_{\cdots} \Big| \quad \asymp \quad \Big|_{\cdots} \Big| \quad \Big|$$

$$\quad\;\; 1 \quad\;\; 2 \quad i-1 \quad i \quad\; i+1 \; i+2 \; l-1 \quad l$$
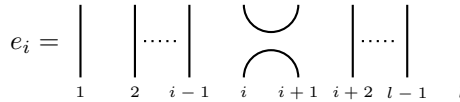
Figure 4.5: Graphical representation of the e_i operator.

We now assign the following rules for multiplying the non-trivial operators e_i. To multiply two operators, we glue the picture corresponding to the operator on the left, on top of the picture corresponding to the operator on the right, respecting two additional rules. The first rule is to consider any two pictures that can be continuously deformed to one another to be the same. The second rule is to consider a closed loop as a factor of some given number d. As an example consider the $l = 4$ case. We, for example, then have the following two relations:

$$e_1 e_2 = \;\; = \;\; = \;\;,$$

$$e_1^2 = \;\; = \;\; = d \;\; = d\, e_1.$$
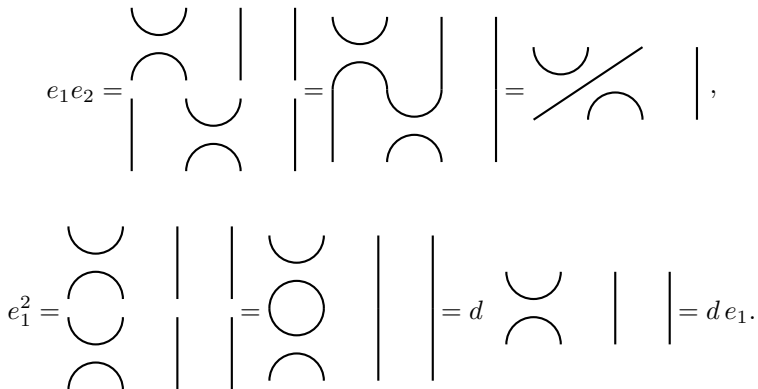
We now start investigating the integrability of the dilute anyon-chain model. Motivated by the graphical representation given in [WNS92] and having a glance at the dilute anyon-chain model, we introduce nine type of graphical operators whose ith part is depicted in Fig. 4.6.

$$
e_{0,i} = \begin{array}{cc} \vdots & \vdots \\ i & i+1 \end{array} \;,\quad
e_{r,i} = \begin{array}{cc} \vdots & | \\ i & i+1 \end{array} \;,\quad
e_{l,i} = \begin{array}{cc} | & \vdots \\ i & i+1 \end{array} \;,\quad
e_{lr,i} = \begin{array}{cc} | & | \\ i & i+1 \end{array}
$$

$$
e_{-,i} = \underset{i \quad i+1}{\times} \;,\quad
e_{+,i} = \underset{i \quad i+1}{\times} \;,\quad
e_{a,i} = \underset{i \quad i+1}{\frown}
$$

$$
e_{c,i} = \underset{i \quad i+1}{\smile} \;,\quad
e_i = \underset{i \quad i+1}{\smile}
$$

Figure 4.6: Operators corresponding to the dilute anyon-chain model.

At other sites that are not explicitly shown in the figure above, a straight line segment is assumed. As becomes clear shortly, these operators will be related to the terms $h_{i,\mu_{00}}$, $h_{i,\mu_{0\fra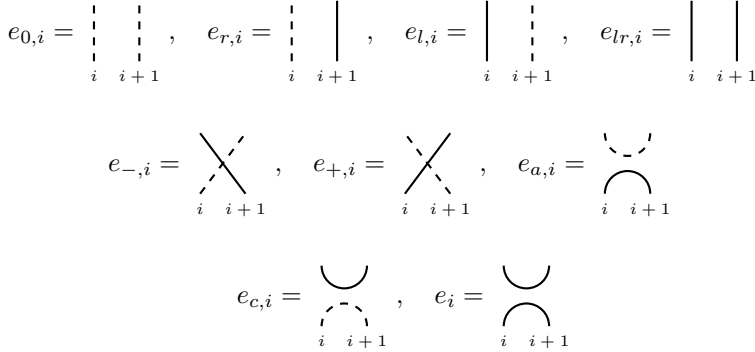c{1}{2}}}$, $h_{i,\mu_{\frac{1}{2}0}}$, $h_{i,\mu_{\frac{1}{2}\frac{1}{2}}}$, $h'_{i,t}$, $h_{i,t}$, $h_{i,\Delta}$, $h'_{i,\Delta}$, and $h_{i,J}$ in the local Hamiltonian (4.12), respectively.

To multiply the operators in Fig. 4.6, as before, we stack the picture corresponding to the operator on the left, on top of the picture corresponding to the operator on the right. Again two pictures that can be continuously deformed to one another are considered to be the same. This time, a closed loop corresponds to a $d_{1/2}$ factor, the quantum dimension of $1/2$ anyon type, and a dashed closed loop corresponds to a $d_0 = 1$ factor. One new rule that we require in this case is that the product of two operators does not vanish only if the operators *match* in the sense that if at some site i from the picture below a dashed (solid) line is terminated, the line originated from the same site i in the picture above must be a dashed (solid) line as well, for all i. For example, $e_{\alpha,i}e_{+,i} = 0$ for all $\alpha \neq r,-$; in addition, $e_{-,i}e_{+,i} = e_{l,i}$ and $e_{r,i}e_{+,i} = e_{+,i}$. Moreover, it is straightforward to convince yourself that the operators $e_{0,i}$, $e_{l,i}$, $e_{r,i}$, and $e_{lr,i}$ act trivially on the matching operators. For example, $e_{0,i}e_{a,i} = e_{a,i}$ and $e_{c,i}e_{0,i} = e_{c,i}$. One can also mention

$$
\begin{aligned}
e_{a,i}e_{c,i} &= d_{1/2}\,e_{0,i}, & e_{a,i}e_i &= d_{1/2}\,e_{a,i}, \\
e_{c,i}e_{a,i} &= e_i, & e_ie_{c,i} &= d_{1/2}\,e_{c,i},
\end{aligned}
\tag{4.54}
$$

as other non-trivial relations between two operators acting on the same site.

Employing the analogy with the dilute loop model considered in [WNS92], we consider the following R-matrices:

$$
\begin{aligned}
R_i(u;\lambda) := &\left[\sin(2\lambda)\cos(3\lambda) + \sin(u)\cos(u+3\lambda)\right] e_{i,0} \\
&+ \sin(2\lambda)\cos(u+3\lambda)\,(e_{i,l} + e_{i,r}) + \sin(2\lambda)\sin(u)\,(e_{i,a} + e_{i,c}) \\
&+ \sin(u)\cos(u+3\lambda)\,(e_{i,+} + e_{i,-}) + \sin(u+2\lambda)\cos(u+3\lambda)\,e_{i,lr} \\
&+ \sin(u)\cos(u+\lambda)\,e_i,
\end{aligned}
$$

defined in terms of the operators in Fig. 4.6, which except for the spectral parameter u, they also depend on an auxiliary parameter λ. Using the multiplication table of the e operators and employing Mathematica, it is a straightforward but a tedious task to verify that, the above matrices satisfy the Yang–Baxter equation (4.43) only if $-2\cos(4\lambda) = d_{1/2}$, or by Eq. (3.8), only if

$$
\lambda = \pm\pi\,\frac{k+2\pm 1}{4(k+2)}. \tag{4.55}
$$

Let λ take one of the values above. To construct the Hamiltonian H_R given by (4.48), we first note that

$$
\begin{aligned}
R_i^{-1}(0;\lambda) &= \frac{1}{\sin(2\lambda)\cos(3\lambda)}\,(e_{0,i} + e_{l,i} + e_{r,i} + e_{lr,i})^{-1} \\
&= \csc(2\lambda)\sec(3\lambda)\,I,
\end{aligned}
$$

and

$$
\begin{aligned}
\frac{\mathrm{d}R_i}{\mathrm{d}u}(u;\lambda)\Big|_{u=0} = &\cos(3\lambda)\,e_{0,i} - \sin(2\lambda)\sin(3\lambda)\,(e_{l,i} + e_{r,i}) \\
&+ \sin(2\lambda)\,(e_{a,i} + e_{c,i}) + \cos(3\lambda)\,(e_{+,i} + e_{-,i}) \\
&+ \cos(5\lambda)\,e_{lr,i} + \cos(\lambda)\,e_i.
\end{aligned}
$$

Therefore,

$$
\begin{aligned}
H_R = \sum_i \Big\{ &-\csc(2\lambda)\,e_{0,i} + \tan(3\lambda)\,(e_{l,i} + e_{r,i}) - \sec(3\lambda)\,(e_{a,i} + e_{c,i}) \\
&-\csc(2\lambda)\,(e_{+,i} + e_{-,i}) - \csc(2\lambda)\sec(3\lambda)\cos(5\lambda)\,e_{lr,i} \\
&-\csc(2\lambda)\sec(3\lambda)\cos(\lambda)\,e_i \Big\}.
\end{aligned}
$$

On the other hand, using relations in (4.54) as a guide and a case-by-case check, one can verify that the operators

$$
\frac{1}{\mu_{00}}\,h_{i,\mu_{00}}, \quad \frac{1}{\mu_{0\frac{1}{2}}}\,h_{i,\mu_{0\frac{1}{2}}}, \quad \frac{1}{\mu_{\frac{1}{2}0}}\,h_{i,\mu_{\frac{1}{2}0}}, \quad \frac{1}{\mu_{\frac{1}{2}\frac{1}{2}}}\,h_{i,\mu_{\frac{1}{2}\frac{1}{2}}},
$$

$$
\frac{1}{t}\,h'_{i,t}, \quad \frac{1}{t}\,h_{i,t}, \quad \frac{\sqrt{d_{1/2}}}{\Delta}\,h'_{i,\Delta},
$$

$$
\frac{\sqrt{d_{1/2}}}{\Delta}\,h_{i,\Delta}, \quad \frac{d_{1/2}}{J}\,h_{i,J},
$$

obey the same algebraic properties met by operators in Fig. 4.6, respectively. Hence, if one replaces the e operators in H_R by their corresponding counterparts from the list above, and letting

$$
\begin{aligned}
\mu_{00} &= -\csc(2\lambda), & t &= -\csc(2\lambda), \\
\mu_{0\frac{1}{2}} = \mu_{\frac{1}{2}0} &= \tan(3\lambda), & \Delta &= -\sqrt{d_{1/2}}\,\sec(3\lambda), \\
\mu_{\frac{1}{2}\frac{1}{2}} &= -\csc(2\lambda)\sec(3\lambda)\cos(5\lambda), & J &= -d_{1/2}\,\csc(2\lambda)\sec(3\lambda)\cos(\lambda),
\end{aligned}
$$

with λ being one of the values given by (4.55), then the Hamiltonian H_R, which is integrable by construction, coincides with the Hamiltonian of the dilute anyon-chain model. Consequently, the dilute anyon-chain model is integrable at, at least, the four points of the parameter space specified by the relations given above, for each λ in (4.55).

Identifying the Critical Points

In this section, we investigate whether or not the dilute anyon-chain model is critical at the points of integrability recognized in the previous section and, if so, we determine the corresponding conformal field theory (CFT) that describes the model at that particular critical point [FMS12,BP09]. The strategy that we follow in this section to accomplish this task—limiting ourselves to $k = 1, 2, 3$ cases and employing the exact diagonalization for systems of small size—is to look at the low-lying part of the energy spectrum of the dilute anyon system at these integrable points and compare the spectrum with the CFT predictions for critical one-dimensional systems. The energy $E(l)$, to order $1/l$, of the states of a one-dimensional system of size l at a critical point describable by a CFT is given by

$$
E(l) = E_s l - \frac{\pi v c}{6l} + \frac{2\pi v}{l}\left(2h_i + n\right) + \cdots, \tag{4.56}
$$

where E_s, the energy per site, and v, the velocity, are non-universal constants. Moreover, c denotes the *central charge* of the corresponding CFT, h_i's are the *scaling dimension*s of the CFT fields, and n is a non-negative integer, which is zero in the case of the *primary* fields and it takes the positive value m for the descendant fields at level m. Because of the non-universal constants in (4.56) for $E(l)$, one cannot directly compare the data gained by the exact diagonalization of the Hamiltonian with the above CFT prediction of the energy spectrum. To overcome this problem, we pursue the following steps.

For a given small system size, we first exactly diagonalize the Hamiltonian to obtain the low-lying part of the energy spectrum and sort it in an ascending order. We then shift the spectrum such that the ground state energy becomes zero. To see now whether a particular CFT indeed describe the model under consideration, we rescale the shifted spectrum such that the energy of the first excited state becomes $2h_{\text{low}}$, where h_{low} denotes the lowest non-vanishing scaling dimension of that CFT. We then compare the low-lying part of the

shifted and rescaled spectrum with the energies obtained from $E = 2h_i + n$ for that CFT. A considerable match, then implies that the particular CFT considered gives a good description of the model.

To see why the strategy outlined above, which will be the basis of recognizing the proper CFT for the dilute anyon-chain model, does in fact work, first note that the CFT corresponding to a physical model (if it exists) has to be unitary. Hence, the scaling dimension of any field is greater than or equal to the scaling dimension h_0 of the identity field, which is equal to zero. The lowest energy E_0 obtained from (4.56) then corresponds to zero value for both n and h_i and, therefore, $E_0 = E_s l - (\pi vc)/(6l)$. If one now shift the energies so that E_0 is set to zero, then we have $E = (2\pi v/l)(2h_i + n)$ and, hence, for the next energy E_1 we have $E_1 = (2\pi v/l)(2h_{\text{low}})$. Therefore, setting E_1 equal to $2h_{\text{low}}$ is equivalent to setting $2\pi v/l$ to one and that in turn is equivalent to having $E = 2h_i + n$, as desired.

Before starting the analysis, noticing one point simplifies the investigation. The values of λ in (4.55) come in two opposite pairs $\pm\lambda_1$ and $\pm\lambda_2$, where

$$\lambda_1 := \pi \frac{k+3}{4\,(k+2)}, \quad \lambda_2 := \pi \frac{k+1}{4\,(k+2)}. \tag{4.57}$$

Furthermore, changing the sign of λ in the relations given for the parameters in terms of λ at the top of the last page, changes the sign of all the parameters except Δ. On the other hand, numerical calculations indicate that the sign of the Δ terms in the Hamiltonian does not affect the energy spectrum. Therefore, the spectrum of H for $-\lambda$ is the same as the spectrum of $-H$ for λ. Hence, in the analysis that follows, instead of considering the four values for λ given by (4.55), we can consider only the two values for λ given in (4.57), provided that in each case we take into account not only the corresponding Hamiltonian but also minus the Hamiltonian as well. Hence, in what follows, we investigate $\pm H_1$ and $\pm H_2$, where H_1 and H_2 denote the Hamiltonian of the dilute anyon-chain model for λ_1 and λ_2, respectively.

The strategy outlined in the previous paragraph of how to identify the CFT corresponding to a critical system works if one has a prior guess, to compare the data with, regarding a suitable CFT that describes the system. In the case of the dilute loop model considered in [WNS92], the system is critical at all four points corresponding to $\pm\lambda_1$ and $\pm\lambda_2$. Moreover, the central charges corresponding to these points given in [WNS92], expressed in terms of parameter k, are as follows:

λ	c	λ	c
$\frac{\pi\,(k+3)}{4\,(k+2)}$	$1 - \frac{6}{(k+2)(k+3)}$	$-\frac{\pi\,(k+3)}{4\,(k+2)}$	$\frac{1}{2} + 1 - \frac{6}{(k+1)(k+2)}$
$\frac{\pi\,(k+1)}{4\,(k+2)}$	$1 - \frac{6}{(k+1)(k+2)}$	$-\frac{\pi\,(k+1)}{4\,(k+2)}$	$\frac{1}{2} + 1 - \frac{6}{(k+2)(k+3)}$

These central charges point in the direction of *unitary minimal-model* CFTs. The unitary minimal models $\mathcal{M}_m$ are labeled by an integer parameter $m \geqslant 3$ and the central charge of $\mathcal{M}_m$, which is given by

$$c = 1 - \frac{6}{m(m+1)}. \tag{4.58}$$

Moreover, the primary fields of the minimal model $\mathcal{M}_m$ is denoted by $\phi_{r,s}$, labeled by two integer parameters r and s, where $1 \leqslant r \leqslant m$ and $1 \leqslant s \leqslant m-1$. In the minimal model $\mathcal{M}_m$, labels (r,s) and $(m+1-r, m-s)$ corresponds to the same primary field and, therefore, there are only $m(m-1)/2$ primary fields for $\mathcal{M}_m$. The scaling dimension $h_{r,s}$ of the primary field $\phi_{r,s}$ is given by

$$h_{r,s} = \frac{[mr - (m+1)s]^2 - 1}{4m(m+1)}. \tag{4.59}$$

The reader should note that the central charge, in its own, is not in general sufficient to determine the corresponding CFT. This is why, in the second accompanied paper, we still needed to investigate the situation for the dilute anyon-chain model considered in the paper. There, we got the following results.

For each value of k, the points corresponding to $\pm\lambda_1$ are critical points. At λ_1 the system is described by the simple minimal model $\mathcal{M}_{k+2}$, and at $-\lambda_1$ the system is described by the product of two minimal models $\mathcal{M}_3 \times \mathcal{M}_{k+1}$, where we identify $\mathcal{M}_2$ with the completely trivial CFT, namely, the one containing just the vacuum state. We also found that, for $k = 1$, the point corresponding to λ_2 is not a critical point, but, for $k \geqslant 2$, it is critical and the system is described by the minimal model $\mathcal{M}_{k+1}$. Finally, for the point corresponding to $-\lambda_2$, we did not succeed in identifying a CFT for the model. For further details, the reader is referred to [GA17].

Part B

Quantum Graphs

Chapter 5

$\mathcal{PT}$-Symmetry and Quantum Star-Graph

This chapter consists of three sections. In Section 5.1, the notion of a $\mathcal{PT}$-symmetric Hamiltonian is introduced. We then see that the spectrum of a $\mathcal{PT}$-symmetric Hamiltonian has reflection symmetry with respect to the real axis of the energy complex plane. Investigating whether or not the converse of the latter statement is true, is a harder problem. This motivates the material in the subsequent sections.

Section 5.2 is a very short introduction on quantum graphs. Quantum graphs are graph-shape objects together with a differential operator and a set of equations, known as vertex conditions, that define the domain of the operator.

Section 5.3, which is based on the third accompanied paper [KMG17], describes a simple model in the context of quantum graphs. As is explained in this section, this models a non-Hermitian operator whose spectrum has reflection symmetry and it is indeed $\mathcal{PT}$-symmetric, where $\mathcal{P}$ is an edge permuting operator and $\mathcal{T}$ is the anti-linear operator of complex conjugation. In other words, we introduce a model for which reflection symmetry of the spectrum implies $\mathcal{PT}$-symmetry.

5.1 $\mathcal{PT}$-Symmetric Quantum Mechanics

It is an axiom of quantum mechanics that physical observables are represented by Hermitian operators. Hermiticiy of the operator in fact certifies reality of the spectrum of the corresponding observable, as is required by a physical theory. In other words, Hermiticity of an operator is a *sufficient*, but *not* necessary, mathematical condition that guarantees the reality of the spectrum of the operator. In 1998, Bessis and Zinn-Justin conjectured that the spectrum of the eigenvalue problem

$$H\psi(x) = E\,\psi(x), \qquad \psi \in L^2(\mathbb{R}), \tag{5.1}$$

with H being the *non-Hermitian* operator

$$H = P^2 + \mathrm{i}\,X^3, \tag{5.2}$$

and P and X being the momentum and the position operators, respectively, is entirely real and positive. Soon afterward, Bender and Boettcher observed

numerically that the spectra of the following class of Hamiltonians:

$$H = P^2 - (\mathrm{i}\,X)^N, \tag{5.3}$$

are entirely real and positive for $N \geqslant 2$ [BB98]. Finally, in 2001, a relatively intricate proof of this conjecture, exploiting ODE/IM correspondence, was given by Dorey et al [DDT01].

The reality of the spectra of the above class of Hamiltonians was interpreted by Bender and Boettcher due to the fact that the above Hamiltonians are $\mathcal{PT}$-symmetric in the sense that

$$[H, \mathcal{PT}] = 0, \tag{5.4}$$

where $\mathcal{P}$ is the *parity* operator that sends x to $-x$ and p to $-p$, and $\mathcal{T}$ is the *time-reversal* operator that sends p to $-p$ and i to $-\mathrm{i}$. The latter is needed for the consistency of the commutation relation $[X, P] = \mathrm{i}$. Note also that:

$$\mathcal{P}^2 = \mathcal{T}^2 = (\mathcal{PT})^2 = I. \tag{5.5}$$

To see why the commutation relation (5.4) may gives rise to a real spectrum for H, we reason, along the lines of [MS04], as follows.

Let H be a $\mathcal{PT}$-symmetric Hamiltonian and let $|\psi\rangle$ be a common eigenstate of H and $\mathcal{PT}$ with eigenvalues E and λ, respectively. We then, using Eq. (5.5), have

$$|\psi\rangle = \mathcal{PTPT}|\psi\rangle = \mathcal{PT}(\lambda\,|\psi\rangle) = \lambda^*\lambda\,|\psi\rangle,$$

and, therefore, $|\lambda| = 1$. On the other hand,

$$0 = (H\mathcal{PT} - \mathcal{PT}H)|\psi\rangle = \lambda(E - E^*)|\psi\rangle,$$

and $E = E^*$, that is, E is real. Consequently, if H is $\mathcal{PT}$-symmetric and if H and $\mathcal{PT}$ are simultaneously diagonalizable[§], then H has a spectrum that is entirely real. Of course, to determine if H and $\mathcal{PT}$ are simultaneously diagonalizable is a highly non-trivial problem.

Consider now the $\mathcal{PT}$-symmetric Hamiltonian H that is not simultaneously diagonalizable with $\mathcal{PT}$. Then there exists an eigenstate $|\chi\rangle$ of H that is not an eigenstate of $\mathcal{PT}$. Since $|\chi\rangle$ is not an eigenstate of $\mathcal{PT}$, $|\phi\rangle := \mathcal{PT}|\chi\rangle$ is a non-zero state that is not parallel to $|\chi\rangle$. Since H is assumed to be $\mathcal{PT}$-symmetric, we have

$$0 = (H\mathcal{PT} - \mathcal{PT}H)|\chi\rangle,$$

which implies

$$H|\phi\rangle = E^*\,|\phi\rangle, \tag{5.6}$$

where E is the eigenvalue of H corresponding to $|\chi\rangle$. In other words, E^* is also an eigenvalue of H. Moreover, if E is a non-degenerate eigenvalue of H, then

---

[§]Note that (5.4) in its own does not in general imply that H and $\mathcal{PT}$ are simultaneously diagonalizable, since $\mathcal{PT}$ is an anti-linear operator rather than being a linear operator.

acting on both sides of (5.6) by $\mathcal{PT}$ implies that E^* is also non-degenerate. One can show that, if E is a d-fold degenerate eigenvalue, then E^* is also d-fold degenerate. The general conclusion regarding the spectrum of a $\mathcal{PT}$-symmetric Hamiltonian is then as follows.

The spectrum of a $\mathcal{PT}$-symmetric Hamiltonian H is either entirely real, and this occurs when H and $\mathcal{PT}$ are simultaneously diagonalizable, or it consists of two disjoint parts. One part is a subset (possibly empty) of the real numbers and onex other part is a list of non-real numbers whose elements can be grouped in conjugate pairs, and this occurs when the $\mathcal{PT}$ symmetry of H is *spontaneously broken*, that is, when H and $\mathcal{PT}$ are not simultaneously diagonalizable. Both cases above can be unified as follows that if H is $\mathcal{PT}$-symmetric, then the spectrum of H has reflection symmetry with respect to the real axis.

From the discussion above, one notes that, even if the Hamiltonian H is non-Hermitian, it is still possible for H to have an entirely/partly real spectrum. As mentioned earlier, this is due to the fact that the Hermiticity, which is a purely mathematical constraint on the Hamiltonian, is in fact a sufficient but not a necessary condition for the reality of the spectrum of H. This was the insight of Bender and Boettcher that associated the reality of the spectrum with a more sensible and physical constraint on the Hamiltonian, that is, $\mathcal{PT}$-symmetry of the Hamiltonian.

A natural question at this stage would be whether or not one can conclude the opposite statement. In other words, if one knows that the spectrum of a non-Hermitian Hamiltonian H has reflection symmetry with respect to the real axis, is it necessarily true that H is $\mathcal{PT}$-symmetric? In the next section and in the context of quantum graphs, we investigate an example of a non-Hermitian operator for which the converse statement turns out to be true as well.

5.2 Quantum Graphs

Although some of the problems that are classified nowadays under the title of quantum graphs have appeared in the literature since 1930s in different areas of physics, mathematics, and chemistry [Pau36]; it is only two decades that quantum graphs has found its role as an independent and fast growing field of research in mathematical physics and science. A main reason for this surge of interest to the field is due to the diversity of its applications and the fact that many problems in science can be modeled naturally in the language of quantum graphs.

In this section, we give a brief introduction to the concepts that are necessary to state the problem we want to solve. For a more thorough introduction the reader is referred to [BK13, Kur]

The reader might recall the definition of a graph, which we call a *discrete graph*, from her elementary courses in discrete mathematics. A discrete graph G is an ordered pair (V, E) composed of a non-empty finite set V, called the

vertex set, and a set E, called the *edge set*, whose elements are two-element subsets of V. Each member of V is called a *vertex* and each element of E is called an *edge*. It is easier to work with a diagram of a discrete graph instead of its abstract definition. This is due to the fact that, in the context of a discrete graph, one does not need to care about geometrical properties of the diagrams representing the graph. All that matters is whether two vertices are connected or not, regardless of the geometry of the line(s) or curve(s) connecting them. Therefore, in a discrete graph, the priority is with the set of vertices and the set of edges is built on the former set.

Since edges are one-dimensional objects, as the first attempt to define a metric graph, it seems natural to consider each edge as an interval on the real line having certain length.

Definition 5.1. A *metric graph* Γ is an ordered pair $(\mathcal{E}, \mathcal{V})$ composed of two sets $\mathcal{E}$ and $\mathcal{V}$. The set $\mathcal{E}$ consists of closed intervals $[x_i, x_j]$ and the set $\mathcal{V}$ is a partition of the set $\mathbb{V}$, which is the set consisting of all end points of the intervals in $\mathcal{E}$. Each interval in $\mathcal{E}$ is called an *edge* and each set in $\mathbb{V}$ is called a *vertex*. The number of elements in each vertex is called the *degree* of that vertex.

Example 5.2. Fig. 5.1 shows a typical metric graph with edges $e_1 = [x_1, x_2]$, $e_2 = [x_3, x_4]$, $e_3 = [x_5, x_6]$, and $e_4 = [x_7, x_8]$, and vertices $v_1 = \{x_1, x_2, x_4\}$, $v_2 = \{x_3\}$, $v_3 = \{x_5, x_8\}$, and $v_4 = \{x_6, x_7\}$.
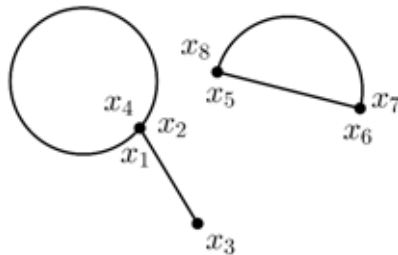
Figure 5.1: A typical metric graph

A function f, defined on a metric graph Γ with N edges, is an N-tuple $(f_1, \ldots, f_N)$ of functions so that the domain of f_j is a function space, like the set of all square-integrable functions, characterized by jth edge e_j of Γ, for all $1 \leqslant j \leqslant N$.

Definition 5.3. A *quantum graph* is a triple $(\Gamma, \mathbf{D}, \text{VC})$, where Γ is a metric graph, $\mathbf{D}$ is a differential expression, and VC is a set of equations, referred to as the *vertex conditions*, that relates the values of the functions, defined on Γ, at the vertices. One can consider VC as the constraints that defines the *domain*

of the differential operator $\mathbf{D}$. The metric graph Γ is then called the *underlying metric graph*.

Depending on the phenomenon that one would like to describe, one may consider different differential expressions for $\mathbf{D}$, and also different VCs. The most widely used differential expressions are the *Laplace*, the *Schrödinger*, and the *magnetic Schrödinger* operators described below.

(i) The *Laplace* operator $\mathbf{D}$:

$$\mathbf{D} := -\frac{\mathrm{d}^2}{\mathrm{d}x^2}. \tag{5.7}$$

This operator corresponds to the free particle.

(ii) The *Schrödinger* operator $\mathbf{D}_v$:

$$\mathbf{D}_v := -\frac{\mathrm{d}^2}{\mathrm{d}x^2} + v(x), \tag{5.8}$$

where $v(x)$ is the *electric potential*.

(iii) The *magnetic Schrödinger* operator $\mathbf{D}_{v,a}$:

$$\mathbf{D}_{v,a} := \left(\mathrm{i}\,\frac{\mathrm{d}}{\mathrm{d}x} + a(x)\right)^2 + v(x), \tag{5.9}$$

where $a(x)$ is the *magnetic potential*.

Obviously, the Laplace and the Schrödinger operators are special cases of the magnetic Schrödinger operator for zero electric potential and/or zero magnetic potential. In this thesis, however, we consider the Laplace operator and denote it by L.

There are also different VCs considered in different contexts. In a quantum graph $(\Gamma, \mathbf{D}, \mathrm{VC})$, the VCs are usually chosen so that the operator $\mathbf{D}$ be a self-adjoint operator on Γ, but, as it is the case in this thesis, this is not a necessity. The VCs considered in this thesis are the *standard* VCs and *Robin* VCs introduced below.

Let $f = (f_1, \ldots, f_N)$ be a function defined on a metic graph with N edges and let v be a vertex of this graph of degree d on edges e_{j_1} till e_{j_d}.

(i) The standard VCs at the vertex v are the following relations:

$$f_{j_1}(v) = \cdots = f_{j_d}(v), \qquad \text{(Continuity at } v)$$
$$\partial_{\boldsymbol{n}} f_{j_1}(v) + \cdots + \partial_{\boldsymbol{n}} f_{j_d}(v) = 0, \qquad \text{(Current conservation at } v)$$

where $\partial_{\boldsymbol{n}}$ denotes the *normal* derivative defined as follows:

$$\partial_{\boldsymbol{n}} f_{j_k}(v) = \begin{cases} +f'_{j_k}(v), & \text{if } v \text{ is the left end point of the interval } e_{j_k}; \\[2mm] -f'_{j_k}(v), & \text{if } v \text{ is the right end point of the interval } e_{j_k}. \end{cases}$$

In other words, the normal derivatives are taken in an *outgoing* direction, namely, they are taken in the directions away from the vertex and into the edge.

(ii) The Robin VCs with given parameters h_{j_1} till h_{j_d} at the vertex v are the following relations:

$$\partial_{\boldsymbol{n}} f_{j_i}(v) = h_i \, f_{j_i}(v), \qquad 1 \leqslant i \leqslant d.$$

One main theme in studying a quantum graph $(\Gamma, \mathbf{D}, \mathrm{VC})$ is to look at the spectrum of the differential operator $\mathbf{D}$ subject to the given set of vertex conditions VC. A complex number λ is an *eigenvalue* of the quantum graph $(\Gamma, \mathbf{D}, \mathrm{VC})$ with N edges, if there exists a non-zero N-tuple $(u_1, \ldots, u_N)$ satisfying all given vertex conditions VC such that $\mathbf{D} u_j = \lambda \, u_j$, for all j.

5.3   Quantum Equilateral Star-Graph

Inspired by the results in the context of $\mathcal{PT}$-symmetric quantum mechanics described in the previous section regarding non-Hermitian Hamiltonians with real spectrum, we investigate similar ideas by looking at a simplified model in the context of quantum graphs. In particular, we cook up a model of a quantum graph for which the reflection symmetry of the spectrum of the corresponding operator with respect to the real axis is indeed equivalent to $\mathcal{PT}$-symmetry, in the sense that is defined later, of the underlying metric graph. The metric graph that we consider here is the equilateral star-graph depicted in Fig. 5.2 and the corresponding operator the one-dimensional Laplace operator $-\mathrm{d}^2/\mathrm{d}x^2$. The corresponding vertex conditions are the standard vertex condition at the internal vertex together with Robin vertex conditions, with at least one non-real Robin parameter, at the external vertices. As becomes clear shortly, on the domain specified by the above vertex conditions the Laplace operator is in general not self-adjoint.

Let N be an integer larger than two. Consider the Hilbert space

$$\mathscr{H} := \mathrm{L}^2(0,1) \times \cdots \times \mathrm{L}^2(0,1), \tag{5.10}$$

as the Cartesian product of N copies of the space $\mathrm{L}^2(0,1)$, which is the space consisting of square-integrable complex-valued functions defined on the interval

$(0, 1)$, equipped with the following inner product:

$$\langle\, \boldsymbol{u} \,,\, \boldsymbol{v} \,\rangle := \sum_{i=1}^{N} \int_{0}^{1} u_i^*(x) v_i(x) \, \mathrm{d}x, \qquad (5.11)$$

for every $\boldsymbol{u} = (u_1, \ldots, u_N)$ and $\boldsymbol{v} = (v_1, \ldots, v_N)$ in $\mathscr{H}$. Let h_1 till h_N, known as Robin parameters, be given complex numbers and let $\boldsymbol{h}$ denote the N-tuple $(h_1, \ldots, h_N)$. We now consider the Laplace operator $L_{\boldsymbol{h}} = -\mathrm{d}^2/\mathrm{d}x^2$ with the domain $\mathrm{Dom}(L_{\boldsymbol{h}})$ consisting of all N-tuples $\boldsymbol{u} = (u_1, \ldots, u_N)$ such that each component u_j belongs to the Sobolev space $W_2^2(0, 1)$ and, moreover, the components satisfy standard vertex conditions at the internal vertex, namely,

$$\begin{aligned} u_1(1) = u_2(1) = \cdots = u_N(1), \\ u_1'(1) + u_2'(1) + \cdots + u_N'(1) = 0, \end{aligned} \qquad (5.12)$$

and the Robin vertex conditions at the external vertices, namely,

$$u_j'(0) = h_j\, u_j(0), \qquad 1 \leqslant j \leqslant N. \qquad (5.13)$$

In the context of quantum graphs, what mentioned above can easily be visualized as the following equilateral star-graph subject to standard vertex conditions at the internal vertex and Robin vertex conditions, with parameters h_1 till h_N, at the external vertices, with the Laplacian $L_{\boldsymbol{h}}$ as the operator acting on it.
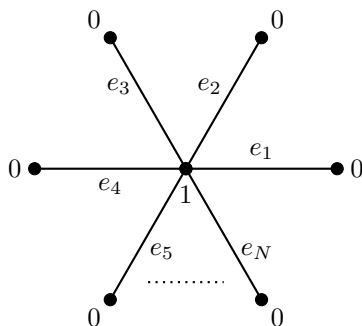
Figure 5.2: Star-graph Γ with N edges.

Using integration by parts, for $\boldsymbol{u}$ and $\boldsymbol{v}$ in $\mathrm{Dom}(L_{\boldsymbol{h}})$, we obtain

$$\langle\, L_{\boldsymbol{h}}\boldsymbol{u} \,,\, \boldsymbol{v} \,\rangle - \langle\, \boldsymbol{u} \,,\, L_{\boldsymbol{h}}\boldsymbol{v} \,\rangle = \sum_{i=1}^{N} (h_i^* - h_i) u_i^*(0) v_i(0), \qquad (5.14)$$

which does not in general vanish, since we allow for complex Robin parameters. Therefore, $L_{\boldsymbol{h}}$ defined above is not necessarily self-adjoint and the spectrum of $L_{\boldsymbol{h}}$ might contain non-real eigenvalues.

5.3.1   Definitions and Notations

To investigate the relation between the symmetries of the underlying metric graph Γ in Fig. 5.2 and the reflection-symmetry of the spectrum of $L_{\boldsymbol{h}}$ with respect to the real axis, we need to define a few notions and fix some notations first.

We use boldface letters to indicate N-tuples. In this context $\boldsymbol{c}_i$, for example, denotes the $(N-1)$-tuple obtained from $\boldsymbol{c}$ by suppressing its ith component.

An N-tuple is said to be *invariant under conjugation* if the non-real components of it can be grouped in conjugate pairs. For example, $\boldsymbol{c} = (-\mathrm{i}, 3, \mathrm{i}, -\mathrm{i}, \mathrm{i})$ is invariant under conjugation, whereas $\boldsymbol{d} = (2, 3\mathrm{i}, 3\mathrm{i}, -3\mathrm{i})$ is not.

The anti-linear operator $\mathcal{T}$ acting on $\mathscr{H}$ is the *time-reversal* operator defined by

$$\mathcal{T}\boldsymbol{u} = \boldsymbol{u}^*, \qquad \boldsymbol{u} \in \mathscr{H}, \tag{5.15}$$

where $\boldsymbol{u}^*$ denotes the N-tuple obtained from $\boldsymbol{u}$ by conjugating all its components.

For $1 \leqslant i \leqslant j \leqslant N$, the linear operator $\mathcal{P}_{i,j}$, which is called the (ij)th edge permutation operator, is an operator with domain $\mathscr{H}$ that interchanges the ith and the jth components of the N-tuple on which it acts, and does not affect other components. Moreover, for $1 \leqslant i \leqslant N$, $\mathcal{P}_{i,i}$ is the identity operator $\mathrm{id}_{\mathscr{H}}$ on $\mathscr{H}$.

A linear operator $\mathcal{S}$ acting on $\mathscr{H}$ is called a symmetry of $L_{\boldsymbol{h}}$ if $L_{\boldsymbol{h}}\mathcal{S} = \mathcal{S}L_{\boldsymbol{h}}$. The operator $L_{\boldsymbol{h}}$ in this case is said to be $\mathcal{S}$-symmetric. The relation $L_{\boldsymbol{h}}\mathcal{S} = \mathcal{S}L_{\boldsymbol{h}}$ implies that, for $\mathcal{S}$ to be a symmetry of $L_{\boldsymbol{h}}$, $\mathrm{Dom}(L_{\boldsymbol{h}})$ has to be invariant under the action of $\mathcal{S}$, that is, $\mathcal{S}\big(\mathrm{Dom}(L_{\boldsymbol{h}})\big) \subseteq \mathrm{Dom}(L_{\boldsymbol{h}})$.

We recall the definition of the mth elementary symmetric polynomial from Subsection 2.5.2. Since, in this chapter, the mth edge of the star-graph Γ is denoted by e_m, we use s_m, instead of e_m, to denote the mth elementary symmetric polynomial. For a non-negative integer m, the mth elementary symmetric polynomial $s_m(x_1, \ldots, x_N)$ in N variables x_1 till x_N is defined to be the constant polynomial that is equal to one, if $m = 0$; the zero polynomial, if $m \geqslant N + 1$; and it is defined by:

$$s_m(x_1, \ldots, x_N) = \sum x_{i_1} \cdots x_{i_m}; \tag{5.16}$$

otherwise. The sum is over all indices i_1 till i_m such that $1 \leqslant i_1 < \cdots < i_m \leqslant N$.

5.4   The Main Theorem

The rest of this chapter is devoted to explaining the strategy pursued in the third accompanied paper [KMG17] to prove Theorem 5.4, which is the main result of the paper. This theorem relates the reflection symmetry, with respect to the real axis, of the spectrum of L_h to a certain symmetry, namely, $\mathcal{PT}$-symmetry, of this operator, where $\mathcal{P}$ is a symmetry of the underlying metric star-graph Γ of Fig. 5.2.

Theorem 5.4. *The spectrum of the operator L_h has reflection symmetry with respect to the real axis if and only if L_h is $\mathcal{PT}$-symmetric, where $\mathcal{P}$ is a symmetry of the underlying metric star-graph Γ.*

5.4.1   Proof of the "only if" part of Theorem 5.4

The proof of the "only if" part of the above theorem is rather straightforward. In fact, the statement expressed in the "only if" part of this theorem follows from the following more general argument, whose proof is given in Appendix A of [KMG17].

Proposition 5.5. *Let $\mathcal{AT}$, where $\mathcal{A}$ is an invertible linear operator defined on a Hilbert space H and $\mathcal{T}$ is the time-reversal operator, be a symmetry for a linear operator L acting on H, namely, $\mathcal{AT}L = L\mathcal{AT}$. Then if λ is an eigenvalue of L with degeneracy d, then $\overline{\lambda}$ is also an eigenvalue of L with the same degeneracy d.*

5.4.2   Proof of the "if" Part of Theorem 5.4

The proof of the "if" part, which claims the reflection symmetry of the spectrum of L_h with respect to the real axis implies its $\mathcal{PT}$-symmetry, is much harder. In the following, we just outline the the strategy employed in [KMG17] to prove this by just reviewing the ideas of the proofs in each step.

First, consider the following theorem, which relates the reflection symmetry of the spectrum of L_h to the reality of the elementary symmetric polynomials $s_1(\boldsymbol{h})$ till $s_N(\boldsymbol{h})$:

Theorem 5.6. *If the spectrum of the operator L_h has reflection symmetry with respect to the real axis, then, for all $1 \leqslant m \leqslant N$, $s_m(\boldsymbol{h})$ is real.*

We first show that the "if" part of Theorem 5.4 follows from the theorem above and, then, concentrate ourselves on the proof of this theorem instead. To do this, we first prove two lemmas. The first one is

Lemma 5.7. *If $\boldsymbol{h}$ is invariant under conjugation, then there exists a symmetry $\mathcal{P}$ of the underlying metric star-graph Γ such that L_h is $\mathcal{PT}$-symmetric.*

The idea of the proof of this lemma is that, if $\boldsymbol{h}$ is invariant under conjugation, then $L_{\boldsymbol{h}}$ is $\mathcal{PT}$-symmetric, where $\mathcal{P}$ is a product of edge permutation operators, defined by $\mathcal{P} = \prod_{j=1}^{m} \mathcal{P}_{2j-1,2j}$. Here m denotes the number of complex conjugate pairs in $\boldsymbol{h}$ and, without loss of generality, we have assumed that the components of $\boldsymbol{h}$ are such that $h_{2j} = h_{2j-1}^*$, for $1 \leqslant j \leqslant m$.

The second lemma is:

Lemma 5.8. *An N-tuple $\boldsymbol{c} = (c_1, \ldots, c_N)$ consisting of complex numbers is invariant under conjugation if and only if, for all $1 \leqslant m \leqslant N$, $s_m(\boldsymbol{c})$ is real.*

To prove this, we employ the identity $\prod_{j=1}^{N}(x + c_j) = \sum_{k=0}^{N} s_k(\boldsymbol{c}) \, x^{N-k}$ and symmetry properties of elementary symmetric polynomials $s_1(\boldsymbol{h})$ till $s_N(\boldsymbol{h})$.

It is now readily seen that Theorem 5.6 together with Lemmas 5.7 and 5.8, implies the "if" part of the main Theorem 5.4. Therefore, to prove the "if" part of Theorem 5.4, we only need to prove Theorem 5.6. In what follows, we briefly discuss the general ideas of the proof. For the actual proof, the reader is referred to [KMG17].

A natural starting point toward a proof of Theorem 5.6 is to determine the secular equation of $L_{\boldsymbol{h}}$, whose solution set is the spectrum of $L_{\boldsymbol{h}}$. If $\lambda := z^2$ is a non-zero eigenvalue of $L_{\boldsymbol{h}}$, then there exists a non-zero $\boldsymbol{u}$ in $\mathrm{Dom}(L_{\boldsymbol{h}})$ so that $L_{\boldsymbol{h}}\boldsymbol{u} = z^2 \, \boldsymbol{u}$. Writing the latter equation in terms of components, we come to the following N second order differential equations:

$$-\frac{\mathrm{d}^2}{\mathrm{d}x^2} u_i(x) = z^2 \, u_i(x), \qquad i = 1, 2, \ldots, N, \tag{5.17}$$

with the general solutions

$$u_i(x) = A_i \cos zx + B_i \sin zx, \qquad i = 1, 2, \ldots, N. \tag{5.18}$$

Applying the vertex conditions (5.12) and (5.13) on the solutions above and requiring that $\boldsymbol{u}$ is non-zero, the secular equation of $L_{\boldsymbol{h}}$ is $D_{\boldsymbol{h}}(z) = 0$, where

$$D_{\boldsymbol{h}}(z) := \sum_{i=1}^{N} \left(\beta_{h_i}(z) \prod_{\substack{j=1 \\ j \neq i}}^{N} \alpha_{h_j}(z) \right), \tag{5.19}$$

and

$$\begin{aligned} \alpha_{h_i}(z) &:= z \cos zx + h_i \sin zx, \\ \beta_{h_i}(z) &:= -z \sin zx + h_i \cos zx. \end{aligned} \tag{5.20}$$

The details of the calculations that give rise to Eq. (5.19) are given in Section 4 of [KMG17]. From this equation, it is seen that $D_{\boldsymbol{h}}$ is an entire function of z. In addition, we have

$$\left(D_{\boldsymbol{h}}(z^*) \right)^* = D_{\boldsymbol{h}^*}(z). \tag{5.21}$$

It is now straightforward to see that, if all Robin parameters are zero, that is, if $\boldsymbol{h} = \boldsymbol{0}$, then Eq. (5.19) reduces to

$$D_{\boldsymbol{0}}(z) = -N\, z^N \sin z (\cos z)^{N-1}, \tag{5.22}$$

with the following solution set:

$$\big\{ n\,\pi \mid n \text{ is an integer} \big\} \bigcup \big\{ n\,\pi + \pi/2 \mid n \text{ an integer} \big\}. \tag{5.23}$$

The roots $n\,\pi$ are each of multiplicity one and the roots $n\,\pi + \pi/2$ are each of multiplicity $N-1$. In what follows, we focus on the first set of roots that are easier to handle.

Consider now the case in which at least one of the Robin parameters is non-zero, and let $\widetilde{z}_n(\boldsymbol{h})$, for some positive integer n, denote a root of the secular equation $D_{\boldsymbol{h}}(z) = 0$. In [KMG17], we show that this root can be written as

$$\widetilde{z}_n(\boldsymbol{h}) = n\,\pi + \Delta_n(\boldsymbol{h}), \tag{5.24}$$

where the deviation term $\Delta_n(\boldsymbol{h})$ takes the following form:

$$\Delta_n(\boldsymbol{h}) = \frac{a_1(\boldsymbol{h})}{n} + \frac{a_3(\boldsymbol{h})}{n^3} + \frac{a_5(\boldsymbol{h})}{n^5} + \cdots, \tag{5.25}$$

for some coefficients $a_i(\boldsymbol{h})$ and for sufficiently large n. This can also be understood perturbatively as follows. Using the following proposition:

Proposition 5.9. *Let $\boldsymbol{c} = (c_1, \ldots, c_N)$, and let i and j be integers such that $1 \leqslant i \leqslant N$ and $0 \leqslant j \leqslant N - 1$. Then*

$$c_i\, s_j(\boldsymbol{c}_i) = s_{j+1}(\boldsymbol{c}) - s_{j+1}(\boldsymbol{c}_i), \tag{5.26}$$

$$\sum_{i=1}^{N} s_j(\boldsymbol{c}_i) = (N - j)\, s_j(\boldsymbol{c}), \tag{5.27}$$

whose proof is given in Appendix B of [KMG17], one can write $D_{\boldsymbol{h}}(z)$, given in (5.19), as follows:

$$D_{\boldsymbol{h}}(z) = -N\, z^N \sin z (\cos z)^{N-1} + z^N \sum_{k=1}^{N} \frac{s_k(\boldsymbol{h})}{z^k}\, f_k(z), \tag{5.28}$$

where

$$f_k(z) := (k - N \sin^2 z)(\sin z)^{k-1}(\cos z)^{N-k-1}, \qquad k = 1, 2, \ldots, N. \tag{5.29}$$

The derivation of the above relations is given in [KMG17]. Therefore, for any non-zero z, we have

$$\frac{D_{\boldsymbol{h}}(z)}{z^N} = -N \sin z (\cos z)^{N-1} + \sum_{k=1}^{N} \frac{s_k(\boldsymbol{h})}{z^k}\, f_k(z). \tag{5.30}$$

For any positive integer n, $n\pi$ is a root of the first term on the right side of (5.30). On the other hand, we have:

$$\left|\frac{s_k(\boldsymbol{h})}{z^k}\right| \leqslant \binom{N}{k}\left(\frac{h}{|z|}\right)^k, \qquad (5.31)$$

where $h := \max\{|h_1|, \ldots, |h_N|\}$. Thus, the second term on the right side of (5.30) can be made arbitrarily small by choosing z inside a circle of some fixed and small radius centered at $n\pi$, for sufficiently large n. Since this term is continuous, one would then expect that the equation $D_{\boldsymbol{h}}(z) = 0$ has a root that is arbitrary close to $n\pi$ for an n that is large enough.

To finalize the proof of Theorem 5.6, one needs to investigate the structure of the coefficients $a_i(\boldsymbol{h})$ in (5.25). We Taylor expand the right side of (5.28) at $z = 0$ and then substitute $n\pi + \Delta_n(\boldsymbol{h})$, with $\Delta_n(\boldsymbol{h})$ given by (5.25), into the Taylor expansion, and write the outcome as a series in n. It turns out that the powers of n that appear in this expansion are n^{N-2i+1}, $i = 0, 1, 2, 3, \ldots$. For $\widetilde{z}_n(\boldsymbol{h}) = n\pi + \Delta_n(\boldsymbol{h})$ to be a root of the secular equation $D_{\boldsymbol{h}}(z) = 0$, it is necessary and sufficient that the coefficients of all powers of n mentioned above vanish. We get the following result:

$$a_{2i-1}(\boldsymbol{h}) = s_1(\boldsymbol{h})\, F_i\big(s_1(\boldsymbol{h}), \ldots, s_{i-1}(\boldsymbol{h})\big) + \frac{i}{\pi^{2i-1}N^i}\big(s_1(\boldsymbol{h})\big)^{i-1} s_i(\boldsymbol{h}), \quad (5.32)$$

for $i = 2, 3, 4, \ldots$, where F_i is a polynomial of degree $2i$ in $i-1$ variables, whose coefficients are real-valued rational functions of N. In addition, we get

$$a_1(\boldsymbol{h}) = \frac{1}{\pi N}\, s_1(\boldsymbol{h}). \qquad (5.33)$$

The important point that reveals itself in Eqs. (5.32) and (5.33) is that $s_i(\boldsymbol{h})$ appears, for the first time, in the equation for $a_{2i-1}(\boldsymbol{h})$ and it appears there with exponent equal to one. Since the spectrum of $L_{\boldsymbol{h}}$ is assumed to possess reflection symmetry with respect to the real axis, $D_{\boldsymbol{h}}(z) = 0$ if and only if $D_{\boldsymbol{h}}(z^*) = 0$ and, by Eq. (5.21), this is equivalent to $D_{\boldsymbol{h}^*}(z) = 0$. Thus, $\widetilde{z}_n(\boldsymbol{h})$ is a root of $D_{\boldsymbol{h}^*}(z)$ as well.

One can now repeat the same procedure mentioned on the paragraph previous to Eq. (5.32) on $D_{\boldsymbol{h}^*}(z)$ instead. This together with $s_m(\boldsymbol{h}^*) = s_m^*(\boldsymbol{h})$, for $m = 1, \ldots, N$, then give rise to the following equations:

$$a_1(\boldsymbol{h}) = \frac{1}{\pi N}\, s_1^*(\boldsymbol{h}), \qquad (5.34)$$

and

$$a_{2i-1}(\boldsymbol{h}) = s_1^*(\boldsymbol{h})\, F_i\big(s_1^*(\boldsymbol{h}), \ldots, s_{i-1}^*(\boldsymbol{h})\big) + \frac{i}{\pi^{2i-1}N^i}\big(s_1^*(\boldsymbol{h})\big)^{i-1} s_i^*(\boldsymbol{h}), \quad (5.35)$$

for all i greater than one.

Eqs. (5.33) and (5.34) imply that $s_1(\boldsymbol{h})$ is real. Assume now that $s_1(\boldsymbol{h})$ till $s_{k-1}(\boldsymbol{h})$, $2 \leqslant k \leqslant N$, are real. Eqs. (5.35) and (5.32), then imply that $s_k(\boldsymbol{h})$ is also real. Hence, all polynomials $s_1(\boldsymbol{h})$ till $s_N(\boldsymbol{h})$ are real and Theorem 5.6 is then proven.

In conclusion, we showed that the spectrum of the operator $L_{\boldsymbol{h}}$, which is not necessarily self-adjoint, has reflection symmetry with respect to the real axis if and only if the N-tuple $\boldsymbol{h} = (h_1, \ldots, h_N)$, consisting of the Robin parameters, is invariant under conjugation.

Bibliography

[ABF84]   George E Andrews, Rodney J Baxter, and Peter J Forrester. Eight-vertex sos model and generalized rogers-ramanujan-type identities. *Journal of Statistical Physics*, 35(3):193–266, 1984.

[AKLT87]   Ian Affleck, Tom Kennedy, Elliott H Lieb, and Hal Tasaki. Rigorous results on valence-bond ground states in antiferromagnets. *Physical review letters*, 59(7):799, 1987.

[Ard02]   Eddy Ardonne. Parafermion statistics and application to non-abelian quantum hall states. *Journal of Physics A: Mathematical and General*, 35(3):447, 2002.

[ARRS01]   Eddy Ardonne, N Read, Edward Rezayi, and Kareljan Schoutens. Non-abelian spin-singlet quantum hall states: wave functions and quasihole state counting. *Nuclear Physics B*, 607(3):549–576, 2001.

[ASW84]   Daniel Arovas, John R Schrieffer, and Frank Wilczek. Fractional statistics and the quantum hall effect. *Physical review letters*, 53(7):722, 1984.

[BB98]   Carl M Bender and Stefan Boettcher. Real spectra in non-hermitian hamiltonians having p t symmetry. *Physical Review Letters*, 80(24):5243, 1998.

[BK13]   Gregory Berkolaiko and Peter Kuchment. *Introduction to quantum graphs*. Number 186. American Mathematical Soc., 2013.

[Bon07]   Parsa Hassan Bonderson. *Non-Abelian anyons and interferometry*. PhD thesis, California Institute of Technology, 2007.

[BP09]   R Blumenhagen and E Plauschinn. Introduction to conformal field theory: With applications to string theory, vol. 779 of lect. *Notes Phys. Springer*, 2009.

[DDT01]   Patrick Dorey, Clare Dunning, and Roberto Tateo. Spectral equiv-
           alences, bethe ansatz equations, and reality properties in ðĪŠńðĪŠŕ-
           symmetric quantum mechanics. *Journal of Physics A: Mathemat-
           ical and General*, 34(28):5679, 2001.

[DPRH+98] R De-Picciotto, M Reznikov, M Heiblum, V Umansky, G Bunin,
           and D Mahalu. Direct observation of a fractional charge. *Physica
           B: Condensed Matter*, 249:395–400, 1998.

[DRR12]   J Dubail, N Read, and EH Rezayi. Real-space entanglement spec-
           trum of quantum hall systems. *Physical Review B*, 85(11):115321,
           2012.

[ENO05]   Pavel Etingof, Dmitri Nikshych, and Viktor Ostrik. On fusion
           categories. *Annals of Mathematics*, pages 581–642, 2005.

[FMS12]   Philippe Francesco, Pierre Mathieu, and David Sénéchal. *Confor-
           mal field theory*. Springer Science & Business Media, 2012.

[FTL+07]   Adrian Feiguin, Simon Trebst, Andreas WW Ludwig, Matthias
           Troyer, Alexei Kitaev, Zhenghan Wang, and Michael H Freedman.
           Interacting anyons in topological quantum liquids: The golden
           chain. *Physical review letters*, 98(16):160409, 2007.

[GA17]   B. Majidzadeh Garjani and E. Ardonne. Anyon chains with pair-
           ing terms. *J. Phys. A: Math. Theor.*, 50(135201), 2017.

[GEA15]   B Majidzadeh Garjani, B Estienne, and Eddy Ardonne. On the
           particle entanglement spectrum of the laughlin states. *Journal of
           Physics A: Mathematical and Theoretical*, 48(28):285205, 2015.

[GR00]   V Gurarie and E Rezayi. Parafermion statistics and quasihole ex-
           citations for the generalizations of the paired quantum hall states.
           Physical Review B, 61(8):5473, 2000.

[Hal79]   Edwin H Hall. On a new action of the magnet on electric currents.
           American Journal of Mathematics, 2(3):287–292, 1879.

[Hal83]   F Duncan M Haldane. Fractional quantization of the hall effect: a
           hierarchy of incompressible quantum fluid states. *Physical Review
           Letters*, 51(7):605, 1983.

[HH09]   Tobias J Hagge and Seung-Moon Hong. Some non-braided fu-
           sion categories of rank three. *Communications in Contemporary
           Mathematics*, 11(04):615–637, 2009.

[HZS07]   Masudul Haque, Oleksandr Zozulya, and Kareljan Schoutens. En-
           tanglement entropy in fermionic laughlin states. *Physical review
           letters*, 98(6):060401, 2007.

[Kac89]   Victor G Kac. *Infinite Dimensional Lie Algebras and Groups:
           Proceedings of the Conference*, volume 7. World scientific, 1989.

[KDP80]   K v Klitzing, Gerhard Dorda, and Michael Pepper. New method
           for high-accuracy determination of the fine-structure constant
           based on quantized hall resistance. *Physical Review Letters*,
           45(6):494, 1980.

[Kit06]   Alexei Kitaev. Anyons in an exactly solved model and beyond.
           Annals of Physics, 321(1):2–111, 2006.

[KMG17]   Pavel Kurasov and Babak Majidzadeh Garjani. Quantum graphs:
           Pt-symmetry and reflection symmetry of the spectrum. *Journal
           of Mathematical Physics*, 58(2):023506, 2017.

[KP06]   Alexei Kitaev and John Preskill. Topological entanglement en-
           tropy. *Physical review letters*, 96(11):110404, 2006.

[Kur]   P. Kurasov. *Spectral theory of quantum graphs and inverse prob-
           lems.* to appear in Birkhäuser.

[Lan30]   LD Landau. Diamagnetismus der metalle. *Zeitschrift für Physik
           A Hadrons and Nuclei*, 64(9):629–637, 1930.

[Lau83]   Robert B Laughlin. Anomalous quantum hall effect: an in-
           compressible quantum fluid with fractionally charged excitations.
           Physical Review Letters, 50(18):1395, 1983.

[LH08]   Hui Li and F Duncan M Haldane. Entanglement spectrum as
           a generalization of entanglement entropy: Identification of topo-
           logical order in non-abelian fractional quantum hall effect states.
           Physical review letters, 101(1):010504, 2008.

[LM77]   Jon M Leinaas and Jan Myrheim. On the theory of identical
           particles. *Il Nuovo Cimento B (1971-1996)*, 37(1):1–23, 1977.

[LW06]   Michael Levin and Xiao-Gang Wen. Detecting topological or-
           der in a ground state wave function. *Physical review letters*,
           96(11):110405, 2006.

[Mac95]   IG Macdonald. Symmetric functions and hall polynomials oxford
           univ. *Press, New York*, 1995.

[MG15]   Babak Majidzadeh Garjani. *On the Rank of the Reduced Density Operator for the Laughlin State and Symmetric Polynomials*, Licentiate thesis, Stockholm University, 2015.

[MR91]   Gregory Moore and Nicholas Read. Nonabelions in the fractional quantum hall effect. *Nuclear Physics B*, 360(2-3):362–396, 1991.

[MS04]   Adam Millican-Slater. *Aspects of PT-symmetric quantum mechanics*. PhD thesis, Durham University, 2004.

[NC00]   Michael A Nielsen and IL Chuang. Quantum computation. *Quantum Information. Cambridge University Press, Cambridge*, 2000.

[NW96]   Chetan Nayak and Frank Wilczek. 2n-quasihole states realize 2n-1-dimensional spinor braiding statistics in paired quantum hall states. *Nuclear Physics B*, 479(3):529–553, 1996.

[Pau36]   Linus Pauling. The diamagnetic anisotropy of aromatic molecules. *The Journal of Chemical Physics*, 4(10):673–677, 1936.

[Rea06]   N Read. Wavefunctions and counting formulas for quasiholes of clustered quantum hall states on a sphere. *Physical Review B*, 73(24):245334, 2006.

[RR96]   N Read and E Rezayi. Quasiholes and fermionic zero modes of paired fractional quantum hall states: the mechanism for non-abelian statistics. *Physical Review B*, 54(23):16864, 1996.

[RSS12]   Iván D Rodríguez, Steven H Simon, and JK Slingerland. Evaluation of ranks of real space and particle entanglement spectra for large systems. *Physical review letters*, 108(25):256806, 2012.

[SCR+12] A Sterdyniak, A Chandran, Nicolas Regnault, B Andrei Bernevig, and Parsa Bonderson. Real-space entanglement spectrum of quantum hall states. *Physical Review B*, 85(12):125308, 2012.

[SGJE97] L Saminadayar, DC Glattli, Y Jin, and B c-m Etienne. Observation of the e/3 fractionally charged laughlin quasiparticle. *Physical Review Letters*, 79(13):2526, 1997.

[Sta99]   Richard P. Stanely. *Enumerative Combinatorics*, volume 2. Cambridge University Press, 1999.

[Tam00]   D Tambara. Representations of tensor categories with fusion rules of self-duality for abelian groups. *Israel Journal of Mathematics*, 118(1):29–60, 2000.

[TSG82]   Daniel C Tsui, Horst L Stormer, and Arthur C Gossard. Two-dimensional magnetotransport in the extreme quantum limit. *Physical Review Letters*, 48(22):1559, 1982.

[Wan10]   Zhenghan Wang. *Topological quantum computation*. Number 112. American Mathematical Soc., 2010.

[Wen95]   Xiao-Gang Wen. Topological orders and edge excitations in fractional quantum hall states. *Advances in Physics*, 44(5):405–473, 1995.

[Wil82a]   Frank Wilczek. Quantum mechanics of fractional-spin particles. *Physical review letters*, 49(14):957, 1982.

[Wil82b]   Frank Wilczek. Quantum mechanics of fractional-spin particles. *Physical review letters*, 49(14):957, 1982.

[Wil13]   RL Willett. The quantum hall effect at 5/2 filling factor. *Reports on Progress in Physics*, 76(7):076501, 2013.

[WNS92]   Sven Ole Warnaar, Bernard Nienhuis, and KA Seaton. New construction of solvable lattice models including an ising model in a field. *Physical review letters*, 69(5):710, 1992.

[ZHSR07]   OS Zozulya, M Haque, K Schoutens, and EH Rezayi. Bipartite entanglement entropy in fractional quantum hall states. *Physical Review B*, 76(12):125310, 2007.

Accompanied Papers